7-1-2012

The role of geological history, topography, and environmental heterogeneity in the diversification of an endemic Andean radiation : the Metallura hummingbirds

Phred Benham

Phred M. Benham
Candidate

Biology
Department

This thesis is approved, and it is acceptable in quality and form for publication:

Approved by the Thesis Committee:

Christopher Witt , Chairperson

Vaishali Katju

Felisa Smith

THE ROLES OF GEOLOGICAL HISTORY, TOPOGRAPHY, AND ENVIRONMENTAL HETEROGENEITY IN THE DIVERSIFICATION OF AN ENDEMIC ANDEAN RADIATION THE METALLURA HUMMINGBIRDS

by

PHRED M. BENHAM

B. S., LOUISIANA STATE UNIVERSITY, 2006

THESIS

Submitted in Partial Fulfillment of the
Requwerements for the Degree of

Master of Science in Biology

The University of New Mexico
Albuquerque, New Mexico

July, 2012

ACKNOWLEDGEMENTS

My major advisor, Chris Witt, provided tremendous assistance and support throughout my time as a Master's student. Libby Beckman, Shane DuBay, Spencer Galen, Andrew Johnson, Sabrina McNew, C. Jonathan Schmitt, Ashley Smiley, and Natalie Wright Were excellent labmates assisting me extensively in the field, the lab, and through many discussions. Several people also provided much needed help in the field, including: Michael Lelevier, Monica Flores, Emil Bautista O., and Homan Castillo. I would like to thank my committee, Vaishali Katju and Felisa Smith, for all of their useful comments and advice. The following people provided access to tissues and specimens at their respective collections: Robb Brumfield, Donna Dittmann, Steve Cardiff, and J. V. Remsen, Jr. (Louisiana State University Museum of Natural Science); John Bates, Shannon Hackett, and David Willard (Field Museum of Natural History); Joel Cracraft and Paul SIet (American Museum of Natural History); Mark Robbins (Kansas University Museum of Natural History); Nate Rice (Academy of Natural Sciences, Philadelphia); and Thomas Valqui (Centro de Ornitologia y Biodiversidad). Andrés M. Cuervo and Jorge Pérez-Emán kindly loaned tissue extracts of *Metallura* from Colombia and Venezuela. Permits for specimen collecting in Peru Were provided by INRENA. Finally, I am grateful for funding from the NSF DEB-1146491, NCRR-NIH P20RR018754, UNM Center for Evolutionary and Theoretical Immunology (CETI), the Frank M. Chapman Memorial Fund, and the Graduate Resmyce Allocation Committee at the University of New Mexico.

The Role of Geological History, Topography, and Environmental Heterogeneity in the Diversification of an Endemic Andean Radiation: the *Metallura* Hummingbirds.

by

Phred M. Benham

B.S. Biological Sciences, Louisiana State University, 2006

M.S. Biology, University of New Mexico, 2012

ABSTRACT

A dynamic geological history, complex topography, and high species richness characterize the tropical Andes. Endemic radiations comprise a major component of this high diversity and evaluating the spatial and temporal context in which these radiations diversified provides an informative framework to understand the processes facilitating speciation in the Andes. *Metallura* hummingbirds are a diverse genus endemic to the Andes that are widely distributed geographically and ecologically making them well suited to investigating Andean speciation.

In the first chapter I apply phylogenetic methods to address the relative roles of geological history, physical barriers, and environmental heterogeneity in the *Metallura* radiation. I found *Metallura* diversification to be primarily associated with Pleistocene glacial cycles. The two main clades recovered in all phylogenetic analyses exhibited contrasting histories of spread through the Andes. One clade, the *M. aeneocauda* superspecies, diverged from south-to-north through the Andes, whereas a second clade, the widespread *M. tyrianthina*, shows a northern origin followed by spread southward. Finally, river valleys played a prominent role in structuring genetic diversity in both

clades. Environment played little role with genetic structure only existing in conjunction with physical barriers.

Secondly, I compare patterns of genetic and morphological variation within Peruvian populations of *Metallura tyrianthina* to evaluate how geographic isolation and environmental heterogeneity interact to drive divergence. Longer bills were found in populations occurring in more seasonal environments regardless of taxonomy or geographic proximity. Conversely, physical barriers structured genetic variation. A more detailed investigation of four populations in southern Peru also revealed that bill length increased in more seasonal environments. However, both morphological and genetic differences were greater in the presence of a physical barrier. These results indicate that the physical barriers and environmental heterogeneity created by a complex Andean topography operate in concert to drive speciation.

TABLE OF CONTENTS

CHAPTER ONE:

Historical Biogeography of an Endemic Andean Radiation: the *Metallura* Hummingbirds

INTRODUCTION

Avian species richness reaches its peak in the tropical Andes (Hawkins et al., 2007). A dynamic geological history and consequent topographic complexity in the Andes facilitated *in situ* radiations that now comprise a substantial component of this high species richness (e.g., McGuire et al., 2007; Sedano & Burns, 2009). Studies also point to recent diversification within many of these radiations compared to clades from the surrounding lowlands (Fjeldsa, 1994; Weir, 2006). Molecular phylogenies with detailed geographic sampling now have the potential to resolve the spatial and temporal history of Andean diversification (e.g., Chaves et al., 2011), but few lineages have been studied.

Allopatric speciation is the most likely and frequent mode of speciation in birds (Coyne & Price, 2000; Price, 2008). Assuming that all speciation events in the Andes are the result of allopatric isolation implies two processes must occur for a lineage to achieve high net diversification. First, multiple barriers to gene flow must exist in order to account for multiple speciation events. Second, range expansion must occur in daughter taxa otherwise net diversification becomes limited as species ranges are divided into smaller components and extinction becomes more likely in these small daughter populations (Weir & Price, 2011; Pigot et al., 2010). Andean topography creates multiple physical barriers to gene flow and these barriers correspond to major breaks in genetic

and phenotypic variation in multiple taxa, thus highlighting the importance of these barriers in the diversification process (Parker et al., 1985; Weir, 2009; Chaves & Smith, 2011). The role of range expansion in species radiations is not as clearly understood in the Andes. Elevational zonation in congeners is one of the best-known and long recognized patterns in Andean birds (Chapman, 1917; Terborgh, 1971). The few clades examined to date have found that these elevational replacements originated in allopatry and displaced one another upon secondary contact (Patton & Smith, 1992; Pérez-Emán, 2005; Parra et al., 2009). This indicates that range expansion across common barriers may allow for multiple cycles of diversification within a lineage.

Periods of uplift and glaciation in the Andes fostered abundant opportunity for both range expansion and fragmentation in Andean taxa (Rull, 2011). Initial uplift began in the Andes during the Paleogene of Peru and Bolivia, however by 10 million years ago (mya) these regions had only reached about half their modern height and a final period of uplift to current elevations occurred between 10-6 mya (Garzione et al., 2008; Hoorn et al., 2010). The initial period of uplift in the northern Andes occurred during the middle Oligocene-to-early Miocene followed by a second period of uplift in the Pliocene 3-5 mya when the Eastern Cordillera of the Colombian Andes attained modern elevations (Gregory-Wodzicki, 2000; Hoorn et al., 1995). The south-to-north procession of uplift created a series of novel montane habitats for organisms to expand into, but also created a topographically complex region that promoted isolation. Glacial cycles in the Andes began with the onset of the Pleistocene 2.4 mya and intensified from 0.9 mya to the last glacial maximum (ca. 12,000 ya) (Hewitt, 2000). Glacial cycles caused major shifts in habitat, at times pushing treeline downslope by 1200 m (Hooghiemstra et al., 2006).

Habitat migration allowed for populations to expand during glacial periods when high elevation habitats spanned river valleys and then diverge in isolation during inter-glacials when habitat returned upslope (Hooghiemstra & Van der Hammen, 2004).

In addition to forming multiple physical barriers, topographic complexity also creates extensive environmental and habitat heterogeneity within the Andes (Sarkinen et al., 2011). Local adaptation to temperature, pressure, or humidity can potentially facilitate diversification along environmental gradients in the Andes. There is evidence for morphological divergence across these ecological gradients despite ongoing gene flow in Andean taxa (Milá et al., 2009), but there is no firm evidence that this type of diversifying selection can lead to reproductive isolation without allopatry (Patton & Smith, 1992; Parra et al., 2009). Rather, environmental heterogeneity likely acts as a catalyst for divergence in conjunction with physical barriers.

The nine currently recognized species and 15 subspecies within *Metallura* comprise an endemic radiation in the Andes belonging to the coquette clade of hummingbirds (Bleiweiss et al., 1997; McGuire et al., 2009), which is also largely endemic to the Andes (Kirchman et al., 2010). Previous molecular and morphological studies of *Metallura* revealed two main clades (Heindl & Schuchmann, 1998; Garcia-Moreno et al., 1999a). The first clade, known as the *M. aeneocauda* superspecies (Zimmer, 1952), consists of six species that replace one another latitudinally from Bolivia to Colombia in humid treeline habitat (Fig. 1a). A second clade comprises the seven subspecies within *Metallura tyrianthina*, which occupy a broad ecological and geographic range (Fig. 1b). *M. tyrianthina* ranges from 1900-4200 m in elevation, although generally it occurs at lower elevations than members of the *M. aeneocauda*

superspecies where they come into contact (Fjeldsa & Krabbe, 1990). *M. phoebe* and populations of *M. tyrianthina* occur in semi-arid scrub of west-facing slopes in the Peruvian Andes, with the former species occurring at higher elevations (Schulenberg et al., 2007). The two clades of *Metallura* span many of the same physical and ecological barriers and these two independent histories of dispersal and divergence within *Metallura* hummingbirds make them an ideal group to investigate the roles of orogeny, glaciation, and physical or ecological barriers in shaping the diversity and biogeography of an Andean endemic radiation.

The genus *Metallura* has long been recognized as a monophyletic group sister to *Chalcostigma* thornbills (but see Peters, 1945) based on morphological (Heindl & Schuchmann, 1998) and molecular data (Garcia-Moreno et al., 1999a; McGuire et al., 2007). Species limits and taxonomic relationships within *Metallura* have changed considerably over the years (Cory, 1918; Peters, 1945; Zimmer, 1952; Garcia-Moreno et al., 1999a; Kirchman et al., 2010). The position of *M. phoebe* remains unresolved with a mtDNA phylogeny (Garcia-Moreno et al., 1999a) placing it among a group of Ecuadorian species in the *M. aeneocauda* superspecies, whereas a more recent multi-locus dataset placed the species as basal to the entire genus (Kirchman et al., 2010). Additionally, the phylogenetic position of *M. iracunda* has remained a mystery although morphological analyses suggest a close relationship with *M. tyrianthina* (Heindl & Schuchmann, 1998).

In the present study I construct a comprehensive, multi-locus phylogeny including all species of *Metallura* and subspecies of *M. tyrianthina* in order to assess the spatial and historical context in which the genus has expanded and diversified.

Specifically, I address: **1)**; the timing of diversification in association with Andean uplift and glaciation; **2)** the role of physical and ecological barriers in structuring genetic variation in *Metallura*; **3)** the history of origin and dispersal throughout the Andes in both clades of *Metallura;* and **4)** concordance of current taxonomy with the molecular phylogeny.

MATERIALS AND METHODS

Samples and Sequencing

The mitochondrial locus NADH dehydrogenase subunit 2 (ND2) was sequenced for 197 samples of *Metallura tyrianthina*, five of *M. iracunda*, three of *M. w. williami*, one of *M. aeneocauda*, one of *M. eupogon*, and one of *M. thereseiae* (Appendix A). Following phylogenetic analyses of ND2 I selected a subset of 70 *M. tyrianthina* samples that included 2-5 individuals from each distinct clade. For these 70 samples I sequenced two autosomal nuclear introns, Adenylate Kinase subunit 1 (AK1) and Beta-Fibrinogen subunit 7 (Bfib7), and the z-linked locus muscle, skeletal receptor tyrosine kinase (MUSK). Five hummingbird species (*Lophornis chalybeus, Aglaiocercus kingi, Oreotrochilus estella, Lesbia nuna,* and *Chalcostigma herrani*) were selected as outgroups from across the coquette clade of hummingbirds (Kirchman et al., 2010). ND2, AK1, and Bfib7 sequence data were obtained from GenBank for the five outgroup species as well as *M. phoebe, M. aeneocauda, M. eupogon, M. theresiae, M. odomae, M. williami atrogularis*, and *M. baroni* (Appendix A). I sequenced MUSK for each of these individual species, as sequence data for MUSK was not available on GenBank.

Genomic DNA was extracted from frozen tissue or muscle tissue preserved in the saline solution RNAlater® (Life Technologies) using a QIAGEN DNeasy tissue kit and following the manufacturer's protocols (QIAGEN inc., Valencia, CA, USA). Primers for each locus were taken from the literature or designed specifically for this project using primer 3 v. 0.4.0 (Rozen & Skaletsky, 2000) (see Table 1 for details). PCR protocols were identical for each locus. 15µl reactions (1µl DNA; 9.05µl H_20; 1.5µl $MgCl_2$ and GeneAmp®10x PCR buffer (Applied Biosystems, Foster City, CA, USA); 0.3µl 10mM

dNTP; 0.75μl of 10mM reverse and forward primer; and 0.15μl AmpliTaq® Gold PCR Polymerase (Applied Biosystems)) ran on a thermal cycler with the following protocol: initial denaturation at 95ºC for 8 minutes; 35 cycles of denaturation at 95ºC for 30 seconds, annealing at 50-62ºC for 30 seconds, and extension at 72ºC for 1minute; and final extension at 72ºC for 10 minutes. The annealing temperature was the only component that varied among loci. ND2 and MUSK annealed best at 50ºC, whereas AK1 and Bfib7 annealed at 62ºC. Following PCR, sequences were cleaned using 1μl exosap-IT and the recommended thermal cycler protocol (USB Corporation, Cleveland, OH, USA). Finally, I sequenced forward and reverse strands of each locus using the PCR primers and ABI BigDye® terminator v. 3.1 (Applied Biosystems) and the associated buffer on an ABI 3130 automated sequencer.

All sequences were manually assembled and edited using Sequencer 4.10.1 (Gene Codes Corporation, Ann Arbor, MI, USA) and aligned using MUSCLE 3.7 (Edgar, 2004). Haplotype reconstruction for nuclear loci with multiple double peaks was conducted using the program PHASE 2.1.1 (Stephens et al., 2001; Stephens & Donnelly, 2003).

Phylogentic analyses

I estimated phylogenies using Bayesian inference (BI) and Maximum Likelihood (ML) methods for an ND2 dataset including all samples and five pruned datasets of 38 samples: one for each nuclear gene, a concatenated nuclear dataset, and a concatenated dataset of all four loci. I used an Akaike Information Criterion (Akaike, 1974) in jModelTest v. 0.1.1 (Posada, 2008; Guindon & Gascuel, 2003) to select an appropriate model of nucleotide substitution for each locus. The models GTR+I+G (ND2), HKY+I

(AK1), HKY+I+G (Bfib7), and HKY+G (MUSK) were selected for all BI analyses. ND2 was also partitioned by codon position. BI analyses were run in MrBayes v. 3.1 (Huelsenbeck & Ronquist, 2003) on the CIPRES Science Gateway (Miller et al., 2010). For each dataset I ran an MCMC analysis for 40 million generations that involved four simultaneous runs of four chains each and a temperature for the heated chains of 0.2 (0.175 for ND2). Trees were sampled every 1000 generations and I discarded the first 10% of trees as burnin. Convergence was assessed using the slide and compare functions in AWTY (Wilgenbusch et al., 2004). Three datasets (Bfib7 only, MUSK only, and concatenated nuclear) showed incomplete convergence after 40 million generations and I re-ran analyses on these datasets, increasing the number of generations to 60 million, sampling every 2000 generations, and decreasing the temperature of the heated chains to 0.15.

ML analyses were performed using RAxML v. 7.2.8 (Stamatakis, 2006), which does not allow for the specification of an HKY model. Instead I use a GTRGAMMA model for each locus. The data were partitioned by codon position for ND2 and by locus for concatenated datasets. ML-optimization in RAxML begins with a randomized maximum parsimony (MP) tree that is obtained by randomly inserting each sample and then optimizing the MP tree by pruning and re-grafting subtrees. The ability to begin each ML-optimization from a distinct MP starting tree improves the ability of RAxML to search the tree topology space and identify a best-scoring ML tree (Stamatakis, 2006). To find the best scoring ML tree I ran 100 inferences of RAxML for each dataset (except ND2 for which I ran 200 inferences), followed by 1000 bootstrap iterations using the

rapid bootstrapping algorithm in RAxML, and finally I printed the support values from the bootstrap analysis to the best-scoring ML topology.

Species tree analysis and Divergence Times

The *Metallura* dataset exhibits short internal branches, a recent history of divergence, and incomplete lineage sorting within nuclear loci. All of these issues can cause discordance among individual gene trees and the true species tree (Flórez-Rodríguez et al., 2010). I use the species tree method *BEAST to construct a multi-locus phylogeny of *Metallura* (Heled & Drummond, 2010). Based on the Bayesian framework implemented in BEAST (Drummond & Rambaut, 2007), *BEAST utilizes coalescent theory to infer the species tree topology and divergence times based on the multiple gene trees and individuals (Heled & Drummond, 2010). *BEAST requires that the tips be specified *a priori* in order to estimate coalescence of gene copies from within each "species". I selected 3-5 individuals from each of the well-supported *M. tyrianthina* ND2 clades following recommendations of the developers (Heled & Drummond, 2010), however only 1-2 individuals were available for other *Metallura* species and outgroups (see below for further details of the MCMC analysis).

To determine if *Metallura* diversification occurred primarily during Andean uplift or Pleistocene glacial cycles I applied both a fossil and a geological calibration to estimate divergence times and rates of molecular evolution across the *Metallura* phylogeny. Fossil swifts in the genus *Scaniacypselus* are known from the middle Eocene (37-48.6 mya) of Denmark and Germany (Harrison, 1984; Peters, 1985). The position of *Scaniacypselus* within Apodidae is well supported through robust phylogenetic analysis of morphological characters (Mayr, 2003) and the sister relationship between Apodidae

and Hemiprocnidae to the exclusion of Trochilidae is supported by multiple molecular and morphological datasets (Hackett et al., 2008, Mayr, 2002). The *Scaniacypselus* fossils were used as a minimum divergence date between Apodidae and Hemiprocnidae. The oceanic islands of the Juan Fernandez Archipelago provide a second calibration point. The endemic Juan Fernandez Firecrown, *Sephanoides fernandensis,* and its sister species *S. sephanoides* belong to the coquette clade of hummingbirds (McGuire et al., 2007). Robinson Crusoe Island is the largest and oldest island of the archipelago and it is estimated to have emerged approximately 4-5 mya based on K-Ar dating of basalt rocks (Stuessy et al., 1984). I use this date to specify a maximum date of divergence between the two *Sephanoides* species.

I applied these two calibration points to a ND2 dataset in BEAST v.1.7.0 (Drummond et al., in press) and the species tree estimated in *BEAST. I incorporated representative samples from GenBank of Apodidae (*Streptoprocne zonaris*), Hemiprocnidae (*Hemiprocne mystacea*), and both *Sephanoides* species. BEAST and *BEAST allow the calibration of certain nodes with mean and standard deviation (sd) and based on these nodes calculates divergence times and substitution rates across the entire phylogeny. Input files were created using BEAUti v. 1.7.0 (Drummond et al., *in press*). Priors for the TMRCA were assigned to the calibrated nodes. For the fossil calibration between Apodidae and Hemiprocnidae I applied a normal prior with mean 42.9 mya and sd 3.5, thus encompassing the entire middle Eocene within the 95% HPD of the prior. For the geological calibration between *Sephanoides* species I also applied a normal prior of 4.23 mya and sd 0.5, which includes a range of 3.5-5 mya within the 95% HPD. Preliminary runs of *BEAST indicated that an uncorrelated relaxed lognormal

clock model (Drummond et al., 2006) was more appropriate for the ND2 data, whereas the three nuclear loci fit a strict clock model (95% HPD of the standard deviation included zero). I performed six independent runs of the ND2 dataset and six runs of the species-tree dataset on the CIPRES Science Gateway (Miller et al., 2010). Each MCMC analysis was run for 200 million generations, sampling every 20000 steps, and the first 10% of trees was discarded as burnin. I combined log files from each independent run using the program LogCombiner v.1.7.1 (Rambaut & Drummond, 2007b), then viewed the combined log file in TRACER v. 1.5 to confirm that ESS values for all priors and the posterior distribution were >200 (Rambaut & Drummond, 2007a), and annotated using TREEANNOTATOR v.1.7.1 (Rambaut & Drummond, 2007c).

Population structure:

Based on current taxonomy and the ND2 phylogeney *Metallura* diversity is closely associated with the following Andean centers of endemism (Cracraft, 1985; Stattersfield et al., 1998; Weir, 2009): (A) North Venezuelan; (B) Meridan; (C) Santa Marta; (D) Perijan; (E) East Colombian; (F) Central Colombian; (G) West Colombian; (H) North Andean; (I) West Peruvian; (J) North Peruvian; (K) Central Peruvian; and (L) Southern Peruvian (Table 2, Fig. 3). To determine the degree to which physical barriers between these centers of endemism structure genetic variation in both *Metallura* clades I calculated corrected pairwise distances (Nei, 1987) and Fst values across certain barriers (Holsinger & Weir, 2009). I also evaluated pairwise distances across ecological boundaries in the Andes within *M. tyrianthina*. Climatic variables of precipitation and seasonality available from worldclim.org (Hijmans et al., 2005) served as proxies for ecology. I determined ecological differences among the 43 sampling localities by plotting

the first principal component (PC1) for seasonality, which explained 82.3% of the variation in seasonality, against PC1 of precipitation (75% of the variation). This analysis revealed six climatically similar clusters (Fig. 2). I further subdivided cluster 1 into three additional sub-clusters. The ecological differences among these clusters are readily apparent, however the interpolated nature of the worldclim dataset can lead to errors where environmental transitions occur over fine spatial scales. Two of the sub-clusters (1a and 1c) are characterized by semi-arid, more seasonal montane scrub on the west slope of the Andes and inter-Andean rain-shadow valleys, whereas the third cluster (1b), only a few kilometers apart from some localities in 1c, is humid, aseasonal montane forest (Stotz et al., 1996). Both pairwise sequence differences and Fst-values were calculated with the program Arlequin v. 3.5 (Excoffier et al., 2005)

Dispersal-Vicariance analysis:

I estimated the history of spread through the Andes for both *Metallura* clades using a Dispersal-Vicariance analysis (DIVA). DIVA optimizes the ancestral distributions of a clade by minimizing the number of dispersal and extinction events and assuming that most speciation occurred through vicariance (Ronquist, 1997). For *Metallura* I implemented a Bayes-DIVA approach in the program RASP (Yu et al., *in press*). The main advantage of Bayes-DIVA is the ability to incorporate phylogenetic uncertainty into the estimation of ancestral distributions by assessing the probability of certain ancestral distributions over the posterior probabilities of multiple tree topologies generated during an MCMC analysis (Nylander et al., 2008). This is especially relevant for the *Metallura* dataset where I had difficulty resolving certain nodes. I utilized 40000 trees obtained from MCMC analyses in BEAST of both the ND2 gene tree and the four-

locus species tree. For each analysis I grouped the centers of endemism, discussed above (Table 2, Fig. 3), into six regions: (A) Venezuela; (B) Sierras de Perijá and Santa Marta; (C) the Eastern Cordillera of the Colombian Andes; (D) the Northern Andes, which includes both the Central and Western Cordillera of Colombia south through Ecuador to northern Peru; (E) Eastern Andes of Peru and Bolivia; and (F) the Western Andes of Peru. Given the linear nature of the Andes as well as Andean bird distributions (Graves, 1988), I constrained the ancestral distributions to include only contiguous ranges, e.g. ancestral taxa could have a distribution that included the regions ABC, but not AEF. Few Andean species exhibit disjunct ranges and no *Metallura* clades or species have a disjunct range.

RESULTS

ND2 sequences were 1041 bp in length and included 257 informative sites with outgroups (24.7%). For the two autosomal nuclear introns I sequenced 503 bp of AK1 (21 informative sites with outgroups (4.2%)) and 629-1013 bp of Bfib7 (38 informative sites with outgroups (3.8%)). The Z-linked locus MUSK was 645 bp in length with 25 informative sites with outgroups (3.8%). Indels were found in both nuclear introns, including a 90 bp indel in the AK1 intron. This indel occurred at intermediate frequencies in populations throughout the range of *Metallura tyrianthina* and it was excised for all phylogenetic analyses. A 15 bp indel was also found in Bfib7. The latter indel caused problems in the sequencing of heterozygous individuals because clean sequence would end abruptly at the starting point of the indel at nucleotide position 629. The indel was also excised from Bfib7 before performing any phylogenetic analyses. There were no internal stop codons, indels, or anomalous substitution patterns in the ND2 sequences that might indicate that I had unknowingly amplified pseudogenes. However, I excluded one sample (FMNH 433155) because it did not align with other sequences and BLAST returned ambiguous matches with a variety of hummingbird species.

Phylogenetic analyses

BI and ML analyses of the ND2 dataset both recovered a monophyletic *Metallura* consisting of two well-supported clades (>70 bootstrap support and >0.95 posterior probability (pp); (Fig. 4)): (1) *M. phoebe* as sister to the *Metallura aeneocauda* superspecies, which exhibited a south-to-north branching pattern with *M. aeneocauda* basal, followed by *M. eupogon* and *M. theresiae*, and finally all species north of the Marañon valley; and (2) all populations within *M. tyrianthina* including *M. iracunda*.

Clade 2 can further be subdivided into three well-supported sub-clades: (2A) a northeastern clade including *M. iracunda* and the subspecies *chloropogon, oreopola, districta,* and *tyrianthina* from the eastern Cordillera of Colombia; (2B) a northern and central Andean clade including populations of *M. t. tyrianthina* from the central and western cordilleras of Colombia south to the Marañon valley in northern Peru and the subspecies *quitensis*; and (2C) a clade comprising all populations of *M. tyrianthina* south of the Marañon valley in Peru and Bolivia. Clades corresponding to many of the isolated cordilleras and centers of endemism Were also supported, however, short internal branches among these different groups made it difficult to resolve the branching pattern within each of the major clades and there was frequent discordance between BI and ML analyses at this level (Fig. 4).

Phylogenetic analyses of individual nuclear genes revealed likely cases of incomplete lineage sorting and generally poor resolution despite evidence for good mixing among the different runs of the MCMC analyses in AWTY. Individual nuclear loci and the concatenated dataset did show some moderate-to-high posterior probability for certain clades, including: a southern Peru clade (south of the Apurimac valley) in all four datasets; high support for a sister relationship among the two Venezuelan populations (MUSK 0.96; and concatenated 0.99); and support for a northern Peru through Ecuador and central and western Colombia clade (MUSK 0.99; concatenated dataset 1.0). The concatenated nuclear dataset also showed 100% support for a monophyletic *M. tyrianthina* that included *M. iracunda* (Fig. 5).

The four-locus concatenated dataset showed overall consistency with the ND2 dataset with high support for the five clades discussed above. BI and ML analyses were

largely congruent with each other, with the exception that the ML phylogeny showed weak support (32 bootstrap) for *M. phoebe* in a basal position to the *M. tyrianthina* and *M. iracunda* clade (Fig. 6).

Species tree and divergence times

The multi-locus species tree strongly supported a monophyletic *Metallura* (0.98 pp) and the two main clades within *Metallura*, however, *M. phoebe* was placed, with weak support (0.56 pp), in a position sister to *M. tyrianthina* rather than sister to the *M. aeneocauda* superspecies. The topology within the *M. aeneocauda* superspecies was largely concordant with both the ND2 and concatenated analyses. The only difference found was a sister relationship between *M. odomae* and *M. w. williami*, which was weakly supported (0.54 pp). Similar to the ND2 gene tree I found *M. baroni* to be nested within *M. williami* and sister to *M. w. atrogularis*, but with very weak support (0.38 pp). Although *M. tyrianthina* including *M. iracunda* is a well-supported clade (0.99 pp) I did not find strong support for many relationships within *M. tyrianthina*. The only clade with support greater than 0.90 pp was a clade from southeast Peru that included populations from Ayacucho (north of the Apurímac valley) basal to birds from Bolivia, Apurimac/Urubamba, and humid southeast Peru. Otherwise a weakly supported topology showed the Venezuelan birds as a basal split, followed by the rest of clade 2A (*M. t. districta, M. t. tyrianthina*, and *M. iracunda*); and then a north Andean clade largely corresponding to 2B (including *M. t. septentrionalis* and northern *M. t. smaragdinicollis*) sister to the well-supported south Peru clade (Fig. 7).

My fossil and geological calibrations of the *Metallura* phylogeny supported an average substitution rate for the ND2 locus of 0.0092 substitutions/site/lineage/million

years (s/s/l/my) (95% HPD: 0.0072-0.0111 s/s/l/my). The nuclear genes are evolving at a much slower rate. Substitution rates for each nuclear gene: AK1: 0.00099 s/s/l/my (95% HPD: 0.00064-0.0013 s/s/l/my); Bfib7: 0.00125 s/s/l/my (95% HPD: 0.00081-0.0016 s/s/l/my); and MUSK: 0.0094 s/s/l/my (95% HPD: 0.00061-0.00119 s/s/l/my).

Divergence times were consistently deeper in the ND2 dataset (Fig. 8) compared to the species tree dataset (Fig. 9), however, both pointed towards extensive diversification within both *Metallura* clades during the Pleistocene glacial cycles. The majority of the temporal discordance between the datasets occurred at deeper nodes in the phylogeny (Table 3).

Population Structure

Corrected pairwise sequence differences across physical barriers ranged from 0.06-3.40% in clade two. In the northern part of the species range sequence divergences were >1%, with the exception of the Rio Mira (0.062%). South of the Marañon valley sequence divergence was <1% across all barriers with a low of 0.082% found across the Huallaga valley in central Peru (Table 4). Sequence divergence within clade 1 ranged from 0.16-8.45% across shared barriers. Fst-values were generally found to correlate with sequence divergence, however, some instances of low sequence divergence still showed high Fst, for example the high Andean ridge in Peru. In contrast, clade 1 species showed greatest divergence within Peru across the high Andes (8.45%) and Apurimac valley (6.05%) although the Huallaga valley again showed recent divergence between species (0.16%). Divergence across the Marañon valley (1.49%) was similar, but less than what was found within *M. tyrianthina* (2.15%).

Ecological barriers alone did not have a strong influence on genetic variation in *M. tyrianthina*. Sequence divergence between ecological barriers that were independent of geological barriers ranged from 0.002-0.324% (Table 5) and always exhibited low Fst values. Furthermore, ecologically similar regions spanned several major physical barriers, such as cluster 3 (Fig. 2), which stretched from northern Peru to Venezuela and sequence divergence across these barriers within cluster 3 ranged from 1.62-3.20% (Table 5).

Dispersal-Vicariance Analysis:

The DIVA analysis of the ND2 (Fig. 10) and species tree (Fig. 11) both revealed a clear southern origin of *Metallura* and clade 1 (*M. aeneocauda* superspecies). The ancestor of clade 1 was likely distributed on both slopes of the Peruvian Andes (Fig. 10), and then diverged in a south-to-north pattern from the southernmost *M. aeneocauda* north to the Ecuadorian group. The origin and spread of the *M. tyrianthina* group is less straightforward. Since the BEAST topology supported a sister relationship between *M. iracunda* and *M. tyrianthina,* clade 2 shows an ancestral origin in the Perijá/ Santa Marta region. However, if *M. iracunda* were excluded the ancestor of *M. tyrianthina* was likely widespread throughout the Andes with clades diverging via vicariance events (Fig. 12). DIVA analysis of the species tree also shows the strongest support for a northern origin of the *M. tyrianthina* clade (Fig. 13). However, if *M. iracunda* were excluded the ancestor of *M. tyrianthina* would appear to have been widespread throughout the Andes before fragmentation by vicariance. Furthermore, all of the probable ancestral distributions include a northern component, but not a southern one (Fig. 13).

DISCUSSION

I found contrasting histories of dispersal through the Andes in the two extant *Metallura* clades. The genus originated ~10 mya ago in the central Andes followed by an initial spread through the Andes and divergence into the two clades. The *M. phoebe* and *M. aeneocauda* superspecies clade (1) shows a clear central Andean origin followed by northward dispersal. The *M. iracunda* and *M. tyrianthina* clade (2), on the other hand, exhibits a northern origin followed by a spread from north-to-south during the Pleistocene. It is unclear exactly when these two clades came into secondary contact, but my results clearly demonstrate allopatric origins of these two parapatrically distributed clades.

Historical Biogeography:

Several studies have highlighted the importance of Andean uplift during the Miocene-Pliocene as a period of diversification within the Andean avifauna (Ribas et al., 2007; Burns & Naoki, 2004; Bates & Zink, 1994). Support for a south-to-north pattern of diversification following uplift is also found in high Andean lizards (Doan, 2003) and the hummingbird *Adelomyia melanogenys* (Chaves et al., 2011). Based on the ND2 gene tree *Metallura* originated in the middle Miocene (~9.9 mya) of the central Andes. This corresponds to a period when the Andes had already achieved at least half of their modern elevation and were beginning a period of accelerated uplift (Gregory-Wodzicki, 2000). The earliest split in *Metallura,* between clades 1 and 2, occurred ~7.9 mya, but whether this divergence occurred as the result of dispersal northward to occupy novel montane habitats cannot be resolved with the present data. An early divide between *M. phoebe* and *M. aeneocauda* of southern Peru occurred about ~7.1 mya. The ancestor of

these species was distributed in both the western and eastern Cordilleras of Peru and the final uplift of the central Andes between 10-6 mya may have split this ancestral population (Garzione et al., 2008). Later spread to the north in clade one post-dates final uplift of the Andes with divergence across the Apurímac valley ~4.9 mya and divergence across the Marañon valley not occurring until the Pleistocene, ~1.5 mya. The species tree supported a central Andean origin during the late Miocene (~6.0 mya) corresponding to the end of uplift in the central Andes (Garzione et al., 2008). The split between clades one and two then occurred ~4.5 mya. *M. aeneocauda* diverged from the rest of the *M. aeneocauda* superspecies about ~2.9 mya and the clade crossed the Marañon valley ~1.6 mya. These later divergence times indicate that mountain uplift had little to do with divergence or spread of the *M. aeneocauda* superspecies northward.

The ND2 gene tree indicated an initial divergence within clade two between *Metallura iracunda* and *M. tyrianthina* ~3.5 mya. *M. iracunda* is currently known only from the isolated Sierra de Perijá and the final uplift of the eastern Cordillera of Colombia 3-5 mya (Hoorn et al., 1995) may have facilitated the subsequent dispersal of *M. tyrianthina* southward. This node, however, received low support and was in conflict with the MrBayes analysis of the ND2 dataset and the concatenated dataset of all four loci. More data and analyses will be required to fully resolve this node and strengthen support for this biogeographical hypothesis. *Metallura tyrianthina* spread and diversified in the Andes almost entwerely within the Pleistocene. Based on the ND2 tree initial divergence occurred between clades A and BC ~2.7 mya and then clades B and C diverged across the Marañon valley ~2.1 mya. Assuming the BEAST topology correctly places *M. iracunda* as sister to *M. tyrianthina* the Bayes-DIVA analysis indicates an

origin of *M. iracunda* in the northern Andes in the Sierra de Perijá and Santa Marta region from where *M. tyrianthina* diverged and spread southward. Bayes-Diva analysis recovered a variety of potential ancestral distributions for the ancestral *M. tyrianthina*. This may be an artifact of the DIVA analysis, which applies a greater cost to dispersal events than vicariance events when optimizing ancestral distributions (Ronquist, 1997), and this analysis may be wrong in its assumption that a widespread distribution was fragmented by vicariance rather than a series of dispersal events. The branching pattern of *M. tyrianthina*, deeper divergences in the north, and a north-to-south sequence of divergence times all support a northern origin of *M. tyrianthina* with subsequent spread to the south. It is difficult to make firm conclusions about the spread and diversification of *M. tyrianthina* based on the species tree. Most nodes were poorly resolved, but the branching pattern does indicate a north-to-south history. Bayes-DIVA analysis showed support for a northern origin of *M. tyrianthina*, but there was also support for a widespread *M. tyrianthina* that then diverged through vicariance. Most studies that examined origins of Andean clades have shown colonizations from Central America (Pérez-Emán, 2005; Weir et al., 2008; Cadena et al., 2007) or a southern origin (Chaves et al., 2011), although the northern Andes have been highlighted as an important center of origin for the diverse *Tangara* tanagers (Burns & Naoki, 2004).

Subsequent diversification within all three clades of *Metallura tyrianthina*, divergence between *M. eupogon* and *M. theresiae*, and diversification within the Ecuadorian and Colombian taxa of the *M. aeneocauda* superspecies all date to the late Pleistocene (<1 mya) for both ND2 and species tree analyses. The last 0.9 myr correspond to an intensification of glaciation in 100 kyr cycles (Ribas et al., 2012).

Pleistocene diversification occurred concurrently with several glacial cycles as evidenced by divergence times betIen currently recognized species occurring as recently as ~0.2 mya betIen *M. baroni* and *M. w. atrogularis* and betIen *M. eupogon* and *M. theresiae* (similar dates for species tree). The impact of glacial cycles on the diversification of Andean taxa has long been discussed (Vuilleumier, 1969; Graves, 1985). In recent years the importance of this period for the generation of contemporary Andean diversity has been confirmed through the applications of molecular clocks to an array of Andean clades, including: *Pionus* parrots (Ribas et al., 2007), *Mucisaxicola* flycatchers (Chesser, 2000); *Cranioleuca* spinetails (Garcia-Moreno et al., 1999b), and *Myioborus* redstarts (Pérez-Emán, 2005). In an analysis of several Andean clades Weir (2006) identified 43% of species diverged within the Pleistocene and 27% diverged during the more intense cycles of the last 1my. Weir (2006) also identified an upturn in the diversification rate of certain lineages during the late Pleistocene further supporting the importance of this time in the formation of extant Andean diversity.

Barriers:

River valleys and intervening tropical lowlands play a major role in structuring genetic diversity in both clades of *Metallura.* The Marañon valley was the most important barrier shared by both *Metallura* clades and there is overlap in the divergence time across the barrier for both clade one (mean: 1.5 mya; 95% HPD: 0.92-2.08 mya) and clade two (mean: 2.1 mya; 95% HPD: 1.38-2.96 mya). Multiple phylogeographic studies have confirmed the importance of the Marañon valley as a major biogeographic barrier (Miller et al., 2007; Weir, 2009; Chaves & Smith, 2011; but see Weir et al., 2008). Otherwise river valleys to the north have isolated populations longer in *M. tyrianthina* compared to

the *M. aeneocauda* superspecies, which instead exhibits greater divergence across southern barriers (Table 5). High Andean ridges appear to play less of a role compared to other species of hummingbird in the Andes (Chaves et al., 2007; Chaves & Smith, 2011), although *M. phoebe* and the *M. aeneocauda* superspecies potentially diverged with the final uplift of the central Andes. More recent divergences in Ecuador (*M. baroni* and *M. williami*) may have occurred across ridges and recent diversification within *M. tyrianthina* across the Cordillera Vilcanota and central Andes in Peru appears to be due to isolation by high montane dispersal barriers.

The genus *Metallura* spans several ecotones between dry west-facing slopes and humid east-facing slopes and across precipitation and seasonality gradients found in the Andes. I did not find a singular role for environmental heterogeneity in promoting diversification within *Metallura*. In all cases where genetic divergence in *Metallura* was found between populations in distinct environments, a potential physical barrier to gene flow was also present conversely, in the absence of barriers there was little divergence indicating ongoing gene flow. Finally, major genetic structure between similar environments was found across physical barriers. My results are similar to a pair of Ecuadorian studies comparing patterns of morphological and genetic variation across environmental gradients (Chaves et al., 2007; Milá et al., 2009).

Substitution rates:

My novel calibrations used to assess divergence timing and substitution rates within coquette hummingbirds revealed a mean molecular substitution rate for the ND2 locus of 0.009 s/s/l/my (95%HPD: 0.007-0.015 s/s/l/my). This substitution rate corresponds to a 1.8% rate of divergence and is close to the 2% rate often reported for the

avian mitochondrial gene Cyt *b* (Lovette, 2004; Weir & Schluter, 2008). The mean is identical to the mean substitution rate derived from the single hummingbird (*Lampornis*) in the Weir and Schluter dataset (2008), which was based on a geological calibration (0.0086 s/s/l/my). ND2 typically evolves faster than Cyt *b*, with estimates for avian ND2 ranging from 2.5-12.3% divergence per million years (Arbogast et al., 2006; Johnson & Weckstein, 2011; Fuchs et al., 2011; Lerner et al., 2011; Patel et al., 2011), however some authors have found similar rates for ND2 and Cyt *b* in tyrant flycatchers (Rheindt et al., 2009) and *Adelomyia* hummingbirds (Chaves et al., 2011).

Substitution rates for nuclear genes were much slower ranging from 0.12-0.25%/my. These nuclear substitution rates are similar to another study examining divergence times in the Hawaiian honeycreepers (Drepaninae) using island formation as a calibration. My studies use in common two nuclear genes, AK1 and Bfib7. For the Hawaiian honeycreepers a substitution rate of 0.16%/ myr was found compared to my 0.12%/ myr and a rate of 0.38%/ myr for Bfib7 compared to my 0.25%/ myr (Lerner et al., 2011).

There were significant differences between the divergence times based on ND2 and those based on the multi-locus species-tree. Estimated divergence times based on the ND2 dataset tended to be much older (Table 3). The ND2 dataset indicated an origin of the coquette clade during the Oligocene (~26.5 mya), an origin of *Metallura* during the middle Miocene (~9.9 mya), and the initial divergences between the two *Metallura* clades during the late Miocene (~7.9 mya). On the other hand, dates estimated based on species-tree analysis pointed to a much more recent origin of the coquette clade during

the middle Miocene (~16.1 mya), origin of *Metallura* in the late Miocene (~6.0 mya), and the split betIen the two clades ~4.5 mya.

These results are consistent with recent studies of North American passerines that also showed significantly older estimates of divergence times based on mitochondrial datasets compared to species tree estimates (McCormack et al., 2010; Walstrom et al., 2011). Species tree analysis more likely reflects the true history of population divergence. Estimates of divergence times based on single gene trees are dependent on ancestral population sizes of that locus. In cases where a single locus exhibits large ancestral population size estimates of divergence times can significantly pre-date the actual population divergence times (Edwards & Beerli, 2000; Arbogast et al., 2002). Multi-locus analyses based on coalescent theory account for this issue by incorporating multiple loci, which contain independent estimates of population parameters and species divergence time, thus reducing variance around the joint estimates (Edwards, 2009; Heled & Drummond, 2010). The magnitude of the discordance between divergent times in mitochondrial versus multi-locus trees could have profound implications for biogeographic inference. For example, this pattern is of serious concern for reconstructing the historical biogeography of Neotropical birds, a group for which most previous divergence time estimates have been based on mitochondrial datasets alone (e.g., Sedano & Burns; 2010, Chaves et al.; 2011, Weir & Price; 2011).

Taxonomic implications:

My phylogenetic analyses of the *Metallura* genus corroborated a sister relationship between *Metallura* and *Chalcostigma* and the two previously supported clades within *Metallura* (Garcia-Moreno et al., 1999a). I found high support for a sister

relationship between *M. phoebe* and the *M. aeneocauda* superspecies in the ND2 dataset, but only moderate support for this relationship in the BI analysis of the four-locus concatenated analysis. ML analysis of the four-locus concatenated dataset placed *M. phoebe* basal to the *M. tyrianthina* clade as did species-tree reconstruction in *BEAST, however both of these were with low support. Finally, the concatenated nuclear dataset placed *M. phoebe* basal to the entire genus with weak support, which is consistent with the topology of Kirchman et al. (2010). My analyses add to the confusion regarding the position of this taxon with respect to other *Metallura* (Garcia-Moreno et al., 1999a; Kirchman et al., 2010). This species diverged soon after the origin of the genus and the presence of a short internal branch at this node has likely led to issues with discordant gene topologies. The exact position of the previously unsequenced *M. iracunda* also remains poorly resolved. Most BI and ML analyses place this species within Clade A of *M. tyrianthina*, however, its precise relationship with other species in this clade was always poorly supported and there was frequent topological discordance among the different analyses. The BEAST analysis of ND2 placed *M. iracunda* sister to all of *M. tyrianthina*, but again this was poorly supported.

The data presented here reveal several inconsistencies with current taxonomy and the species limits in the genus are in need of re-evaluation. The species status of members within the *M. aeneocauda* superspecies has been questioned previously (Zimmer, 1952) and their allopatric distribution makes species status extremely difficult to evaluate (Graves, 1980). My analyses show little sequence divergence (<1%) between *M. eupogon* and *M. theresiae* and between *M. williami* and *M. baroni*. Phenotypically these taxa are distinct and *M. williami* has been reported to occur sympatrically with *M. baroni* and *M.*

odomae (Fjeldsa & Krabbe, 1990; Ridgely & Greenfield, 2001; Tinoco et al., 2009). There is no evidence of hybridization among these overlapping species, but further exploration of these possible contact zones is clearly needed. The mitochondrial phylogeney of Garcia-Moreno et al. (1999a) revealed a polyphyly of two sampled subspecies of *M. williami*. The ND2 dataset here showed *M. williami* to be paraphyletic due to the placement of *M. baroni* within *M. williami*. Analyses of the four-locus concatenated dataset placed *M. w. williami* in a position basal to *M. odomae, M. baroni,* and other *M. williami,* but this was poorly supported. Based on my results I cannot confirm polyphyly in this species, nor can I effectively test the potential existence of multiple species within *M. williami*.

I found *M. iracunda* of the Sierra de Perijá to be embedded within clade A of *M. tyrianthina* for most analyses (but see above). This clade included the subspecies: *M. t. chloropogon, M. t. oreopola, M. t. tyrianthina,* and *M. t. districta,* which occurs syntopically with *M. iracunda.* These syntopic populations are 3.8% divergent mitochondrially suggesting effective reproductive isolation. The precise phylogenetic relationships of *M. iracunda* to the other subspecies in *M. tyrianthina* were never well resolved and will likely require more loci. The placement of *M. iracunda* within *M. tyrianthina* and genetic divergence among all subspecies strongly suggests that *M. tyrianthina* may comprise multiple biological species, however, like the *M. aeneocauda* superspecies, many of these subspecies are allopatrically distributed and it will be difficult to assign species status. In the future, rigorous analysis of morphological and vocal characteristics among all populations of *M. tyrianthina* with comparisons to characteristics of sympatrically occurring species may provide the basis to assign species

status to certain populations of *M. tyrianthina* (Tobias et al., 2010; Cadena & Cuervo, 2010).

Finally, *Metallura* are one of many Andean genera that exhibit a pattern of altitudinal replacement (Terborgh, 1971; Garcia-Moreno et al., 1999a; Cadena, 2007). Altitudinal replacement is commonly thought to be the result of competitive displacement when two taxa come into secondary contact (Diamond, 1973; Terborgh & Weske, 1975). Although I did not explicitly test the potential causes of altitudinal replacement between *Metallura tyrianthina* (lower) and the *Metallura aeneocauda* superspecies (higher) my results indicate that these two taxa originated at opposite ends of the Andes and potentially displaced one another upon secondary contact. The *M. aeneocauda* superspecies overall has larger body size than *M. tyrianthnina* and this varies clinally from the southern, larger *M. aeneocauda* to the diminutive Ecuadorian species (Heindl & Schuchmann, 1998). Whether these differences in body size are the result of climatic differences between the southern and northern Andes (Fig. 2) and allow the *M. aeneocauda* superspecies to dominate *M. tyrianthina* at higher elevations remains to be tested. Phylogenies of other Andean genera also point to a southern origin for higher elevation taxa. *Myioborus* redstarts (Pérez-Emán, 2005) and *Coeligena* hummingbirds (Parra et al., 2009) both show the southernmost species in a basal position to northern species in the high elevation group, whereas a northern species is basal to lower elevation taxa. Similar to *Metallura* the higher elevation species in both of these genera also have larger body mass compared to the lower (Dunning, 1993), but again future work is needed to test the generality of this pattern.

CHAPTER ONE

FIGURES

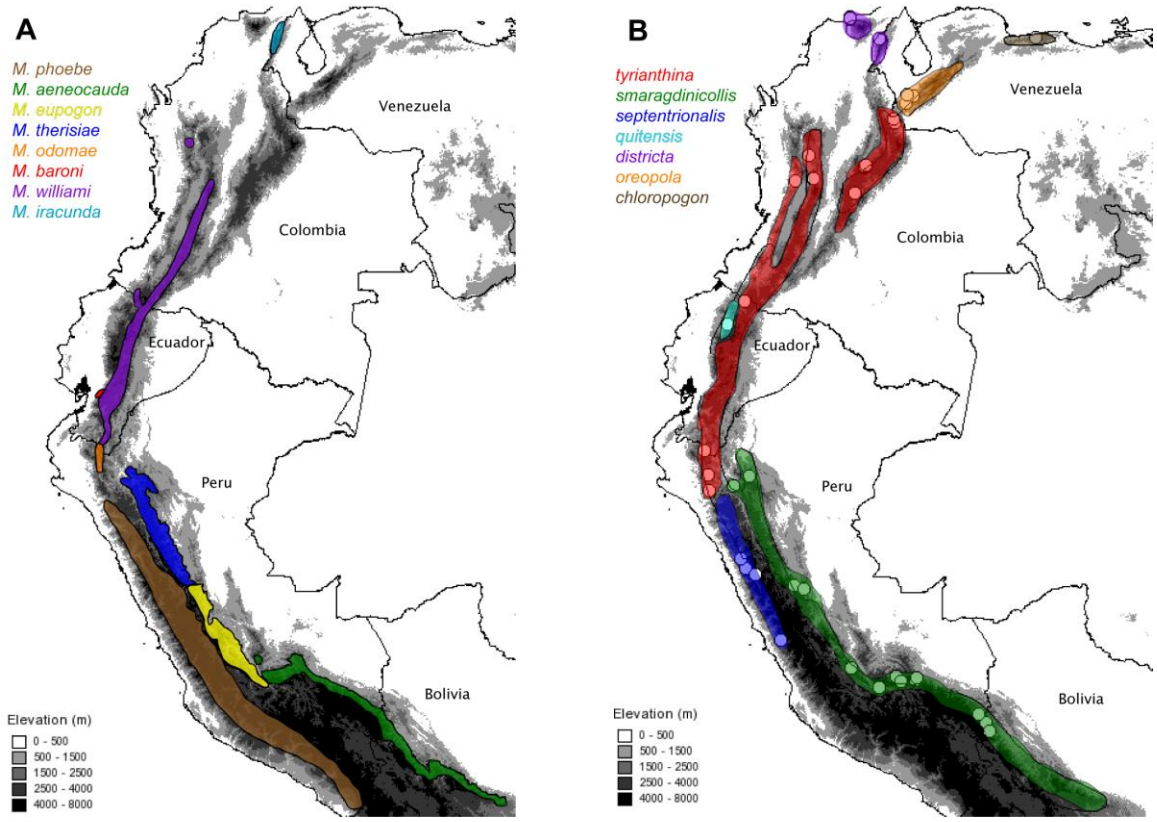

Figure 1: Distribution maps for all Metallura species. (A) Geographic distribution of the *Metallura aeneocauda* superspecies and *M. iracunda*. (B) Geographic distributions of each described subspecies of *M. tyrianthina*. Circles represent localities of all *M. tyrianthina* tissue samples.

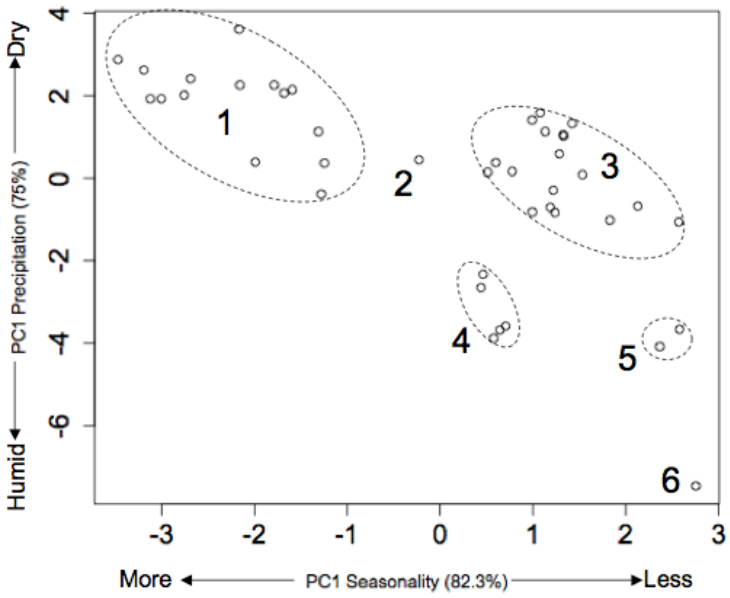

Figure 2: PC1 of seasonality and precipitation data. Numbered clusters are mapped onto Fig. 3. (1) Most Peruvian and Bolivian localities, this cluster was further sub-divided to separate typically drier and more seasonal scrub in the western Andes (1a) and inter-Andean valleys (1b) from humid and aseasonal montane forest of the eastern Andes (1c); (2) Incahuasi, department of Lambayeque, Peru; (3) this cluster stretches from northern Peru just south of the North Peru low through Ecuador to the Eastern Cordillera of Colombia and Venezuela; (4) Sierra de Santa Marta and Perijá; (5) Central Cordillera of Colombia; and (6) Western Cordillera of Colombia.

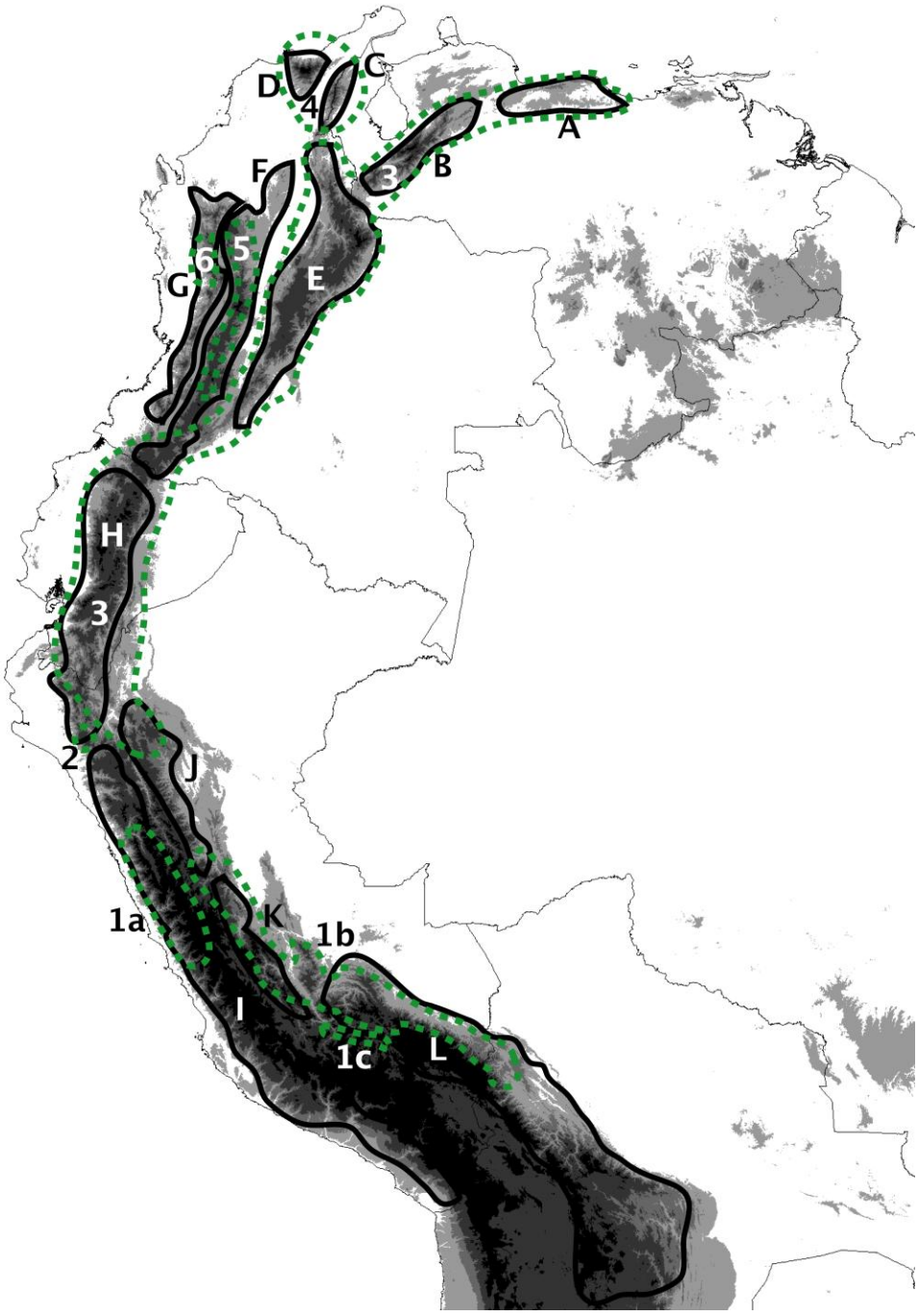

Figure 3: Map of the Tropical Andes showing relevant centers of endemism for *Metallura* species outlined in black and lettered (Cracraft 1985, Stattersfield et al. 1998, Weir 2009). Climatically similar regions (Fig. 3) are outlined in a dashed green line.

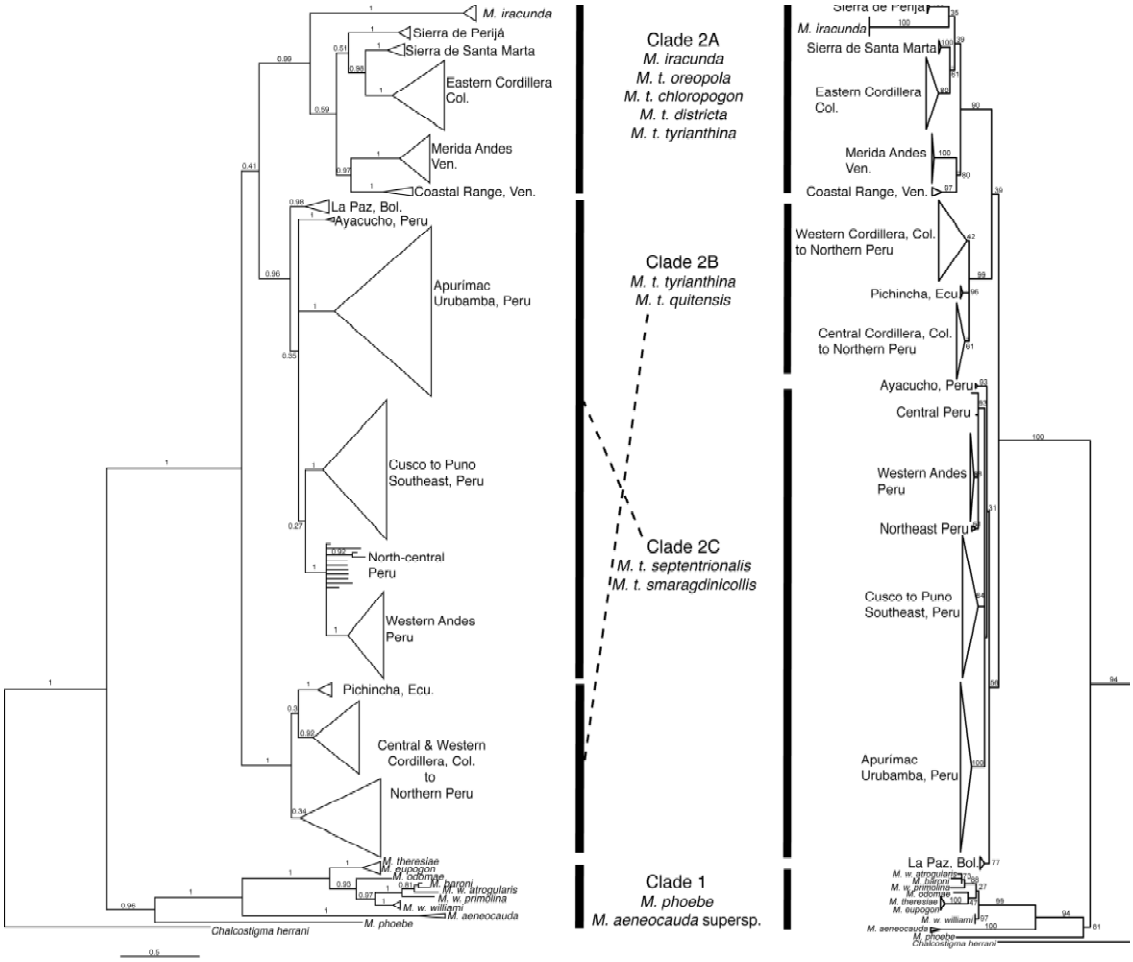

Figure 4: (A) Bayesian phylogeny and (B) Maximum Likelihood phylogeny of the entire ND2 dataset. Each triangle represents a supported clade and the geographic distribution of each of these clades is labeled. Posterior probability and bootstrap values for each node are printed above branches. Dotted lines highlight discordances in topology between the Bayesian and Likelihood trees

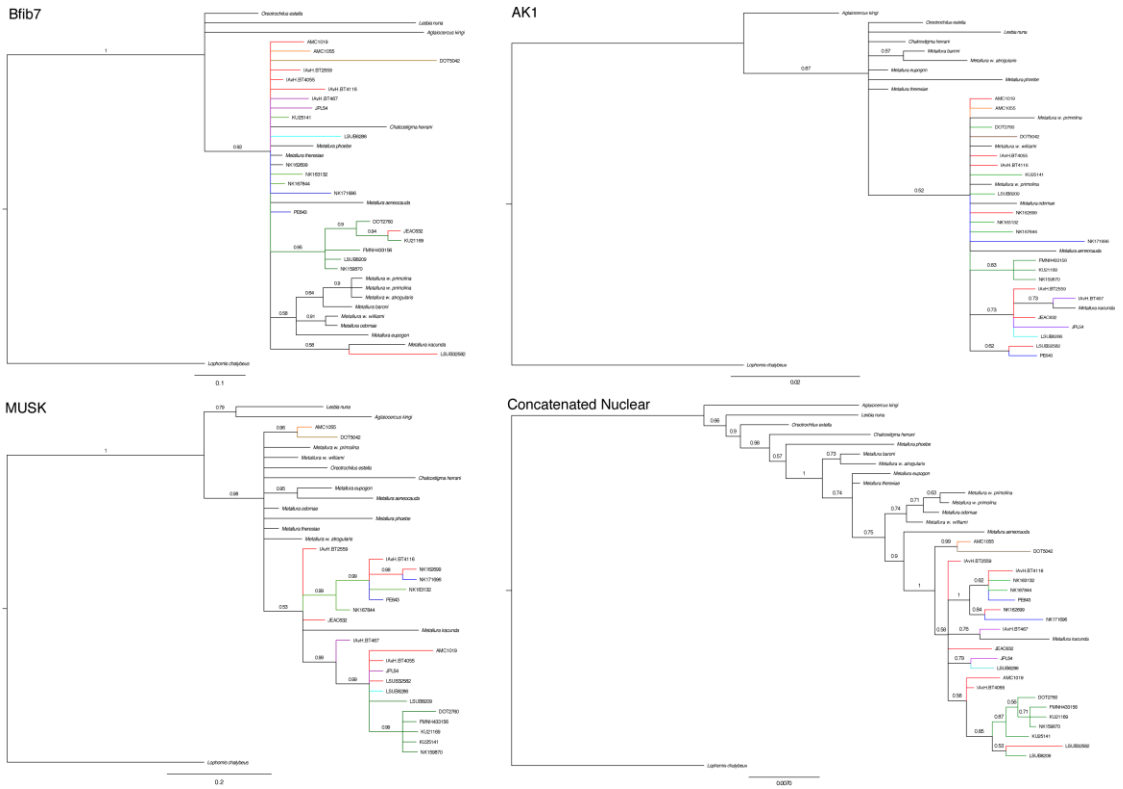

Figure 5: Bayesian trees of each individual nuclear gene and the concatenated nuclear dataset. Colors correspond to different subspecies of *M. tyrinanthina:* (red) *tyrianthina*; (orange) *oreopola*; (brown) *chloropogon*; (violet) *districta*; (blue) *septentrionalis*; (green) *smaragdinicollis;* and (teal) *quitensis*.

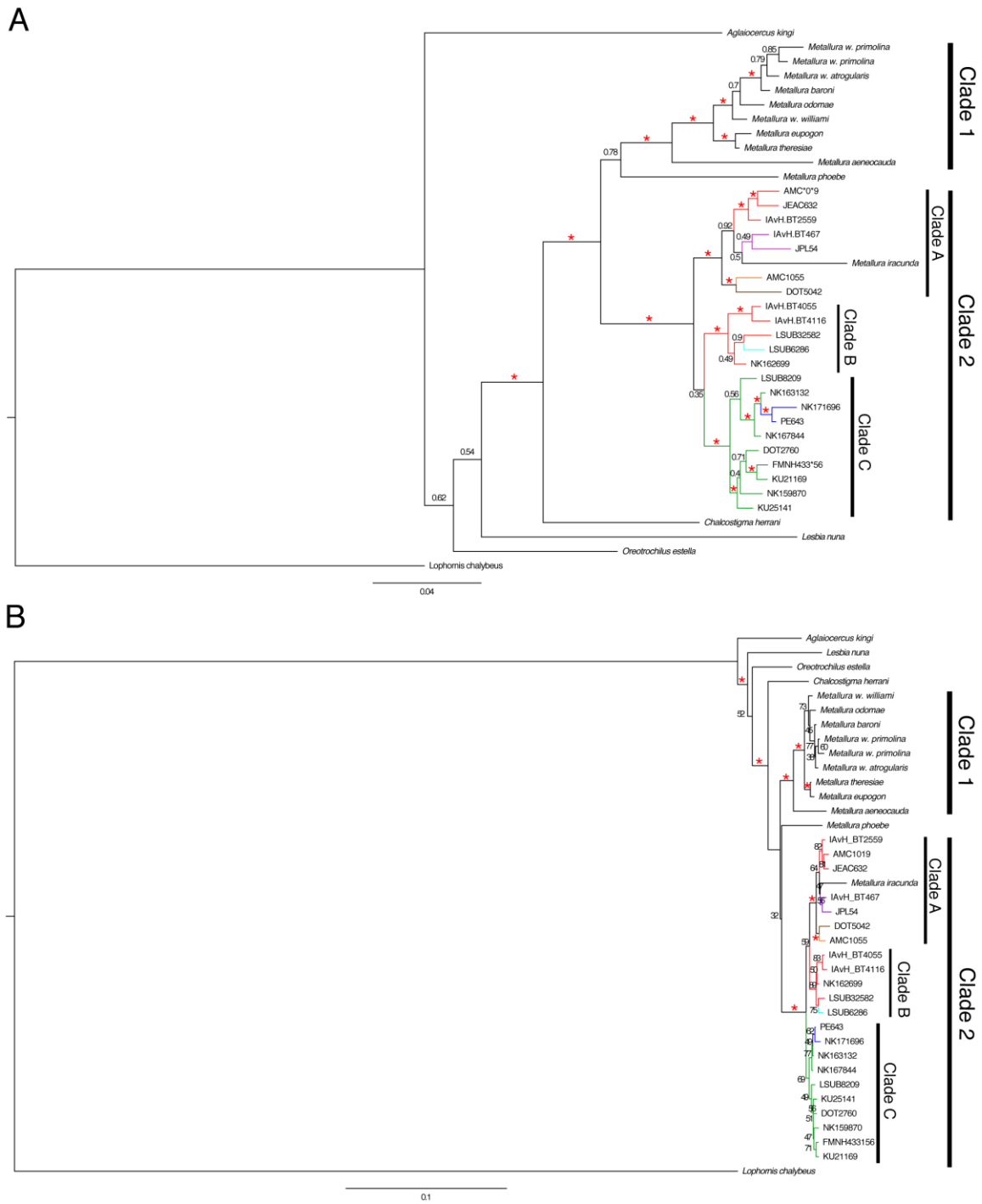

Figure 6: Bayesian (A) and Maximum Likelihood (B) trees of the concatenated dataset. Red asterices indicate >0.95 posterior probability or >90 bootstrap support for nodes. Topologies are largely identical (not branch lengths) with the exception of *M. phoebe*. Colored branches signify subspecies of *M. tyrianthina* (see fig. 1): *tyrianthina* (red); *septentrionalis* (blue); *smaragdinicollis* (green); *quitensis* (teal); *districta* (violet); *oreopola* (orange); and *chloropogon* (brown).

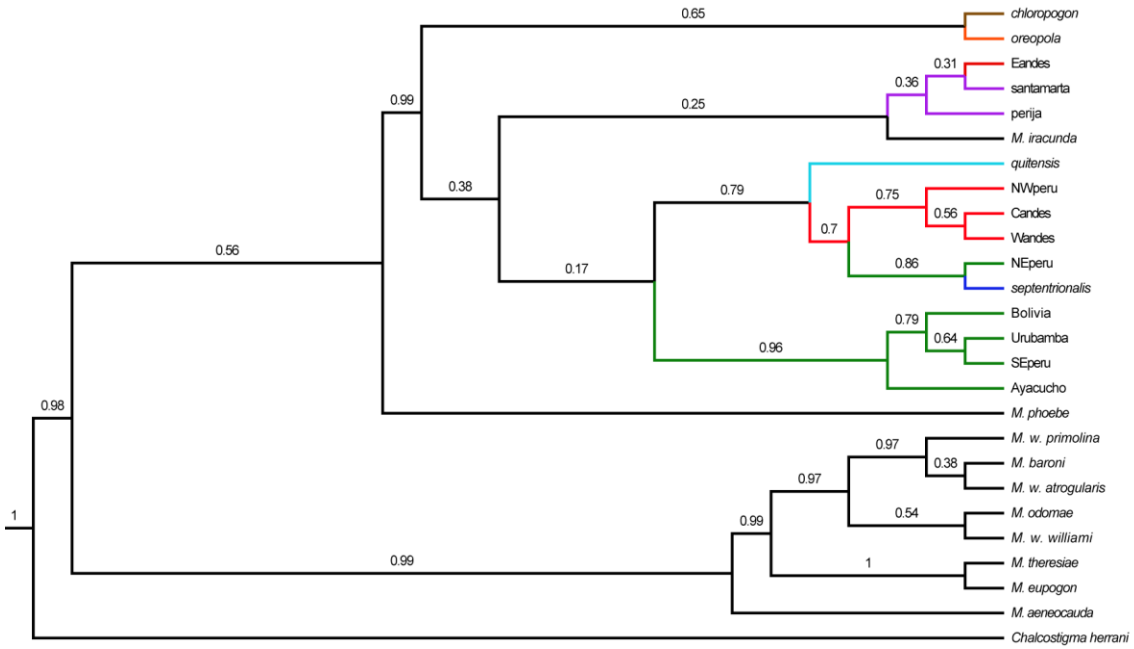

Figure 7: Species tree from *BEAST. Posterior probability support values printed above branch. Colored branches signify subspecies within *M. tyrianthina*: (brown) *M. t. chloropogon;* (orange) *M. t. oreopola*; (violet) *M. t. districta*; (red) *M. t. tyrianthina*; (teal) *M. t. quitensis*; (green) *M. t. smaragdinicollis*; (blue) *M. t. septentrionalis*.

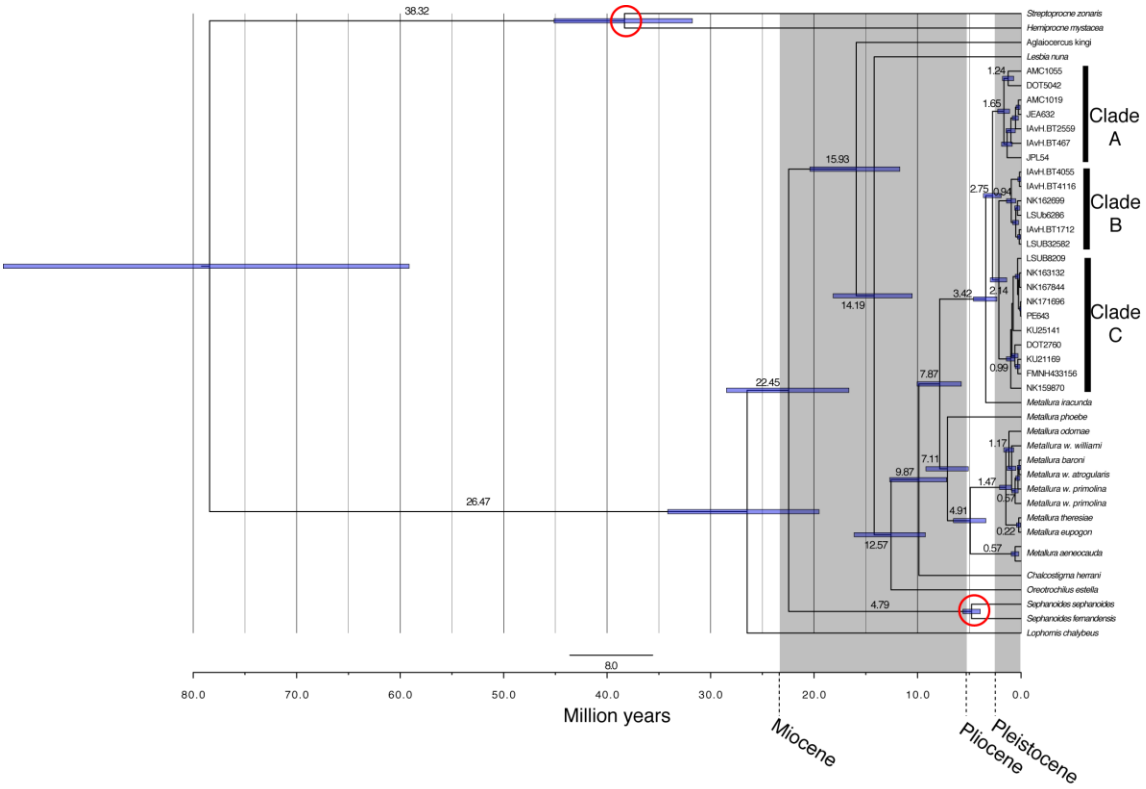

Figure 8: Divergence times plotted on ND2 BEAST phylogeny. Mean divergence times for each node printed on branches. Node bars represent the 95% HPD distribution around each mean divergence time. Red circles around nodes indicate the two calibration points used to infer divergence times and substitution rates across the phylogeny.

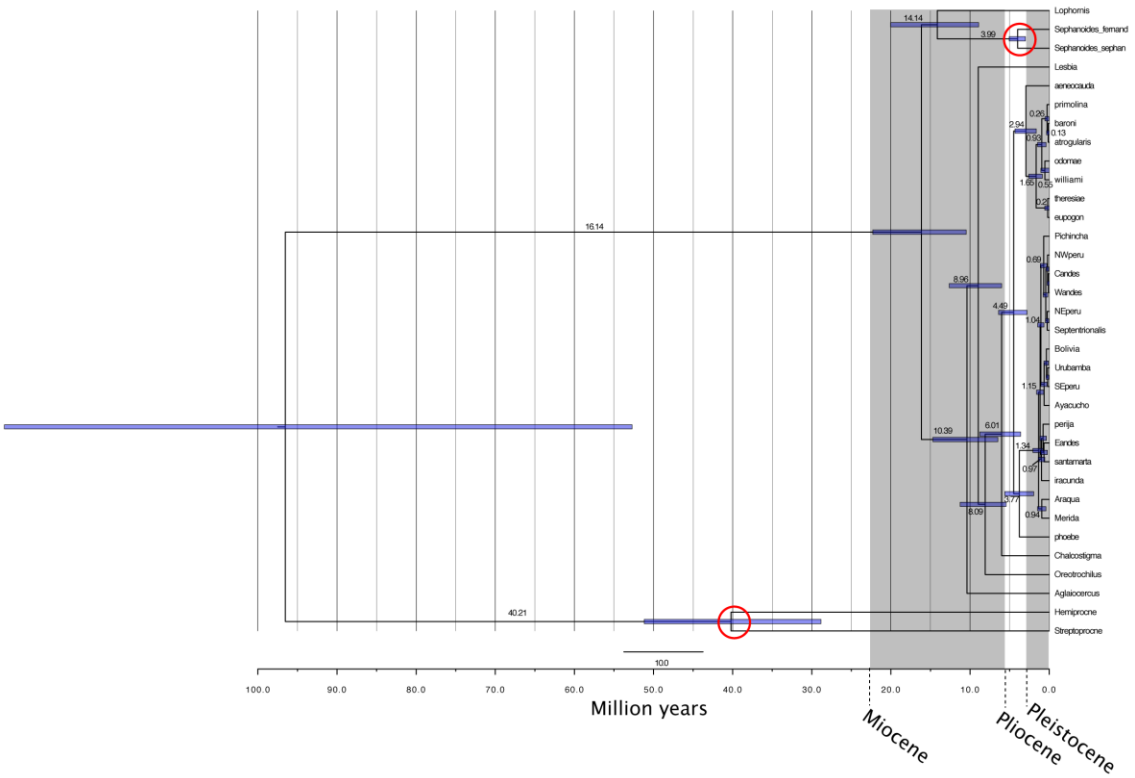

Figure 9: Species tree from *BEAST with 95% HPD of divergence times plotted on each node (violet bars). The mean divergence time for each node is printed above the branches. Red circles surround the nodes used for calibrating divergence times on the phylogeny.

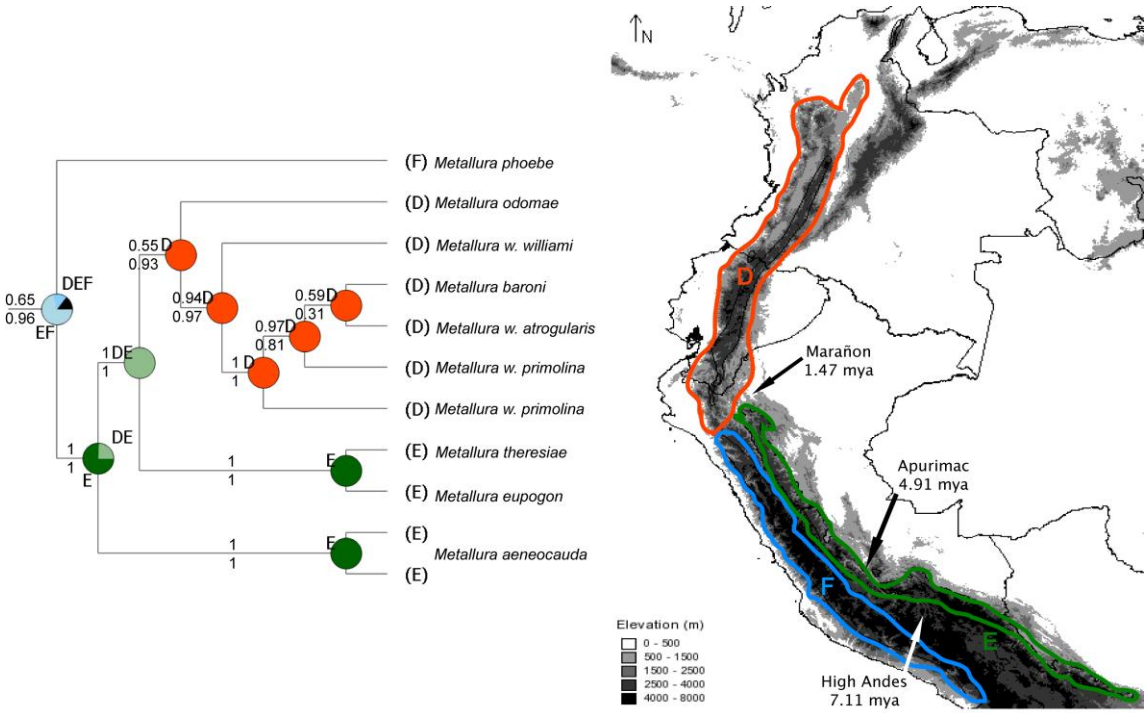

Figure 10: DIVA analysis of the ND2 topology for clade one. Letters at tips correspond to the current distribution of each taxon and the distributions at each nodes: (A) Venezuela Andes; (B) Sierras de Perijá and Santa Marta; (C) East Colombian Andes (D) North Andean; (E) East Peruvian; (F) West Peruvian. At each node the probability of each distribution is proportional. Numbers above branches indicate posterior probability from BEAST analysis and below branches posterior probability of MrBayes analysis. Arrows on map show estimated mean divergence times across barriers.

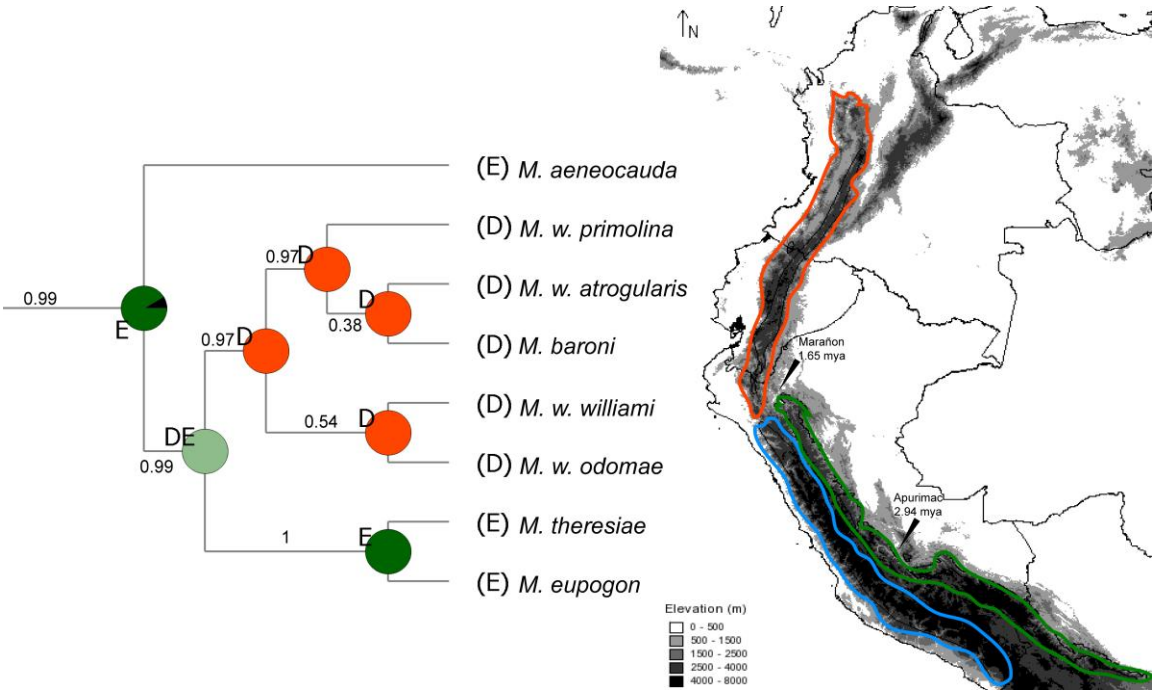

Figure 11: DIVA analysis of the *BEAST topology for clade one. Support values of the species tree printed to branches. Regions specified by letters: (D) Northern Andes from central and Istern Colombia to Northern Peru; (E) Eastern Andes of Peru and Bolivia; (F) Western Andes of Peru. Letters at tips are the extant range of each species. Pie charts at nodes exhibit the proportion of topologies that support a certain ancestral distribution (lettered). Divergence times across the Apurímac and Marañon valley are plotted on the map.

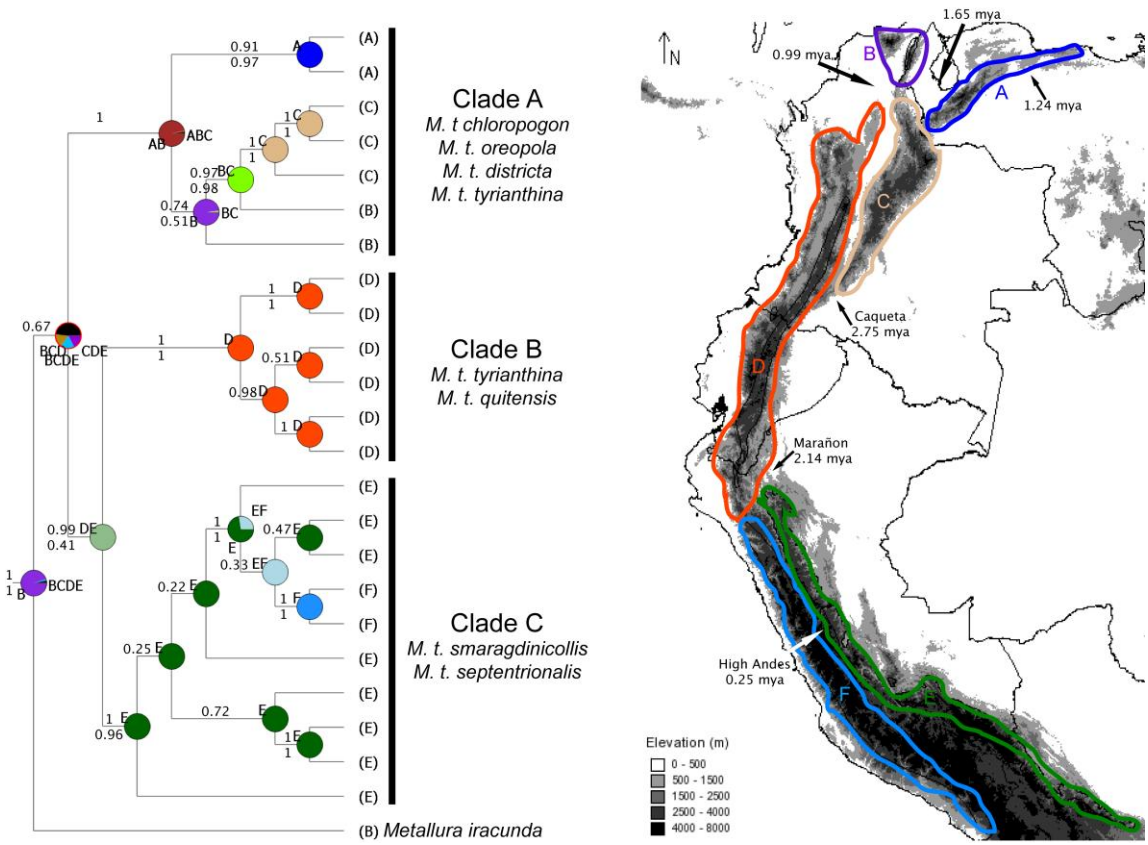

Figure 12: DIVA analysis of the ND2 topology of clade two. Letters at tips correspond to the current distribution of each taxon and the distributions at each nodes: (A) Venezuela Andes; (B) Sierras de Perijá and Santa Marta; (C) East Colombian Andes (D) North Andean; (E) East Peruvian; (F) West Peruvian; (G) lowland; (H) extralimital. At each node the probability of each distribution is proportional. Numbers above branches indicate posterior probability from BEAST analysis and below branches posterior probability of MrBayes analysis. Branches without posterior probability values below branch indicate conflicting nodes betIen BEAST and MrBayes analyses. Arrows on map show estimated mean divergence times across barriers.

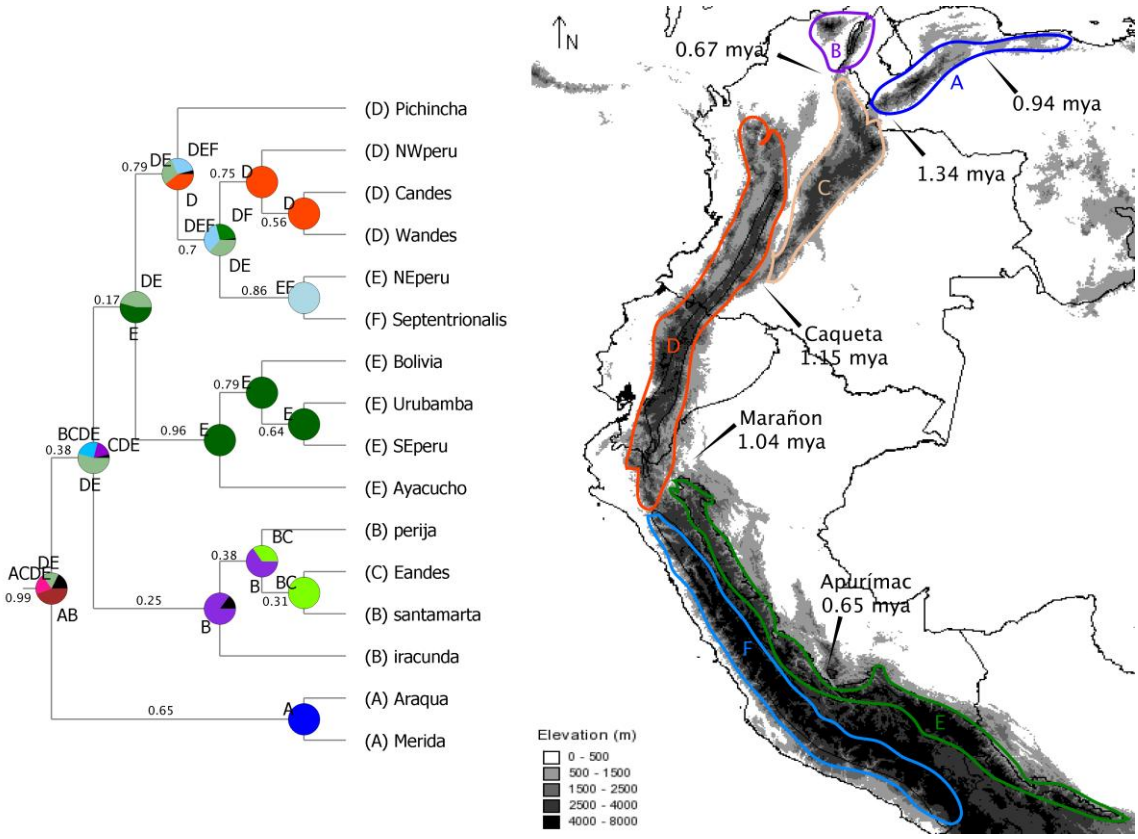

Figure 13: *M. tyrianthina* bayes-DIVA analysis using the species tree from *BEAST. Regions used for ancestral distribution reconstruction are plotted onto the map of the Andes. Support values of the species tree printed to branches. Regions specified by letters are (A) Venezuelan montane regions; (B) Sierras de Santa Marta and Perijá; (C) Eastern Cordillera of the Colombian Andes; (D) Northern Andes from central and Western Colombia to Northern Peru; (E) Eastern Andes of Peru and Bolivia; (F) Western Andes of Peru. Letters at tips are the extant range of each population. Pie charts at nodes exhibit the proportion of topologies that support a certain ancestral distribution (lettered). Divergence times across major barriers plotted on map.

CHAPTER ONE

TABLES

Table 1: Primers used or designed for this study.

Locus	Primer	Sequence (5' to 3')	Reference
ND2	L5219	CCCATACCCCGAAAATGATG	Sorensen et al. 1999
ND2	H6313	CTCTTATTTAAGGCTTTGAAGGC	Sorensen et al. 1999
ND2	LND2MTYR	CCCAAAATTAACACTAATGACCTTTT	This study
MUSK	MUSK F3	GCTGTACTTCCATGCACTACAATG	This study
MUSK	MUSK R3	ATCCTCAAATTTCCCGAATCAAG	This study
Bfib7	Bfib7LM	ATCTTCTTTGGAGCACTGTTTTCTT	This study
Bfib7	Bfib7RM	TGTACTTCAGTACCTATGACAGAGACAA	This study
Bfib7	LBfib7-477	TTAAACAGGACATGCTATATGTCTCC	This study
AK1	AK1LM	AACAGGGAGAGGAGTTTGAGAAG	This study
AK1	AK1RM	GTTTGACCATCGTCTCCTTCC	This study

Table 2: Andean centers of endemism and physical barriers that define each center (Cracraft 1985, Stattersfield et al. 1998, Weir 2009). TL signifies tropical lowlands. Letters A-L correspond to map of Andean centers of endemism (Fig. 3).

		Physical Boundaries			
	Area of Endemism	North	South	East	West
A	Venezuelan Montane	TL	TL	TL	TL
B	Meridan Montane	TL	Tachira	TL	TL
C	Perijan Montane	TL	Rio de Oro	TL	TL
D	Santa Marta Montane	TL	TL	TL	TL
E	East Colombian	Rio de Oro	Caqueta	Tachira	Magdalena
F	Central Colombian	TL	Mira	Magdalena	Cauca
G	West Colombian	TL	Patia	Cauca	TL
H	Ecuadorian	Mira	Marañon	TL	TL
I	West Peruvian	Marañon	Chile	High Andes	TL
J	North Peruvian	Marañon	Huallaga	TL	High Andes
K	Central Peruvian	Huallaga	Apurimac	TL	High Andes
L	South Peruvian	Apurimac	Cochabamba	TL	High Andes

Table 3: Divergence times (in millions of years ago (mya)) at particular nodes for the ND2 dataset and Species tree dataset. Dashes indicate conflicting nodes between the ND2 gene tree and species tree.

Divergence	ND2 dataset	Species Tree
Swift-Treeswift	38.3	40.2
Coquette clade	26.5	16.1
Sephanoides	4.8	4.0
Chalcostigma-Metallura	9.9	6.0
Clade 1-Clade 2	7.9	4.5
M. phoebe- M. aeneocauda	7.1	-
M. aeneocauda-M. eupogon/theresiae	4.9	2.9
M. eupogon/theresiae-Ecuador	1.5	1.6
M. iracunda- M. tyrianthina	3.4	-
Clade 2A-Clades 2BC	2.7	-
Clade 2B-Clade 2C	2.1	-

Table 4: Corrected pairwise differences (%) across major Andean barriers for (A) *M. tyrianthina* (based on 832bp) and (B) *Metallura aeneocauda* superspecies (based on 917bp). Fst-values are for *M. tyrianthina* only. * indicates p-values: ***=0, **= <0.01, *= <0.05, ns= >0.05.

Barrier	A % sequence divergence	Fst	B % sequence divergence
North Venezuela lowlands	1.62	0.936 **	-
Tachira depression	2.63	0.912 ***	-
Rio de Oro	2.10	0.869 ***	-
Santa Marta	1.85	0.969 ns	-
Magdalena valley	3.40	0.887 ***	-
Caqueta Valley	3.20	0.887 ***	-
Cauca Valley	0.92	0.567 ns	-
Patia Valley	1.18	0.723 ***	-
Mira Valley	0.06	0.160 *	0.44
Marañon Valley	2.15	0.848 ***	1.49
Huallaga Valley	0.08	0.186 *	0.16
Apurimac Valley	0.39	0.341 ***	5.42
High Andes Peru	0.32	0.692 ***	7.96

Table 5: Corrected pairwise differences (%) and Fst-values across major ecological barriers (see Fig. 2) for *M. tyrianthina* (based on 832bp of ND2). * indicates p-values: ***=0, **= <0.01, *= <0.05, ns= >0.05.

Cluster comparison	% sequence divergence	Fst (p-value)	Physical barrier present
3 & 4	1.30	0.808***	Rio de Oro
3 & 2	0.11	0.237 ***	No
2 & 1a	2.55	0.962***	Maranon valley
3 & 5	0.06	0.160*	Mira valley
3 & 6	1.15	0.723***	Patia valley
3 & 1a	2.31	0.896***	Marañon valley
3 & 1b	0.11	0.324 ns	No
1a & 1b	0.23	0.766***	High Andes
1b & 1c	1.08	0.861***	Cordillera Vilcanota
1b & Paucartambo	0.002	-0.03ns	No
5 & 6	0.89	0.567*	Cauca Valley

Chapter 2:

Topographic complexity promotes genetic and morphological diversity in the Andean Hummingbird *Metallura tyrianthina*.

INTRODUCTION

The high ridges and deep river valleys of the Andes cause physical barriers to dispersal and extensive environmental heterogeneity, both of which promote diversification (Price, 2008). Allopatric isolation interrupts gene flow between populations, allowing for the stochastic accumulation of genetic and phenotypic differences that can culminate in reproductive incompatibility (Mayr, 1942; Price, 2008). Environmental heterogeneity can cause divergent selective pressures leading to divergence of functional characteristics and evolution of the species ecological niche (Coyne & Orr, 2004). Both isolation and ecological selection are thought to be required for related species to achieve stable coexistence, the final stage of the diversification process. However, the relative importance of these two forces in driving primary divergence and setting overall diversification rates are major questions in evolutionary biology (Price, 2008; Weir & Price, 2011). The Andean landscape provides a natural laboratory for testing these mechanisms by jointly analyzing spatial patterns of gene flow, neutral genetic divergence, and functional divergence.

Deep river valleys divide the main chain of the Andes at several localities from Venezuela to Bolivia. Additionally, the high Andean ridge effectively prevents dispersal between populations distributed on eastern and western slopes of the Andes. These barriers are frequently linked to range boundaries between sister species or mitochondrial phylogeographic breaks between conspecific populations (Parker et al., 1985; Weir,

2009; Chaves et al., 2011). Although these barriers currently limit gene flow and range expansion, it is doubtful that stochastic divergence in allopatry can fully account for inter-population divergence, especially considering that little evidence exists for speciation through genetic drift alone (Moya et al., 1995; Rundle et al., 1998; Price, 2008; Coyne & Orr, 2004). An expectation of genetic drift would be general concordance between neutral genetic variation and phenotypic variation (Cadena et al., 2011); however, discordant patterns between phenotypic diversity and genetic diversity are commonly encountered in birds including Andean taxa (Greenberg et al., 1998; Humphries & Winker, 2010; Cadena et al., 2007; Iir et al., 2008). Thus, spatial patterns of functional and neutral variation need to be considered in light of both environmental heterogeneity and dispersal barriers to understand diversification.

Patterns of spatial variation within widespread polytypic species are critical empirical evidence regarding causes of diversification. The high Andean Hummingbird, *Metallura tyrianthina*, comprises seven subspecies that span numerous physical barriers and ecotones betIen Venezuela and Bolivia (Schuchmann, 1999). Within Peru alone, three of these subspecies occur: *M. t. tyrianthina* is found north and west of the Marañon valley in humid montane forests and edge; *M. t. sepetentrionalis* ranges south to Lima along the drier Western Cordillera of Peru occupying semi-arid montane scrub; and *M. t. smaragdinicollis* occurs throughout the eastern Andes of Peru existing in both humid montane forests along east-facing slopes and semi-arid montane scrub in rain-shadow valleys and west-facing slopes (Fig. 1) (Schulenberg et al., 2007).

The ecological and geographic distribution of these three subspecies allows for morphological and genetic comparisons among: **a)** distinct subspecies allopatrically

distributed in similar environments; **b)** distinct subspecies allopatrically distributed in different environments; and **c)** a single subspecies that occurs parapatrically in distinct environments. I use these comparisons to address the following questions: **1)** Are patterns of genetic and morphological variation concordant? **2)** To what extent do physical versus ecological barriers structure genetic variation? And **3)** what roles do environmental variation and physical barriers play in shaping morphological diversity?

METHODS

Morphological analyses:

Sampling:

I measured bill length (exposed culmen), width, and depth (at base of bill); wing length; and the outer (r5) and inner (r1) rectrix for 245 museum specimens to the nearest 0.01mm using digital calipers (Appendix B). All measurements were measured after they had been dried to avoid issues with shrinkage (Winker, 1993). Specimens were only included if they had full data on locality and mass. To assess environmental differences among specimen localities I obtained bioclimatic data at 30-second resolution from worldclim.org. The climatic variables include measures of temperature, precipitation and seasonality (Table 1). These data are derived from interpolated climate surfaces available for the entire globe at 30-arc second spatial resolution and were gathered from several independent sources between 1950-2000 (Hijmans et al., 2005). Principal component analysis was used to obtain a single axis of temperature, precipitation, and seasonality that were used for subsequent analyses (for loadings see Table 2).

For all morphological analyses specimen localities were clustered into six regions isolated by either physical barriers (e.g. the Marañon Valley) or environmental differences. These regions include: (A) northwest Peru, north of the Marañon valley; (B) eastern Andes south of the Marañon valley and north of the Huallaga valley; (C) the central Andes bounded by the Huallaga and Apurímac valleys; (D) the humid southern Andes south of the Apurímac valley; (E) the drier southern Andes on west-facing slopes; and (F) the western Andes (Fig. 1).

Statistical Analyses:

All statistical analyses were conducted using the open source program R (http://www.r-project.org/). Preliminary analyses indicated that bill length was the only character that varied among more than a single locality. A simple linear regression of bill length versus body mass indicated a weak, but significant relationship ($p<0.05$) and for all statistical analyses I corrected bill length for body mass using the formula: $\ln((\sqrt[3]{}\text{mass})*\text{Bill length})$. Sexual dimorphism in bill length and shape is widely encountered within Trochilidae (Bleiweiss, 1999; Temeles et al., 2010). I used a two-tailed t-test (Zar, 2010) to determine whether bill length varied between the sexes for the entire dataset and within each region. Differences were detected for neither bill length nor mass corrected bill length and for all subsequent analyses males and females were analyzed together. I assessed variation in bill length among the six localities using a one-way analysis of variance (ANOVA). A pairwise-t-test was then conducted to assess which of the six regions differed from the others using a holm correction for multiple comparisons (Dalgaard, 2008).

I tested the influence of different climatic variables on bill length polymorphism using an information-theoretic approach. I performed regression analyses with bill length as the dependent variable and PC1 of temperature, precipitation, and seasonality used as explanatory variables. The likelihood of each of the fifteen possible combinations among the explanatory variables was evaluated using an Akaike Information Criterion corrected for sample size (AICc). Each model was ranked using ΔAICc and Akaike weights to determine, which of my hypothesized models best explains bill length variation in Peru (Johnson & Omland, 2004).

Cusco:

To further evaluate the interacting roles of isolation and environment I narrowed my focus to four populations within the department of Cusco in southeast Peru. Two populations were found within humid montane forest on east-facing slopes adjacent to two other populations occurring in semi-arid montane scrub on west-facing slopes (Fig. 5). Although climatic differences and a corresponding turnover in the flora and fauna between humid and dry sites are readily apparent the worldclim dataset did not show differences among the four sites. This error likely derives from the interpolated nature of the dataset, which makes sudden environmental transitions difficult to track. As a result I do not incorporate any climatic data into the analysis of bill length polymorphism among these four sites. I compared bill length variation among these four localities: Carrizales (n=6); Urubamba (n=21); Paucartambo (n=7); Pillahuata (n=19), using a one-way ANOVA and pairwise t-test using a holm method to correct for multiple comparisons.

Molecular analyses:

Sequencing:

I sequenced the mitochondrial locus NADH dehydrogenase, subunit 2 (ND2) for 137 individuals of *M. tyrianthina* from throughout Peru (Appendix B). Additionally, I sequenced three nuclear loci for 47 individuals from the four Cusco populations (Carrizales (n=6); Urubamba (n=21); Paucartambo (n=7); and Pillahuata (n=13)). These included two nuclear introns (Adenylate Kinase, subunit 1(AK1); beta-fibrinogen, subunit 7 (Bfib7)) and the Z-linked locus muscle, skeletal, tyrosine receptor kinase (MUSK). Extraction, PCR, and sequencing protocols follow those described previously (see chapter 1). All sequences were manually assembled and edited using Sequencer v.

4.10.1 (Gene Codes Corporation, Ann Arbor, MI, USA) and aligned using MUSCLE v. 3.7 (Edgar, 2004). Haplotype reconstruction for nuclear loci with multiple double peaks was conducted using the program PHASE v. 2.1.1 (Stephens et al., 2001; Stephens & Donnelly, 2003).

Phylogenetic analysis:

I constructed an ND2 phylogeny of all Peruvian samples using Bayesian methods in MrBayes v. 3.1 (Ronquist & Huelsenbeck, 2003) and run on the CIPRES Science Gateway (Miller et al., 2010). As an outgroup, ND2 sequence of *Metallura phoebe* was obtained from GenBank (Ascension number: EU042569.1). I selected a GTR+I+G model as an appropriate model of nucleotide substitution using an Akaike Information Criterion (Akaike, 1974) implemented in jmodeltest v.0.1 (Posada, 2008; Guindon & Gascuel, 2003). I also partitioned the ND2 dataset by codon position. I ran an MCMC analysis of four simultaneous runs, consisting of four chains, and a temperature for heated chains of 0.175 for 40 million generations sampling every 1000 generations. I assessed convergence using the program AWTY (Wilgenbusch et al., 2004) and discarded the first 10% of trees as burnin.

Population genetics analyses:

Using the ND2 phylogeny as a guide I calculated a variety of population parameters for each well-supported clade, including: nucleotide diversity, haplotype diversity, Tajima's D, and Fu's F. I also assessed inter-clade structure using corrected pairwise differences (Nei, 1987) and Fst-values (Holsinger & Weir, 2009). All population parameters were calculated in Arlequin v.3.5 (Excoffier et al., 2005).

For the four Cusco populations I calculated the number of haplotypes for each locus in DNaSP (Librado & Rozas, 2009), and subsequently visualized these as a haplotype network using a median-joining method in NETWORK v. 4.6.10 (Bandelt et al., 1999). The program IMa2 is a coalescent genealogy sampler that implements an isolation with migration (IM) model to estimate a variety of population parameters including migration rates among populations (Hey & Nielsen, 2007). IMa is particularly useful for recently diverged populations that may be diverging with ongoing gene flow (Kuhner, 2009). I utilized IMa2 to assess migration rates among the four Cusco populations using the four-locus dataset. Migration rates estimated from preliminary analyses of all four populations showed flat prior distributions that spanned a broad range of the posterior probability. This can indicate that there was an insufficient number of loci or information to accurately estimate the posterior distribution of the model parameters (Hey, 2010). I simplified analyses to instead conduct pairwise comparisons between humid and dry populations distributed along the Manu road (Paucartambo and Pillahuata) and across the Cordillera de Vilcanota (Urubamba and Carrizales). For each locus I specified a mutation rate with error (equal to mutations per locus per year (μ/l/y)) derived from the multi-locus dataset analyzed in *BEAST using novel geological and fossil calibrations for hummingbirds (see chapter 1 for details). These mutation rates were: ND2: 9.5×10^{-6} μ/l/y (95% HPD: 7.5×10^{-6}, 1.2×10^{-5} μ/l/y); AK1: 1.0×10^{-6} μ/l/y (95% HPD: 7.0×10^{-7}, 1.3×10^{-6} μ/l/y); Bfib7: 1.3×10^{-6} μ/l/y (95%HPD: 8.5×10^{-7}, 1.6×10^{-6} μ/l/y); and MUSK: 9.8×10^{-7} μ/l/y (95% HPD: 6.4×10^{-7}, 1.2×10^{-6} μ/l/y). I specified the upper bound for a uniform prior for the migration rate (-m: 1.259), population size (-q 7.94), and splitting times (-t 3.176) based on the geometric mean of

nucleotide diversity for each locus and following the developer's recommendations (Hey, 2011). For each comparison I ran an MCMC analyses for 25000 steps post-burnin using 50 heated chains with a geometric heating scheme that ranged from -ha 0.975 to –hb 0.75.

RESULTS

Morphological analyses:

The results of the one-way ANOVA revealed that there were significant differences (F-value=60.456; df=5; p<<0.0001) in bill length among the six regions. The pairwise t-test indicated that populations of the northwest (A), northeast (B), and the central Andes had identical bill lengths (p=1.00 after holm correction, Fig. 2). Populations from the humid east-facing slopes (D) were significantly longer than populations from A, B, and C. Finally, populations from the drier west-facing slopes (E) and western Andes (F) Were significantly longer than all other populations (A-D), however differences between E and F were not statistically different (p=0.1252) (Fig. 2).

Seasonality was the single best model explaining bill length variation, containing 50.4% of the Akaike weight. The second best model was seasonality and temperature holding 21.5% of the weight (ΔAICc =1.7), and third seasonality and precipitation (18.4%, ΔAICc=2.019) (Table 5). The linear regression of bill length versus seasonality exhibited a highly significant relationship (p<<0.0001) and adjusted r^2 = 0.4036 (Fig. 4).

Populations distributed on the drier west-facing slopes of the Andes in Cusco have significantly longer bills than populations on the humid east-facing slopes (Fig. 6). However, bill length in Urubamba was found to be significantly longer than all three of the other populations and longer bill length in Paucartambo was only weakly significant compared to birds from the adjacent humid slopes at Pillahuata (p=0.037). There were no differences in bill length between the two humid sites (p=0.399).

Molecular analyses:

ND2 sequences were 1041 bp in length and included 76 informative sites (7.3%). Indels were found in both nuclear introns, including a 90bp indel in the AK1 intron and a 15bp indel found in the Bfib7 intron. This caused problems in sequencing Bfib7 for heterozygous individuals because clean sequence would end abruptly at the starting point of the indel at nucleotide position 629. Before any population analyses could be performed all indels and gaps were removed from nuclear loci leaving: 337 bp of AK1 (4 informative sites (1.2%)), 629 bp of Bfib7 (5 informative sites (0.8%)), and 594 bp of MUSK with 4 informative sites (0.7%). There were no internal stop codons, indels, or anomalous substitution patterns in the ND2 sequences that might indicate that I had unknowingly amplified pseudogenes. However, I excluded one sample (FMNH 433155) because it did not align with other sequences and BLAST returned ambiguous matches with a variety of hummingbird species.

Six well-supported mitochondrial clades (posterior probability>0.9) were found with the Bayesian phylogeny in Peru (Fig. 3). The nominate subspecies comprises one clade (A) isolated north of the Marañon valley and >2% divergent from all other populations (Table 4a). Structure among the other clades can be associated with physical barriers, including: the high Andes which isolate *M. t. septentrionalis* and central and northern *Smaragdinicollis* (0.24% divergent); individuals from Ayacucho isolated by the Mantaro river to the north (0.67% divergent) and Aprurímac to the south (0.79-1.04% divergent); and a unique clade occupying the upper Apurímac and Urubamba valleys potentially isolated by the Cordillera de Vilcanota (0.91% divergent) (Table 4a). The region E from the morphological analyses fell out with two distinct clades: clade F from

the Urubamba and Apurímac valleys and the population from near Paucartambo, Peru falling out in clade G (Fig. 3). Fst values largely corresponded to corrected pairwise differences among clades (Table 5b). A single individual from the same locality as clade G showed closer affinities to an extra-limital haplogroup from Bolivia (see Chapter 1).

The nominate subspecies in clade A exhibited much higher nucleotide diversity relative to other populations in Peru, except for clade D (Table 3). Tajima's D and Fu's F values were significantly negative for most of the clades in Peru (Table 3). These values indicate deviations from selective neutrality or recent, rapid expansion throughout Peru (Gillespie, 2004).

ND2 between Urubamba and the other three populations differed by at least eight mutation steps (Fig. 7), which is consistent with phylogenetic structure (0.91% divergence) and Fst values (0.85) (Table 4). The three nuclear loci do not show any clear geographic pattern among different haplotypes (Fig. 7). Migration parameters calculated with IMa largely confirm these patterns. Mean migration rate between drier (Paucartambo) and more humid (Pillahuata) sites along the Manu road was about 0.64 in both directions, whereas across the Cordillera de Vilcanota migration rate was between 0.04-0.057 and not significantly different from zero (Table 6). I also calculated population migration rate (2NM), which is more informative then just migration rate as it takes into account the effect of population size in immigration of genes into a population. These results further supported that little to no migration is occurring across the Cordillera de Vilcanota (2NM is equal to 0.046-0.077) compared to the Manu road where mean population migration rate is greater than 1 (Table 6).

DISCUSSION

Birds in climatically similar regions had similar bill lengths. A model of seasonality best explains bill length variation in Peru with populations in more seasonal environments showing an increase in bill length. Similarities and differences in bill length were not concordant with subspecies classification or genetic variation. Based on the ND2 phylogeny populations have colonized more seasonal habitats on west-facing slopes three times independently (Fig. 3) and each of these transitions to west-facing slopes corresponds to an increase in bill length. Likewise despite major genetic divergence across the Marañon valley between the nominate subspecies and other Peruvian populations (>2%) this did not correspond to divergence in bill length.

Among the four populations I investigated in southern Peru I found a similar pattern of bill length polymorphism with birds on west-facing slopes showing increased bill length relative to birds on adjacent east-facing slopes. However, I also found significant differences in bill length between birds at the two west-facing sites of Urubamba (longer bills) and Paucartambo (shorter bills). These differences in bill length between Urubamba and Paucartambo correspond closely to genetic structure at the ND2 locus. Urubamba birds belong to a unique haplogroup, whereas shorter-billed birds from Paucartambo belong to a haplogroup that includes both populations from east-facing slopes (Carrizales and Pillahuata) (Fig. 7). Migration and population migration rates calculated with multi-locus data in IMa2 also confirm that there is greater gene flow between populations distributed along the Manu road than populations distributed on either side of the Cordillera de Vilcanota (Table 6). The topography of the region further matches bill length and genetic variation. Separating populations at Paucartambo and

Pillahuata along the Manu road is a low elevation ridge reaching maximum elevations of only 4000 m and for much of its length not surpassing elevations of 3600-3800 m. Although this elevation is enough to create a rain-shadow effect betwen eastern and western slopes it is likely not effective in preventing dispersal in a species that ranges to 4200 m (Schulenberg et al., 2007). On the other hand, the Cordillera de Vilcanota, which separates the Urubamba and Carrizales populations, reaches well above 5000 m and snowline with the lowest passes still above 4300 m and the elevational range of *M. tyrianthina*. Based on these concordant patterns of bill length variation, genetic divergence, and topography it is tempting to conclude that the greater morphological and genetic divergence found in the Urubamba populations results from the release of homogenizing gene flow, whereas, bill length divergence in the Paucartambo birds is limited by ongoing gene exchange with humid forest populations. It is also possible that this pattern is the result of recent colonization of Paucartambo from Pillahuata and enough time for equal molecular and morphological divergence has not occurred.

My results corroborate a growing body of literature in numerous taxa showing a central role for ecological differences in shaping morphological variation rather than geographic barriers which structure genetic variation (Smith et al., 1997; Schneider et al., 1999; Smith et al., 2004; Chaves et al., 2007; Milá et al., 2009; Smith et al., 2011). Many of these studies found morphological divergence to occur independently of genetic divergence leading the authors to conclude that sufficiently strong selection can outweigh the homogenizing effects of gene flow. Divergence with gene flow across ecological gradients is theoretically possible (Gavrilets, 2000; Gavrilets et al., 2000; Doebeli & Dieckmann, 2003; Pinho & Hey, 2010), however evidence from natural systems for

divergence with gene flow has been notoriously difficult to obtain (Coyne & Orr, 2004). One of the major obstacles to identifying speciation with gene flow is showing that populations may actually become reproductively isolated rather than just persisting as a phenotypic cline (Coyne & Orr, 2004). Phylogenetic analyses of species parapatrically distributed across environmental gradients have further indicated that speciation primarily occurs in allopatry (Patton & Smith, 1992; Parra et al., 2009). I found that populations existing in different environments and separated from sister populations by a physical barrier were genetically distinct and showed greater bill length divergence compared to populations that were only separated by distinct environments. These results suggest that gene flow does have a negative effect on divergence and that spatial features promoting both physical and ecological isolation will lead to a greater degree of divergence. Although, it remains to be seen whether evolution of bill length variation can be linked to the development of reproductive isolation in hummingbirds.

On the other extreme my results conflict with the notion that speciation in Andean birds can occur via stochastic fixation of plumage or morphological characters through drift alone. I found that populations occurring in similar climates do not show divergence in bill length despite showing the greatest levels of molecular divergence. I did not evaluate plumage variation in *M. tyrianthina* in the present study, which also varies (mostly among the three subspecies). The nominate subspecies north of the Marañon has a reddish tail, whereas other Peruvian subspecies have purplish tails. Further work is needed to determine whether divergence in plumage characteristics is the result of natural selection, sexual selection, or stochastic processes. Major reviews of speciation have found little support in the literature for speciation occurring as the result of genetic drift

alone (Coyne & Orr, 2004; Price, 2008). Although stochastic processes have been proposed for certain phenotypic patterns in Andean birds (Remsen, 1984) recent evidence points to the rapid pace at which plumage characteristics become fixed in populations relative to neutral loci, thus suggesting an important role of selection (Cadena et al., 2011). Strong selective gradients exist in the Andes. The north-to-south axis of the Andes spans a broad latitudinal gradient, which is associated with climatic differences (Fjeldsa & Krabbe, 1990). This climatic cline is fragmented at several points that could serve to isolate populations in distinct environments. Additionally, from east-to-west in the central Andes a major precipitation gradient exists that would also serve to drive divergence in species, such as *M. tyrianthina*. To further understanding of the complex processes underlying speciation in the Andes potential selective pressures and how they may drive population divergence in isolation should be investigated.

Pinpointing the precise selective pressures driving bill length polymorphism in *M. tyrianthina* is difficult since climatic variables are strongly correlated with a multitude of ecological factors. Potential factors impacting bill length polymorphism in *M. tyrianthina* may include: (1) a direct role of climate; (2) competitive release from other hummingbird species; or (3) turnover of floral communities between different environments. Climatic variation underlies the premise of Allen's rule that states endotherms will have shorter appendages in colder environments to prevent heat loss from extremities (Zink & Remsen, 1986; Symonds & Tattersall, 2010). A bird's bill can also be a major engine of thermoregulation and improves the ability of an individual to shed excess body heat (Hagan & Heath, 1980; Tattersall et al., 2009). This may be especially important in water-limited environments where shedding excess heat through the skin can lead to

water loss. Increased bill size has been linked to high summer temperatures in saltmarsh sparrow species of North America (Greenberg et al., 2011). Expectations for variation in direct response to climate do not seem to fit patterns of bill length variation found in *M. tyrianthina.* Although daily temperatures can be quite warm in the high Andes especially in drier environments it never reaches the high temperatures encountered by saltmarsh sparrows in North America or the tropical lowlands. A more significant pressure may be the cold nighttime temperature that would select against long bill length. However, even within similar humid environments *M. tyrianthina* and other *Metallura* species show an opposite trend to Allen's rule with populations and species at higher latitudes showing an increase in bill length (Heindl & Shuchmann, 1998).

There is a drastic decrease in the diversity of hummingbird communities as one moves from the humid eastern to dry western Andes. Hummingbird species are intensely competitive both intra- and inter-specifically (Altshuler, 2006). A diverse array of bill shapes and sizes is encountered in these diverse hummingbird communities as well and competition has been suggested as a mechanism driving divergence in hummingbird bills (at least between the sexes) to prevent populations from competing for the same resources (Temeles & Kress, 2003). *M. tyrianthina* has a relatively short bill compared to other hummingbirds in the diverse east Andean communities and an increase in bill length on west-facing, species-poor slopes may allow *M. tyrianthina* populations found there to exploit a greater variety of floral resources. This would be similar to a mechanism of competitive release found in many island birds where species converge on a more generalist phenotype (Grant & Grant, 2008).

Hummingbird bills have repeatedly been shown to co-evolve with flower morphology (Temeles, 2000; Temeles et al., 2002; Temeles & Kress, 2003; Temeles et al., 2009; Nattero et al., 2010). In addition to turnover in the fauna between eastern and western slopes of the Andes there is extensive turnover in the flora as well. Variation in bill length within *M. tyrianthina* could be the result of hummingbird bills tracking variation in flower morphology between humid and dry slopes in the Andes. Future work should examine differences in preferred food plants in *M. tyrianthina* between eastern and western slopes and whether these differences correspond to an increase in corolla length matching an increase in *M. tyrianthina* bill length.

CHAPTER TWO

FIGURES

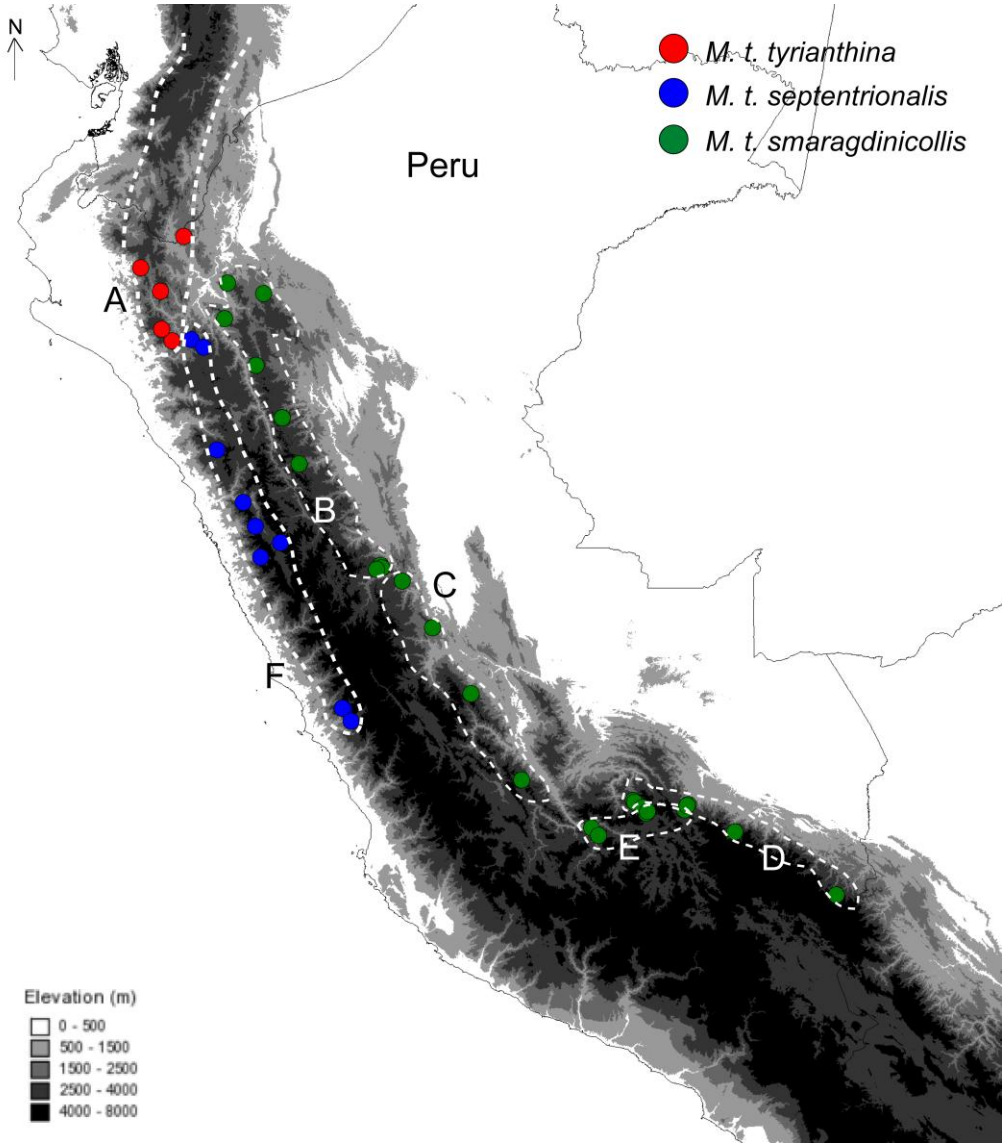

Figure 1: Distribution of *Metallura tyrianthina* in Peru. Dots correspond to sampling localities and colors correspond to each subspecies. Dotted lines and letters encompass regions used for morphological analyses. (A) NW; (B) NE; (C) E-Central; (D) SE Peru wet sites; (E) SE Peru dry sites; and (F) W-Central.

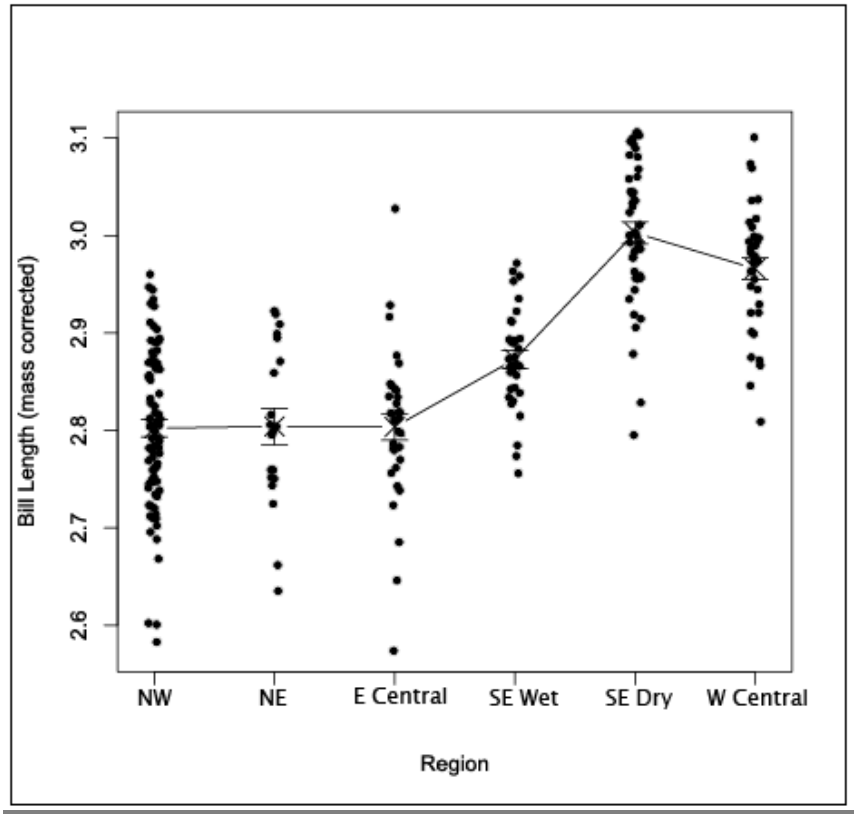

	NW	NE	E Central	SE Wet	SE Dry
NE	1.00	-			
E Central	1.00	1.00	-		
SE Wet	<0.0001	0.0064	0.0011	-	
SE Dry	<0.0001	<0.0001	<0.0001	<0.0001	-
W Central	<0.0001	<0.0001	<0.0001	<0.0001	0.1252

Figure 2: Bill length (mass corrected) variation among regions in Peru. Lines connect the means of each region in the plot. Table of Pairwise comparisons (holm corrected) among the six regions in Fig. 1.

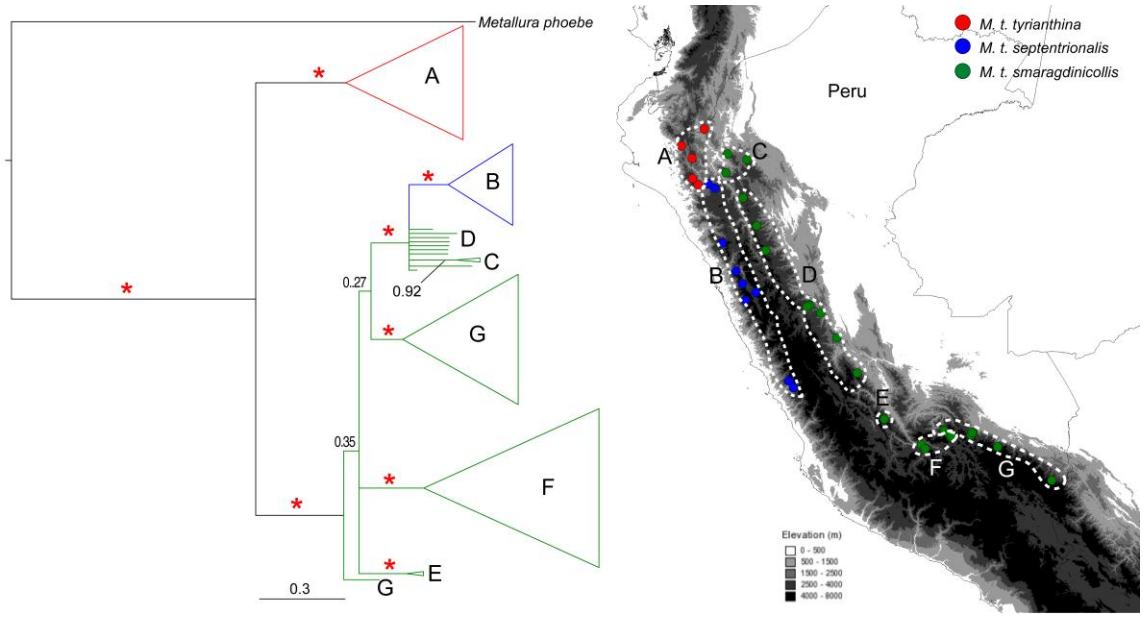

Figure 3: Bayesian phylogeny of ND2 for all Peruvian populations and map showing the distribution of each clade. Red asterices signify posterior probability support of 1.0. Colors correspond to each subspecies. Letters do not signify the same regions that were used for morphological analyses. (A) nominate subspecies from north Ist of the Marañon Valley (Lambayeque & Cajamarca); (B) *M. t. septentrionalis* from west slope of Peru (tissues from Lima & Ancash); (C) northeast Peru (San Martin & Amazonas); (D) Central Peru (Huánuco, Pasco & Junín); (E) Ayacucho; (F) Apurimac and Urubamba; (E) southeast Peru (Cusco & Puno) also single individual at base is from Cusco, but shares haplotypes with a Bolivian clade.

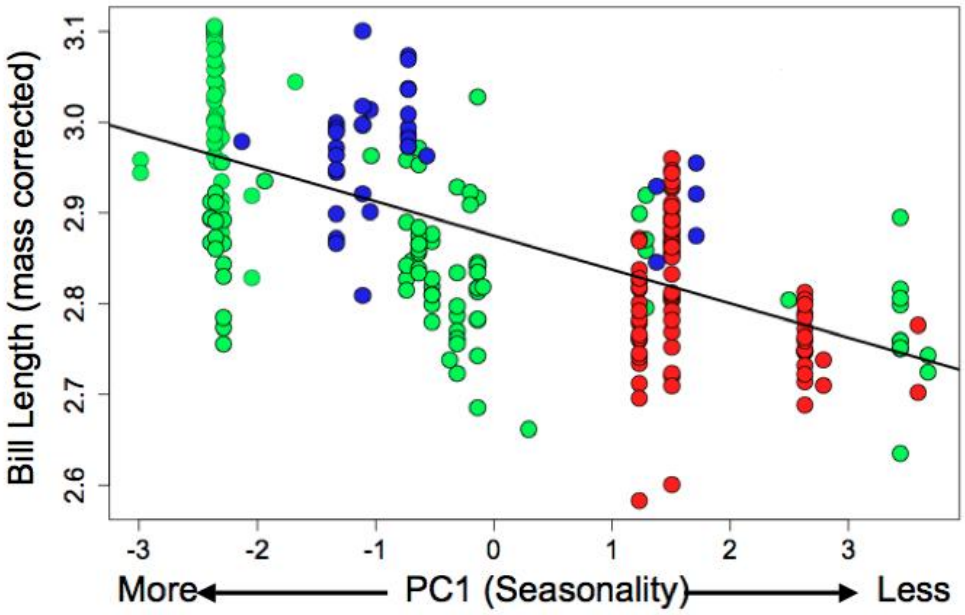

Figure 4: Bill length (mass corrected) versus PC1 of seasonality (82.9% of the variation). The linear regression model was highly significant ($p<<0.0001$) with an adjusted r^2 of 0.4036. Colored circles correspond to the currently recognized subspecies of *M. tyrianthina*: (red) *M. t. tyrianthina*; (blue) *M. t. septentrionalis*; (green) *M. t. smaragdinicollis.*

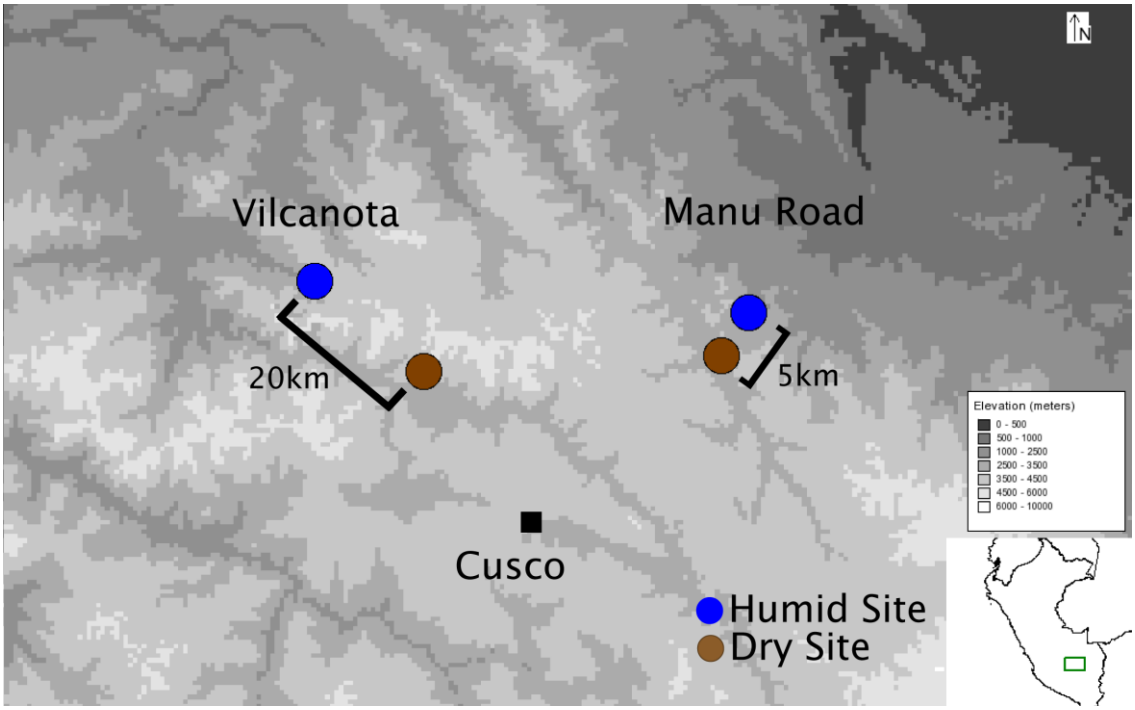

Figure 5: Map of sampling sites from the department of Cusco, Peru. One pair of sites from the humid (Carrizales) and dry (Urubamba) sides of the Cordillera de Vilcanota separated by ca. 20 km. A second pair of sites from along the Manu road with a humid (Pillahuata) and dry (Paucartambo) site from either side of Acjanaco pass ca. 5 km apart. The Cordillera de Vilcanota ranges in elevation from ca. 4300 m to above 5000 m, whereas sites along the Manu road are separated by a cordillera between 3600-4000 m in elevation.

A

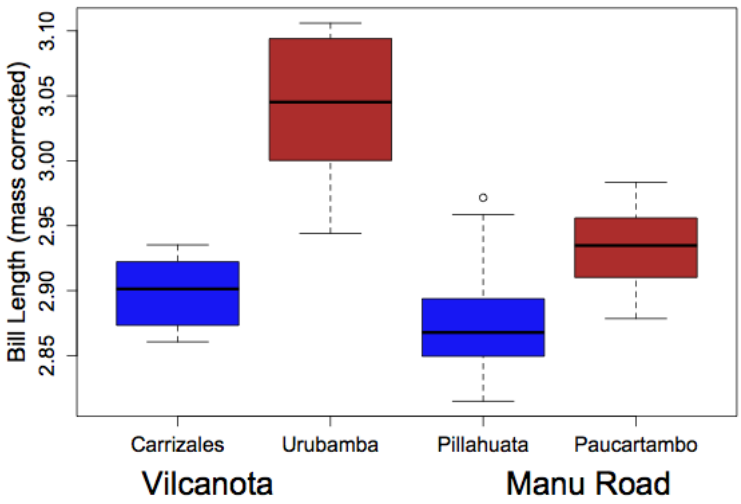

B

	Carrizales	Urubamba	Pillahuata
Urubamba	1.3e-7	-	-
Pillahuata	0.399	4.3e-14	-
Paucartambo	0.399	8.7e-6	0.037

Figure 6: (A) Bill length (mass corrected) differences among the four Cusco localities. Blue represents the two humid sites and brown the two drier sites. (B) p-values for pairwise t-test of mass corrected bill length among the four localities (holm corrected).

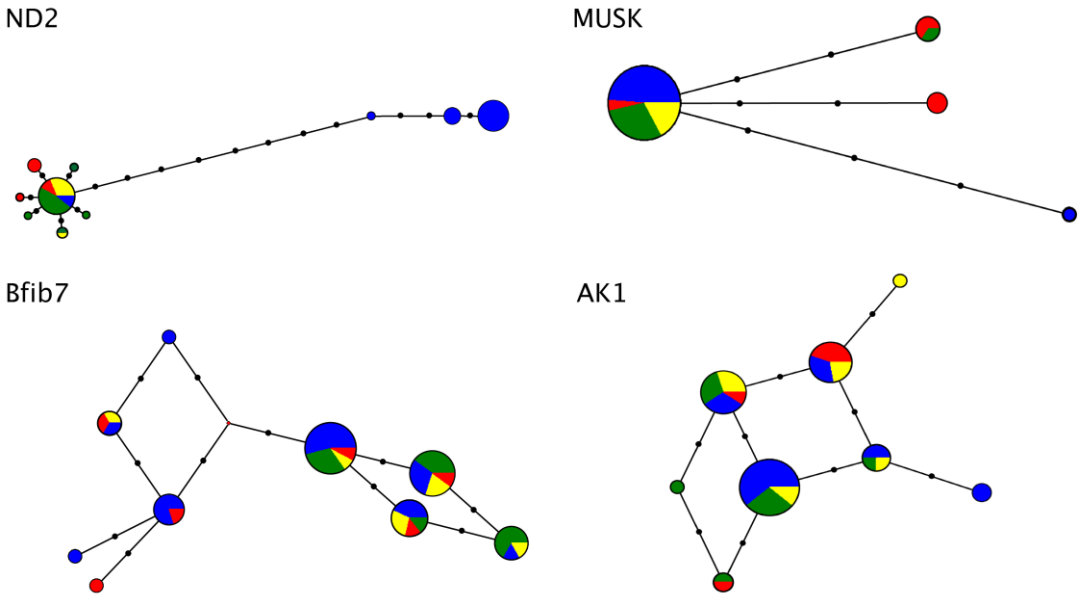

Figure 7: Haplotype networks for each locus from the four Cusco localities (Fig. 4): Pillahuata (green), Paucartambo (yellow), Carrizales (red), and Urubamba (blue). Each dot along lines connecting haplotypes represents a single mutational step. Note figures not drawn to the same scale. For ND2, Urubamba birds are separated from other 3 populations by 0.91% sequence divergence and an Fst of 0.85.

CHAPTER TWO

TABLES

Table 1: Bioclimatic variables from worldclim.org broken down by category.

Category	Bioclimatic Variable	
Temperature:	Bio1	Annual Mean Temperature
	Bio3	Isothermality (2/7) (* 100)
	Bio5	Max Temperature of Warmest Month
	Bio6	Min Temperature of Coldest Month
	Bio8	Mean Temperature of Wettest Quarter
	Bio9	Mean Temperature of Driest Quarter
	Bio10	Mean Temperature of Warmest Quarter
	Bio11	Mean Temperature of Coldest Quarter
Precipitation:	Bio12	Annual Precipitation
	Bio13	Precipitation of Wettest Month
	Bio14	Precipitation of Driest Month
	Bio16	Precipitation of Wettest Quarter
	Bio2	Mean Monthly Temperature Range
	Bio17	Precipitation of Driest Quarter
	Bio18	Precipitation of Warmest Quarter
	Bio19	Precipitation of Coldest Quarter
Seasonality:	Bio2	Mean Monthly Temperature Range
	Bio4	Temperature Seasonality (STD * 100)
	Bio7	Temperature Annual Range (5-6)
	Bio15	Precipitation Seasonality (CV)

Table 2: Loadings from Principal Component analysis of temperature, precipiation, and seasonality Bioclim variables.

Temperature	Comp.1	Comp.2	Comp.3	Comp.4
bio1	-0.385	-0.15	0.56	-0.706
bio3	-0.147	0.825	0.506	-0.174
bio5	-0.344	-0.398	0.439	-0.431
bio6	-0.357	0.321	-0.734	-0.141
bio8	-0.381	-0.116	0.728	0.538
bio9	-0.385	-0.266	0.424	-0.696
bio10	-0.378	-0.174	0.309	-0.117
bio11	-0.385	-0.305	0.534	0.403
Proportion of Variance:	0.8373	0.1555	0.0034	0.0026
Cumulative proportion:	0.8373	0.9928	0.9963	0.9989

Precipitation	Comp.1	Comp.2	Comp.3	Comp.4
bio12	-0.417	0.107	-0.309	-0.494
bio13	-0.353	0.474	0.193	0.716
bio14	-0.378	-0.412	0.149	-0.811
bio16	-0.333	0.518	-0.508	-0.107
bio17	-0.383	-0.394	0.146	0.334
bio18	-0.388	0.175	0.77	-0.421
bio19	-0.387	-0.375	-0.12	0.102
Proportion of Variance:	0.7801	0.1795	0.0307	0.0076
Cumulative proportion:	0.7801	0.9596	0.9904	0.9980

Seasonality	Comp.1	Comp.2	Comp.3	Comp.4
bio2	-0.517	-0.223	0.619	0.548
bio4	-0.504	-0.187	-0.777	0.326
bio7	-0.531	-0.35	0.108	-0.764
bio15	-0.444	0.891		
Proportion of Variance:	0.8293	0.1093	0.0578	0.0037
Cumulative proportion:	0.8293	0.9386	0.9963	1

Table 3: Standard indices of molecular diversity for each clade. Data based on 845bp ND2. Sample size is n. Nucleotide diversity (π) and haplotype diversity (Hd). Asterices following Fu's F and Tajima's D equal: non-significant (ns), * $p < 0.05$, ** $p < 0.01$, *** $p < 0.001$.

Population	n	Variable sites	π	Hd	Fu's F	Tajima's D
Clade A	30	26	0.003505	0.967	-26.34 ***	-1.98 **
Clade C	7	2	0.000815	0.8571	-9.76 ***	-0.27 ns
Clade B	21	1	0.000115	0.9524	-3.4e38 ***	-1.16 ns
Clade D	5	2	0.003762	0.8	-1.9 *	-1.18 *
Clade E	2	1	0.001103	0.5	0 ns	0 ns
Clade F	41	12	0.001742	0.9756	-27.63 ***	-1.32 ns
Clade G	30	12	0.001462	0.9565	-28.17 ***	-2.04 **

Table 4: Among population comparisons based on 845bp ND2 data. (A) percent corrected pairwise differences among all populations. (B) Fst values among populations. All values were significant.

A

	A	B	C	D	E	F
Clade A	-					
Clade B	2.39	-				
Clade C	2.17	0.24	-			
Clade D	2.02	0.24	0.01	-		
Clade E	2.03	1.07	0.83	0.67	-	
Clade F	2.41	1.24	1.01	0.85	1.04	-
Clade G	2.13	0.9	0.67	0.43	0.79	0.91

B

	A	B	C	D	E	F
Clade A	*					
Clade B	0.91	*				
Clade C	0.86	0.89	*			
Clade D	0.84	0.77	0.07	*		
Clade E	0.84	0.99	0.91	0.63	*	
Clade F	0.90	0.91	0.86	0.82	0.86	*
Clade G	0.88	0.91	0.82	0.69	0.83	0.85

Table 5: AICc analysis statistics of regression models for bill length. [seas] seasonality; [prec] precipitation; and [temp] temperature.

Model	logL	k	AICc	ΔAICc	Model weights
[seas]	258.125	3	-510.1482	0	0.5040
[seas][temp]	258.3109	4	-508.4516	1.6966	0.2158
[seas][prec]	258.1497	4	-508.1292	2.019	0.1837
[temp][prec][seas]	258.5459	4	-506.8434	3.3048	0.0966
[temp][prec]	245.0125	4	-481.8547	28.2935	0
[prec]	233.3506	3	-460.5996	49.5486	0
[temp]	200.96	3	-395.8135	114.3347	0

Table 6: Migration rates and population migration rates from IMa2 analysis betIen humid and dry sites across the Manu Rd and the Cordillera de Vilcanota. In each case the mean and range encompassed within the 95% HPD are presented. A > signifies the dwerection of migration. M is migration rate, μ the mutation rate, and N effective population size.

	Manu		Vilcanota	
	mean	95% HPD	mean	95% HPD
Migration rate (M/μ):				
humid>dry	0.6404	0.067-1.258	0.057	0.0-0.173
dry>humid	0.6424	0.067-1.258	0.044	0.0-0.132
Population migration rates (2NM):				
humid>dry	1.468	0.0-3.67	0.046	0.0-0.14
dry>humid	1.704	0.0-3.89	0.077	0.0-0.237

APPENDIX A:

TISSUE SAMPLES USED IN CHAPTER ONE

This appendix presents samples used in the present study with voucher number, collection where specimen is deposited, and general locality. For individuals where MUSK was unavailable on GenBank I sequenced the same individual. Museum acronyms: Louisiana State University Museum of Natural Science (LSUMNS); Field Museum of Natural History (FMNH); American Museum of Natural History (AMNH); University of Kansas Museum of Natural History (KUMNH); Instituto Alexander von Humboldt (IAvH); Andrés M. Cuervo (AMC); Museum of SouthIstern Biology (MSB); Academy of Natural Sciences, Philadelphia (ANSP).

Taxon	Voucher Number	Smyce	Department	Country
Aglaiocercus kingi	8017	LSUMNS	Pasco	Peru
Chalcostigma herrani	6277	LSUMNS	Pichincha	Ecuador
Hemiprocne mystacea		GenBank	Western Province	Soloman Islands
Lesbia nuna	3615	LSUMNS	Huánuco	Peru
Lophornis chalybeus	9399	LSUMNS	Pando	Bolivia
Oreotrochilus estella	103835	LSUMNS	Ayacucho	Peru
Sephanoides fernandensis		GenBank	Robinson Crusoe Is.	Chile
Sephanoides sephanoides	1126	AMNH	Bariloche	Argentina
Streptoprocne zonaris		GenBank	Wiwapatu Mountain	Guyana
Metallura aeneocauda	172611	MSB	Cusco	Peru
Metallura aeneocauda	1236	LSUMNS	La Paz	Bolivia
Metallura baroni		GenBank		Ecuador
Metallura eupogon	8293	LSUMNS	Pasco	Peru
Metallura iracunda	AMC 869	AMC	Cesar	Colombia
Metallura iracunda	AMC 874	AMC	Cesar	Colombia
Metallura iracunda	JPL 56	AMC	Cesar	Colombia
Metallura iracunda	JPL 59	AMC	Cesar	Colombia
Metallura iracunda	JPL 68	AMC	Cesar	Colombia
Metallura odomae	353	LSUMNS	Cajamarca	Peru
Metallura phoebe	103876	LSUMNS	Arequipa	Peru
Metallura theresiae	3534	LSUMNS	Huánuco	Peru
Metallura theresiae	167722	MSB	Amazonas	Peru
Metallura w. atrogularis	5939	LSUMNS	Morona-Santiago	Ecuador
Metallura w. primolina	19018	ANSP	Carchi	Ecuador
Metallura w. primolina	5938	LSUMNS	Pichincha	Peru
Metallura w. williami	IAvH.BT 1655	IAvH	Caldas	Colombia

Metallura w. williami	IAvH.BT 1717	IAvH	Caldas	Colombia
Metallura w. williami	IAvH.BT 1822	IAvH	Caldas	Colombia
Metallura t. chloropogon	DOT 5042	AMNH	Araqua	Venezuela
Metallura t. chloropogon	DOT 5043	AMNH	Araqua	Venezuela
Metallura t. chloropogon	DOT 5044	AMNH	Araqua	Venezuela
Metallura t. districta	AMC 876	AMC	Cesar	Colombia
Metallura t. districta	JPL 54	AMC	Cesar	Colombia
Metallura t. districta	JPL 69	AMC	Cesar	Colombia
Metallura t. districta	NGP 039	AMC	Cesar	Colombia
Metallura t. districta	AMC 998	AMC	Magdalena	Colombia
Metallura t. districta	AMR 61	AMC	Magdalena	Colombia
Metallura t. districta	IAvH.BT 467	IAvH	Magdalena	Colombia
Metallura t. districta	IAvH.BT 472	IAvH	Magdalena	Colombia
Metallura t. oreopola	JPL 263	AMC	Barrosa	Venezuela
Metallura t. oreopola	JPL 264	AMC	Barrosa	Venezuela
Metallura t. oreopola	JPL 265	AMC	Barrosa	Venezuela
Metallura t. oreopola	JPL 266	AMC	Barrosa	Venezuela
Metallura t. oreopola	JPL 272	AMC	Barrosa	Venezuela
Metallura t. oreopola	JPL 273	AMC	Barrosa	Venezuela
Metallura t. oreopola	JPL 274	AMC	Barrosa	Venezuela
Metallura t. oreopola	AMC 1123	AMC	China	Venezuela
Metallura t. oreopola	AMC 1055	AMC	Guaraque	Venezuela
Metallura t. oreopola	AMC 1066	AMC	Guaraque	Venezuela
Metallura t. oreopola	JEM 182	AMC	Inia	Venezuela
Metallura t. oreopola	JEM 183	AMC	Inia	Venezuela
Metallura t. quitensis	6272	LSUMNS	Pichincha	Peru
Metallura t. quitensis	6286	LSUMNS	Pichincha	Peru
Metallura t. quitensis	6311	LSUMNS	Pichincha	Peru
Metallura t. quitensis	6334	LSUMNS	Pichincha	Peru
Metallura t. septentrionalis	171541	MSB	Ancash	Peru
Metallura t. septentrionalis	171543	MSB	Ancash	Peru
Metallura t. septentrionalis	171548	MSB	Ancash	Peru
Metallura t. septentrionalis	171549	MSB	Ancash	Peru
Metallura t. septentrionalis	171553	MSB	Ancash	Peru
Metallura t. septentrionalis	171592	MSB	Ancash	Peru
Metallura t. septentrionalis	173877	MSB	Ancash	Peru
Metallura t. septentrionalis	171724	MSB	Caraz	Peru
Metallura t. septentrionalis	171752	MSB	Caraz	Peru
Metallura t. septentrionalis	171654	MSB	Carhuaz	Peru
Metallura t. septentrionalis	171656	MSB	Carhuaz	Peru
Metallura t. septentrionalis	171665	MSB	Carhuaz	Peru
Metallura t. septentrionalis	171670	MSB	Carhuaz	Peru
Metallura t. septentrionalis	171677	MSB	Carhuaz	Peru
Metallura t. septentrionalis	171696	MSB	Carhuaz	Peru
Metallura t. septentrionalis	171714	MSB	Carhuaz	Peru
Metallura t. septentrionalis	171718	MSB	Carhuaz	Peru
Metallura t. septentrionalis	171719	MSB	Carhuaz	Peru
Metallura t. septentrionalis	PE6 12	MSB	Lima	Peru
Metallura t. septentrionalis	PE6 18	MSB	Lima	Peru

Metallura t. septentrionalis	PE6 43	MSB	Lima	Peru
Metallura t. septentrionalis	163357	MSB	Lima	Peru
Metallura t. smaragdinicollis	167844	MSB	Amazonas	Peru
Metallura t. smaragdinicollis	168886	MSB	Apurimac	Peru
Metallura t. smaragdinicollis	169122	MSB	Apurimac	Peru
Metallura t. smaragdinicollis	169136	MSB	Apurimac	Peru
Metallura t. smaragdinicollis	169152	MSB	Apurimac	Peru
Metallura t. smaragdinicollis	169159	MSB	Apurimac	Peru
Metallura t. smaragdinicollis	169162	MSB	Apurimac	Peru
Metallura t. smaragdinicollis	169170	MSB	Apurimac	Peru
Metallura t. smaragdinicollis	169180	MSB	Apurimac	Peru
Metallura t. smaragdinicollis	169183	MSB	Apurimac	Peru
Metallura t. smaragdinicollis	169190	MSB	Apurimac	Peru
Metallura t. smaragdinicollis	169212	MSB	Apurimac	Peru
Metallura t. smaragdinicollis	169213	MSB	Apurimac	Peru
Metallura t. smaragdinicollis	169216	MSB	Apurimac	Peru
Metallura t. smaragdinicollis	169220	MSB	Apurimac	Peru
Metallura t. smaragdinicollis	169233	MSB	Apurimac	Peru
Metallura t. smaragdinicollis	169234	MSB	Apurimac	Peru
Metallura t. smaragdinicollis	169241	MSB	Apurimac	Peru
Metallura t. smaragdinicollis	169242	MSB	Apurimac	Peru
Metallura t. smaragdinicollis	169248	MSB	Apurimac	Peru
Metallura t. smaragdinicollis	172670	MSB	Apurimac	Peru
Metallura t. smaragdinicollis	KU-25113	KUMNH	Ayacucho	Peru
Metallura t. smaragdinicollis	KU-25141	KUMNH	Ayacucho	Peru
Metallura t. smaragdinicollis	159812	MSB	Cusco	Peru
Metallura t. smaragdinicollis	159838	MSB	Cusco	Peru
Metallura t. smaragdinicollis	159846	MSB	Cusco	Peru
Metallura t. smaragdinicollis	159847	MSB	Cusco	Peru
Metallura t. smaragdinicollis	159851	MSB	Cusco	Peru
Metallura t. smaragdinicollis	159862	MSB	Cusco	Peru
Metallura t. smaragdinicollis	159867	MSB	Cusco	Peru
Metallura t. smaragdinicollis	159870	MSB	Cusco	Peru
Metallura t. smaragdinicollis	159871	MSB	Cusco	Peru
Metallura t. smaragdinicollis	159879	MSB	Cusco	Peru
Metallura t. smaragdinicollis	159881	MSB	Cusco	Peru
Metallura t. smaragdinicollis	159883	MSB	Cusco	Peru
Metallura t. smaragdinicollis	159884	MSB	Cusco	Peru
Metallura t. smaragdinicollis	159885	MSB	Cusco	Peru
Metallura t. smaragdinicollis	159888	MSB	Cusco	Peru
Metallura t. smaragdinicollis	159893	MSB	Cusco	Peru
Metallura t. smaragdinicollis	159895	MSB	Cusco	Peru
Metallura t. smaragdinicollis	159896	MSB	Cusco	Peru
Metallura t. smaragdinicollis	159897	MSB	Cusco	Peru
Metallura t. smaragdinicollis	168288	MSB	Cusco	Peru
Metallura t. smaragdinicollis	168292	MSB	Cusco	Peru
Metallura t. smaragdinicollis	172400	MSB	Cusco	Peru
Metallura t. smaragdinicollis	172402	MSB	Cusco	Peru
Metallura t. smaragdinicollis	172404	MSB	Cusco	Peru

Metallura t. smaragdinicollis	172405	MSB	Cusco	Peru
Metallura t. smaragdinicollis	172409	MSB	Cusco	Peru
Metallura t. smaragdinicollis	172618	MSB	Cusco	Peru
Metallura t. smaragdinicollis	172619	MSB	Cusco	Peru
Metallura t. smaragdinicollis	172622	MSB	Cusco	Peru
Metallura t. smaragdinicollis	172623	MSB	Cusco	Peru
Metallura t. smaragdinicollis	172635	MSB	Cusco	Peru
Metallura t. smaragdinicollis	172642	MSB	Cusco	Peru
Metallura t. smaragdinicollis	172644	MSB	Cusco	Peru
Metallura t. smaragdinicollis	172645	MSB	Cusco	Peru
Metallura t. smaragdinicollis	175554	MSB	Cusco	Peru
Metallura t. smaragdinicollis	175557	MSB	Cusco	Peru
Metallura t. smaragdinicollis	175558	MSB	Cusco	Peru
Metallura t. smaragdinicollis	175559	MSB	Cusco	Peru
Metallura t. smaragdinicollis	175560	MSB	Cusco	Peru
Metallura t. smaragdinicollis	397849	FMNH	Cusco	Peru
Metallura t. smaragdinicollis	397851	FMNH	Cusco	Peru
Metallura t. smaragdinicollis	429932	FMNH	Cusco	Peru
Metallura t. smaragdinicollis	429933	FMNH	Cusco	Peru
Metallura t. smaragdinicollis	429934	FMNH	Cusco	Peru
Metallura t. smaragdinicollis	433153	FMNH	Cusco	Peru
Metallura t. smaragdinicollis	433154	FMNH	Cusco	Peru
Metallura t. smaragdinicollis	433156	FMNH	Cusco	Peru
Metallura t. smaragdinicollis	433157	FMNH	Cusco	Peru
Metallura t. smaragdinicollis	433158	FMNH	Cusco	Peru
Metallura t. smaragdinicollis	163120	MSB	Huánuco	Peru
Metallura t. smaragdinicollis	163132	MSB	Huánuco	Peru
Metallura t. smaragdinicollis	163154	MSB	Huánuco	Peru
Metallura t. smaragdinicollis	163196	MSB	Huánuco	Peru
Metallura t. smaragdinicollis	163214	MSB	Huánuco	Peru
Metallura t. smaragdinicollis	128	MSB	Junin	Peru
Metallura t. smaragdinicollis	213	MSB	Junin	Peru
Metallura t. smaragdinicollis	218	MSB	Junin	Peru
Metallura t. smaragdinicollis	228	MSB	Junin	Peru
Metallura t. smaragdinicollis	DOT 2609	AMNH	La Paz	Peru
Metallura t. smaragdinicollis	DOT 2716	AMNH	La Paz	Peru
Metallura t. smaragdinicollis	DOT 2751	AMNH	La Paz	Peru
Metallura t. smaragdinicollis	DOT 2760	AMNH	La Paz	Peru
Metallura t. smaragdinicollis	8209	LSUMNS	Pasco	Peru
Metallura t. smaragdinicollis	172370	MSB	Pasco	Peru
Metallura t. smaragdinicollis	21169	KUMNH	Puno	Peru
Metallura t. smaragdinicollis	21195	KUMNH	Puno	Peru
Metallura t. smaragdinicollis	43683	LSUMNS	San Martin	Peru
Metallura t. smaragdinicollis	43711	LSUMNS	San Martin	Peru
Metallura t. tyrianthina	IAvH.BT 2276	IAvH	Boyacá	Colombia
Metallura t. tyrianthina	IAvH.BT 4116	IAvH	Antioquia	Colombia
Metallura t. tyrianthina	JEAC 632	AMC	Boyaca	Colombia
Metallura t. tyrianthina	IAvH.BT 4151	IAvH	Boyacá	Colombia
Metallura t. tyrianthina	IAvH.BT 4158	IAvH	Boyacá	Colombia

Metallura t. tyrianthina	IAvH.BT 4169	IAvH	Boyacá	Colombia
Metallura t. tyrianthina	IAvH.BT 4175	IAvH	Boyacá	Colombia
Metallura t. tyrianthina	IAvH.BT 4186	IAvH	Boyacá	Colombia
Metallura t. tyrianthina	IAvH.BT 6967	IAvH	Boyacá	Colombia
Metallura t. tyrianthina	31974	LSUMNS	Cajamarca	Peru
Metallura t. tyrianthina	32000	LSUMNS	Cajamarca	Peru
Metallura t. tyrianthina	32073	LSUMNS	Cajamarca	Peru
Metallura t. tyrianthina	32098	LSUMNS	Cajamarca	Peru
Metallura t. tyrianthina	32101	LSUMNS	Cajamarca	Peru
Metallura t. tyrianthina	32431	LSUMNS	Cajamarca	Peru
Metallura t. tyrianthina	32520	LSUMNS	Cajamarca	Peru
Metallura t. tyrianthina	32582	LSUMNS	Cajamarca	Peru
Metallura t. tyrianthina	IAvH.BT 1712	IAvH	Caldas	Colombia
Metallura t. tyrianthina	IAvH.BT 1737	IAvH	Caldas	Colombia
Metallura t. tyrianthina	IAvH.BT 1911	IAvH	Caldas	Colombia
Metallura t. tyrianthina	IAvH.BT 1946	IAvH	Caldas	Colombia
Metallura t. tyrianthina	15688	ANSP	Carchi	Ecuador
Metallura t. tyrianthina	IAvH.BT 2559	IAvH	Cundinamarca	Colombia
Metallura t. tyrianthina	162559	MSB	Lambayeque	Peru
Metallura t. tyrianthina	162566	MSB	Lambayeque	Peru
Metallura t. tyrianthina	162572	MSB	Lambayeque	Peru
Metallura t. tyrianthina	162584	MSB	Lambayeque	Peru
Metallura t. tyrianthina	162591	MSB	Lambayeque	Peru
Metallura t. tyrianthina	162599	MSB	Lambayeque	Peru
Metallura t. tyrianthina	162600	MSB	Lambayeque	Peru
Metallura t. tyrianthina	162602	MSB	Lambayeque	Peru
Metallura t. tyrianthina	162605	MSB	Lambayeque	Peru
Metallura t. tyrianthina	162606	MSB	Lambayeque	Peru
Metallura t. tyrianthina	162611	MSB	Lambayeque	Peru
Metallura t. tyrianthina	162653	MSB	Lambayeque	Peru
Metallura t. tyrianthina	162670	MSB	Lambayeque	Peru
Metallura t. tyrianthina	162689	MSB	Lambayeque	Peru
Metallura t. tyrianthina	162696	MSB	Lambayeque	Peru
Metallura t. tyrianthina	162699	MSB	Lambayeque	Peru
Metallura t. tyrianthina	162700	MSB	Lambayeque	Peru
Metallura t. tyrianthina	162704	MSB	Lambayeque	Peru
Metallura t. tyrianthina	162712	MSB	Lambayeque	Peru
Metallura t. tyrianthina	162719	MSB	Lambayeque	Peru
Metallura t. tyrianthina	162816	MSB	Lambayeque	Peru
Metallura t. tyrianthina	AMC 1019	AMC	Norte de Santander	Colombia
Metallura t. tyrianthina	AMC 930	AMC	Norte de Santander	Colombia
Metallura t. tyrianthina	SS 1159	AMC	Norte de Santander	Colombia
Metallura t. tyrianthina	SS 1178	AMC	Norte de Santander	Colombia
Metallura t. tyrianthina	SS 1193	AMC	Norte de Santander	Colombia
Metallura t. tyrianthina	SS 1328	AMC	Norte de Santander	Colombia
Metallura t. tyrianthina	IAvH.BT 4055	IAvH	Risaralda	Colombia
Metallura t. tyrianthina	IAvH.BT 4056	IAvH	Risaralda	Colombia
Metallura t. tyrianthina	JEAC 502	AMC	Santander	Colombia
Metallura t. tyrianthina	JEAC 503	AMC	Santander	Colombia

APPENDIX B:

SPECIMENS AND TISSUES USED FOR CHAPTER 2

This appendix presents museum specimens and tissue samples used for morphological measurements and sequence data for chapter two. This includes tissue numbers, catalog numbers; museum collection; Specific locality within Peru; coordinates used to obtain worldclim data; and whether the specimen was used for tissue only (T), morphological measurements (S), or both (B). Museum acronyms: Louisiana State University Museum of Natural Science (LSUMNS); Field Museum of Natural History (FMNH); University of Kansas Museum of Natural History (KUMNH); Museum of SouthIstern Biology (MSB); Centro de Ornitologia y Biodiversidad (CORBIDI). Specimens without catalog information have not been cataloged at their respective institutions.

Tissue #	Catalog #	Museum	Species	Locality	Use
		GenBank	*Metallura phoebe*		T
171724	34998	MSB	*septentrionalis*	Dpto. Ancash, Prov. Caraz; 14.0km SW Caraz	B
171752	35026	MSB	*septentrionalis*	Dpto. Ancash, Prov. Caraz; 14.0km SW Caraz	B
171654	34928	MSB	*septentrionalis*	Dpto. Ancash, Prov. Carhuaz; 16.0km SE Carhuaz	B
171656	34930	MSB	*septentrionalis*	Dpto. Ancash, Prov. Carhuaz; 16.0km SE Carhuaz	B
171665	34939	MSB	*septentrionalis*	Dpto. Ancash, Prov. Carhuaz; 16.0km SE Carhuaz	B
171670	34944	MSB	*septentrionalis*	Dpto. Ancash, Prov. Carhuaz; 16.0km SE Carhuaz	B
171677	34951	MSB	*septentrionalis*	Dpto. Ancash, Prov. Carhuaz; 16.0km SE Carhuaz	B
171696	34970	MSB	*septentrionalis*	Dpto. Ancash, Prov. Carhuaz; 16.0km SE Carhuaz	B
171714	34988	MSB	*septentrionalis*	Dpto. Ancash, Prov. Carhuaz; 16.0km SE Carhuaz	B
171718	34992	MSB	*septentrionalis*	Dpto. Ancash, Prov. Carhuaz; 16.0km SE Carhuaz	B
171719	34993	MSB	*septentrionalis*	Dpto. Ancash, Prov. Carhuaz; 16.0km SE Carhuaz	B
171710		MSB	*septentrionalis*	Dpto. Ancash, Prov. Carhuaz; 16.0km SE Carhuaz	S
171541	34815	MSB	*septentrionalis*	Dpto. Ancash, Prov. Santa; Macate	B
171543	34817	MSB	*septentrionalis*	Dpto. Ancash, Prov. Santa; Macate	B
171548	34822	MSB	*septentrionalis*	Dpto. Ancash, Prov. Santa; Macate	B
171549	34823	MSB	*septentrionalis*	Dpto. Ancash, Prov. Santa; Macate	B
171553	34827	MSB	*septentrionalis*	Dpto. Ancash, Prov. Santa; Macate	B
171592	34866	MSB	*septentrionalis*	Dpto. Ancash, Prov. Santa; Macate	B
173877	36046	MSB	*septentrionalis*	Dpto. Ancash;	T
	86026	LSUMNS	*septentrionalis*	Dpto. Ancash; 31 km (by road) E Paraicoto	S
	86027	LSUMNS	*septentrionalis*	Dpto. Ancash; 31 km (by road) E Paraicoto	S

	86029	LSUMNS	*septentrionalis*	Dpto. Ancash; 31 km (by road) E Paraicoto	S
	86030	LSUMNS	*septentrionalis*	Dpto. Ancash; 31 km (by road) E Paraicoto	S
	86031	LSUMNS	*septentrionalis*	Dpto. Ancash; 31 km (by road) E Paraicoto	S
	86032	LSUMNS	*septentrionalis*	Dpto. Ancash; 31 km (by road) E Paraicoto	S
	86033	LSUMNS	*septentrionalis*	Dpto. Ancash; 31 km (by road) E Paraicoto	S
	86034	LSUMNS	*septentrionalis*	Dpto. Ancash; 31 km (by road) E Paraicoto	S
	86035	LSUMNS	*septentrionalis*	Dpto. Ancash; 31 km (by road) E Paraicoto	S
	86036	LSUMNS	*septentrionalis*	Dpto. Ancash; 31 km (by road) E Paraicoto	S
	84491	LSUMNS	*septentrionalis*	Dpto. Cajamarca; 11.3km by road SW of Cutervo	S
	84490	LSUMNS	*septentrionalis*	Dpto. Cajamarca; 2 km SE Cutervo	S
	84492	LSUMNS	*septentrionalis*	Dpto. Cajamarca; 2 km SE Cutervo	S
	84488	LSUMNS	*septentrionalis*	Dpto. Cajamarca; 7 km N, 3 km E Chota	S
	84489	LSUMNS	*septentrionalis*	Dpto. Cajamarca; 7 km N, 3 km E Chota	S
	91951	LSUMNS	*septentrionalis*	Dpto. La Libertad; 22 road km W Shorey	S
	91952	LSUMNS	*septentrionalis*	Dpto. La Libertad; Quebrada La Caldera, 7km NE Tayabamba	S
168207	27001	MSB	*septentrionalis*	Dpto. Lima	T
18	31016	MSB	*septentrionalis*	Dpto. Lima	T
43	31038	MSB	*septentrionalis*	Dpto. Lima	T
163357	28467	MSB	*septentrionalis*	Dpto. Lima; dist. San Pedro de Casta; Pariangancha	B
	331184	LSUMNS	*smaragdinicollis*	Dpto. Amazonas; 20km W Leymebamba	S
	331185	LSUMNS	*smaragdinicollis*	Dpto. Amazonas; 20km W Leymebamba	S
	331187	LSUMNS	*smaragdinicollis*	Dpto. Amazonas; 20km W Leymebamba	S
	331188	LSUMNS	*smaragdinicollis*	Dpto. Amazonas; 20km W Leymebamba	S
	87552	LSUMNS	*smaragdinicollis*	Dpto. Amazonas; Cordillera Colan, E La Peca	S
	87553	LSUMNS	*smaragdinicollis*	Dpto. Amazonas; Cordillera Colan, E La Peca	S
	87554	LSUMNS	*smaragdinicollis*	Dpto. Amazonas; Cordillera Colan, E La Peca	S
	87555	LSUMNS	*smaragdinicollis*	Dpto. Amazonas; Cordillera Colan, E La Peca	S
	87558	LSUMNS	*smaragdinicollis*	Dpto. Amazonas; Cordillera Colan, E La Peca	S
	87556	LSUMNS	*smaragdinicollis*	Dpto. Amazonas; Cordillera Colan, E La Peca, ridge w of peaks	S
	87557	LSUMNS	*smaragdinicollis*	Dpto. Amazonas; Cordillera Colan, E La Peca, ridge w of peaks	S
	87550	LSUMNS	*smaragdinicollis*	Dpto. Amazonas; Cordillera Colan, SE La Peca	S
	87551	LSUMNS	*smaragdinicollis*	Dpto. Amazonas; Cordillera Colan, SE La Peca	S
	80488	LSUMNS	*smaragdinicollis*	Dpto. Amazonas; km404 on Balsas Leymebamba rd.	S
167844	32672	MSB	*smaragdinicollis*	Dpto. Amazonas; Prov. Utcubamba, dist. Lonya Grande	B
168886	33660	MSB	*smaragdinicollis*	Dpto. Apurimac	T
172670	35855	MSB	*smaragdinicollis*	Dpto. Apurimac;	T
169122	33896	MSB	*smaragdinicollis*	Dpto. Apurimac; 5 km W Huanipaca, Ccocha	B
169136	33910	MSB	*smaragdinicollis*	Dpto. Apurimac; 5 km W Huanipaca, Ccocha	T
169152	33926	MSB	*smaragdinicollis*	Dpto. Apurimac; 5 km W Huanipaca, Ccocha	B
169159	33933	MSB	*smaragdinicollis*	Dpto. Apurimac; 5 km W Huanipaca, Ccocha	T
169162	33936	MSB	*smaragdinicollis*	Dpto. Apurimac; 5 km W Huanipaca, Ccocha	T
169170	33944	MSB	*smaragdinicollis*	Dpto. Apurimac; 5 km W Huanipaca, Ccocha	B
169180	33954	MSB	*smaragdinicollis*	Dpto. Apurimac; 5 km W Huanipaca, Ccocha	B
169183	33957	MSB	*smaragdinicollis*	Dpto. Apurimac; 5 km W Huanipaca, Ccocha	T
169190	33964	MSB	*smaragdinicollis*	Dpto. Apurimac; 5 km W Huanipaca, Ccocha	B
169212	33986	MSB	*smaragdinicollis*	Dpto. Apurimac; 5 km W Huanipaca, Ccocha	T
169213	33987	MSB	*smaragdinicollis*	Dpto. Apurimac; 5 km W Huanipaca, Ccocha	B
169216	33990	MSB	*smaragdinicollis*	Dpto. Apurimac; 5 km W Huanipaca, Ccocha	B
169220	33994	MSB	*smaragdinicollis*	Dpto. Apurimac; 5 km W Huanipaca, Ccocha	T

169233	34007	MSB	*smaragdinicollis*	Dpto. Apurimac; 5 km W Huanipaca, Ccocha	B
169234	34008	MSB	*smaragdinicollis*	Dpto. Apurimac; 5 km W Huanipaca, Ccocha	T
169241	34015	MSB	*smaragdinicollis*	Dpto. Apurimac; 5 km W Huanipaca, Ccocha	T
169242	34016	MSB	*smaragdinicollis*	Dpto. Apurimac; 5 km W Huanipaca, Ccocha	B
169248	34022	MSB	*smaragdinicollis*	Dpto. Apurimac; 5 km W Huanipaca, Ccocha	B
169123		MSB	*smaragdinicollis*	Dpto. Apurimac; 5 km W Huanipaca, Ccocha	S
169137		MSB	*smaragdinicollis*	Dpto. Apurimac; 5 km W Huanipaca, Ccocha	S
16999		CORBIDI	*smaragdinicollis*	Dpto. Ayacucho; 2 km S Ccano	B
17168		CORBIDI	*smaragdinicollis*	Dpto. Ayacucho; 2 km S Ccano	B
25113		KUMNH	*smaragdinicollis*	Dpto. Ayacucho; 2 km S Ccano	T
25141		KUMNH	*smaragdinicollis*	Dpto. Ayacucho; 2 km S Ccano	T
	433153	FMNH	*smaragdinicollis*	Dpto. Cusco, Paucartambo, La Esperanza	T
	433154	FMNH	*smaragdinicollis*	Dpto. Cusco, Paucartambo, La Esperanza	B
	433156	FMNH	*smaragdinicollis*	Dpto. Cusco, Paucartambo, La Esperanza	B
	433157	FMNH	*smaragdinicollis*	Dpto. Cusco, Paucartambo, La Esperanza	T
	433158	FMNH	*smaragdinicollis*	Dpto. Cusco, Paucartambo, La Esperanza	T
	433160	FMNH	*smaragdinicollis*	Dpto. Cusco, Paucartambo, La Esperanza	S
	429933	FMNH	*smaragdinicollis*	Dpto. Cusco, Paucartambo, Pillahuata	B
	429935	FMNH	*smaragdinicollis*	Dpto. Cusco, Paucartambo, Pillahuata	S
	397844	FMNH	*smaragdinicollis*	Dpto. Cusco, Paucartambo, Puesto de Vigilancia de Acjanaco	S
	397845	FMNH	*smaragdinicollis*	Dpto. Cusco, Paucartambo, Puesto de Vigilancia de Acjanaco	S
	397849	FMNH	*smaragdinicollis*	Dpto. Cusco, Paucartambo, Puesto de Vigilancia de Acjanaco	T
	397850	FMNH	*smaragdinicollis*	Dpto. Cusco, Paucartambo, Puesto de Vigilancia de Acjanaco	S
	397851	FMNH	*smaragdinicollis*	Dpto. Cusco, Paucartambo, Puesto de Vigilancia de Acjanaco	T
	397852	FMNH	*smaragdinicollis*	Dpto. Cusco, Paucartambo, Puesto de Vigilancia de Acjanaco	S
	291606	FMNH	*smaragdinicollis*	Dpto. Cusco, Pillahuata, km#126 on Cosñipata Hwy.	S
	311776	FMNH	*smaragdinicollis*	Dpto. Cusco, Pillahuata, km#126 on Cosñipata Hwy.	S
	311778	FMNH	*smaragdinicollis*	Dpto. Cusco, Pillahuata, km#126 on Cosñipata Hwy.	S
168793		MSB	*smaragdinicollis*	Dpto. Cusco, Prov. Marcapata, Distrito Corani, Chile Chile	S
172642	35827	MSB	*smaragdinicollis*	Dpto. Cusco, Prov. Paucartambo; 9.6km NE Paucartambo	B
172644	35829	MSB	*smaragdinicollis*	Dpto. Cusco, Prov. Paucartambo; 9.6km NE Paucartambo	B
172645	35830	MSB	*smaragdinicollis*	Dpto. Cusco, Prov. Paucartambo; 9.6km NE Paucartambo	B
172635	35820	MSB	*smaragdinicollis*	Dpto. Cusco; 2.5km E Carrizales, Puente de la Swerena	B
172618	35803	MSB	*smaragdinicollis*	Dpto. Cusco; 3.7km SE Carrizales	B
172619	35804	MSB	*smaragdinicollis*	Dpto. Cusco; 3.7km SE Carrizales	B
172622	35807	MSB	*smaragdinicollis*	Dpto. Cusco; 3.7km SE Carrizales	B
172623	35808	MSB	*smaragdinicollis*	Dpto. Cusco; 3.7km SE Carrizales	B
	433153	FMNH	*smaragdinicollis*	Dpto. Cusco; Paucartambo, La Esperanza	S
	433161	FMNH	*smaragdinicollis*	Dpto. Cusco; Paucartambo, La Esperanza	S
	429932	FMNH	*smaragdinicollis*	Dpto. Cusco; Paucartambo, Pillahuata	T
	429934	FMNH	*smaragdinicollis*	Dpto. Cusco; Paucartambo, Pillahuata	T
	429935	FMNH	*smaragdinicollis*	Dpto. Cusco; Paucartambo, Pillahuata	S
175554	36590	MSB	*smaragdinicollis*	Dpto. Cusco; Prov. Paucartambo, Distrito Challabamba	B
175557	36593	MSB	*smaragdinicollis*	Dpto. Cusco; Prov. Paucartambo, Distrito Challabamba	B
175558	36594	MSB	*smaragdinicollis*	Dpto. Cusco; Prov. Paucartambo, Distrito Challabamba	B
175559	36595	MSB	*smaragdinicollis*	Dpto. Cusco; Prov. Paucartambo, Distrito Challabamba	B
172400	35674	MSB	*smaragdinicollis*	Dpto. Cusco; Prov. Paucartambo, distrito Pillahuata	B
172402	35676	MSB	*smaragdinicollis*	Dpto. Cusco; Prov. Paucartambo, distrito Pillahuata	B
172404	35678	MSB	*smaragdinicollis*	Dpto. Cusco; Prov. Paucartambo, distrito Pillahuata	B

172405	35679	MSB	*smaragdinicollis*	Dpto. Cusco; Prov. Paucartambo, distrito Pillahuata	B
172409	35683	MSB	*smaragdinicollis*	Dpto. Cusco; Prov. Paucartambo, distrito Pillahuata	B
159881	27214	MSB	*smaragdinicollis*	Dpto. Cusco; Prov. Urubamba	B
168292	33073	MSB	*smaragdinicollis*	Dpto. Cusco; Prov. Urubamba	B
175560	36596	MSB	*smaragdinicollis*	Dpto. Cusco; Prov. Urubamba, near Carrizales	B
159846	27185	MSB	*smaragdinicollis*	Dpto. Cusco; Prov. Urubamba, 7.9 km NW Urubamba	B
159847	27186	MSB	*smaragdinicollis*	Dpto. Cusco; Prov. Urubamba, 7.9 km NW Urubamba	B
159870	27205	MSB	*smaragdinicollis*	Dpto. Cusco; Prov. Urubamba, 7.9 km NW Urubamba	B
159885	27216	MSB	*smaragdinicollis*	Dpto. Cusco; Prov. Urubamba, 7.9 km NW Urubamba	B
159812	31191	MSB	*smaragdinicollis*	Dpto. Cusco; Prov. Urubamba, 7.9 km NW Urubamba	B
159838	31192	MSB	*smaragdinicollis*	Dpto. Cusco; Prov. Urubamba, 7.9 km NW Urubamba	B
159851	31193	MSB	*smaragdinicollis*	Dpto. Cusco; Prov. Urubamba, 7.9 km NW Urubamba	B
159862	31195	MSB	*smaragdinicollis*	Dpto. Cusco; Prov. Urubamba, 7.9 km NW Urubamba	B
159867	31196	MSB	*smaragdinicollis*	Dpto. Cusco; Prov. Urubamba, 7.9 km NW Urubamba	B
159871	31197	MSB	*smaragdinicollis*	Dpto. Cusco; Prov. Urubamba, 7.9 km NW Urubamba	B
159879	31198	MSB	*smaragdinicollis*	Dpto. Cusco; Prov. Urubamba, 7.9 km NW Urubamba	B
159883	31199	MSB	*smaragdinicollis*	Dpto. Cusco; Prov. Urubamba, 7.9 km NW Urubamba	B
159884	31200	MSB	*smaragdinicollis*	Dpto. Cusco; Prov. Urubamba, 7.9 km NW Urubamba	B
159893	31201	MSB	*smaragdinicollis*	Dpto. Cusco; Prov. Urubamba, 7.9 km NW Urubamba	B
159895	31202	MSB	*smaragdinicollis*	Dpto. Cusco; Prov. Urubamba, 7.9 km NW Urubamba	B
159897	31203	MSB	*smaragdinicollis*	Dpto. Cusco; Prov. Urubamba, 7.9 km NW Urubamba	B
168288	33069	MSB	*smaragdinicollis*	Dpto. Cusco; Prov. Urubamba, Ollantaytambo	B
159888	27219	MSB	*smaragdinicollis*	Dpto. Cusco; Prov. Urubamba; 7.9km NW Urubamba	B
159896	27225	MSB	*smaragdinicollis*	Dpto. Cusco; Prov. Urubamba; 7.9km NW Urubamba	B
	73903	LSUMNS	*smaragdinicollis*	Dpto. Huanuco; base of Bosque Tapra above Acomayo	S
163132	31567	MSB	*smaragdinicollis*	Dpto. Huanuco; Prov. Pachitea, Chincho Ocomayo, Carpish Tunnel	B
163154	31589	MSB	*smaragdinicollis*	Dpto. Huanuco; Prov. Pachitea, Chincho Ocomayo, Carpish Tunnel	B
163196	31631	MSB	*smaragdinicollis*	Dpto. Huanuco; Prov. Pachitea, Chincho Ocomayo, Carpish Tunnel	B
163214	31649	MSB	*smaragdinicollis*	Dpto. Huanuco; Prov. Pachitea, Chincho Ocomayo, Carpish Tunnel	B
163121		MSB	*smaragdinicollis*	Dpto. Huanuco; Prov. Pachitea, Chincho Ocomayo, Carpish Tunnel	S
163198		MSB	*smaragdinicollis*	Dpto. Huanuco; Prov. Pachitea, Chincho Ocomayo, Carpish Tunnel	S
163120	31555	MSB	*smaragdinicollis*	Dpto. Huanuco; Prov. Pachitea; Chincho ocomayo, Carpish Tunnel	B
168227	27020	MSB	*smaragdinicollis*	Dpto. Junin	T
213	31164	MSB	*smaragdinicollis*	Dpto. Junin;	T
218	31169	MSB	*smaragdinicollis*	Dpto. Junin;	T
228	31179	MSB	*smaragdinicollis*	Dpto. Junin;	T
	127598	LSUMNS	*smaragdinicollis*	Dpto. Junin; Pampa Huasi, 12km SE Calabaza	S
	127599	LSUMNS	*smaragdinicollis*	Dpto. Junin; Pampa Huasi, 12km SE Calabaza	S
	127588	LSUMNS	*smaragdinicollis*	Dpto. Junin; via Satipo, Chanchuleo, ca. 8km SE de Calabaza	S
	127590	LSUMNS	*smaragdinicollis*	Dpto. Junin; via Satipo, Chanchuleo, ca. 8km SE de Calabaza	S
	127592	LSUMNS	*smaragdinicollis*	Dpto. Junin; via Satipo, Chanchuleo, ca. 8km SE de Calabaza	S
	127594	LSUMNS	*smaragdinicollis*	Dpto. Junin; via Satipo, Chanchuleo, ca. 8km SE de Calabaza	S
	127595	LSUMNS	*smaragdinicollis*	Dpto. Junin; via Satipo, Chanchuleo, ca. 8km SE de Calabaza	S
	127596	LSUMNS	*smaragdinicollis*	Dpto. Junin; via Satipo, Chanchuleo, ca. 8km SE de Calabaza	S
	91953	LSUMNS	*smaragdinicollis*	Dpto. La Libertad; Mashua, E Tayabamba on trail to Ongon	S
	91954	LSUMNS	*smaragdinicollis*	Dpto. La Libertad; Mashua, E Tayabamba on trail to Ongon	S
172370	35644	MSB	*smaragdinicollis*	Dpto. Pasco;	T
	128363	LSUMNS	*smaragdinicollis*	Dpto. Pasco; 2 km NW Punta de Saria on Pozuzo-Chaglla trail	S
	128364	LSUMNS	*smaragdinicollis*	Dpto. Pasco; 2 km NW Punta de Saria on Pozuzo-Chaglla trail	S

	105801	LSUMNS	*smaragdinicollis*	Dpto. Pasco; Cumbre de Ollon, ca 12 km E Oxapampa	S
	128352	LSUMNS	*smaragdinicollis*	Dpto. Pasco; Millpo, E Tambo de Vacas on Pozuzo-Chaglla trail	S
	128353	LSUMNS	*smaragdinicollis*	Dpto. Pasco; Millpo, E Tambo de Vacas on Pozuzo-Chaglla trail	S
8218	128354	LSUMNS	*smaragdinicollis*	Dpto. Pasco; Millpo, E Tambo de Vacas on Pozuzo-Chaglla trail	S
	128355	LSUMNS	*smaragdinicollis*	Dpto. Pasco; Millpo, E Tambo de Vacas on Pozuzo-Chaglla trail	S
	128356	LSUMNS	*smaragdinicollis*	Dpto. Pasco; Millpo, E Tambo de Vacas on Pozuzo-Chaglla trail	S
	128357	LSUMNS	*smaragdinicollis*	Dpto. Pasco; Millpo, E Tambo de Vacas on Pozuzo-Chaglla trail	S
	128358	LSUMNS	*smaragdinicollis*	Dpto. Pasco; Millpo, E Tambo de Vacas on Pozuzo-Chaglla trail	S
	128359	LSUMNS	*smaragdinicollis*	Dpto. Pasco; Millpo, E Tambo de Vacas on Pozuzo-Chaglla trail	S
	128360	LSUMNS	*smaragdinicollis*	Dpto. Pasco; Millpo, E Tambo de Vacas on Pozuzo-Chaglla trail	S
	128361	LSUMNS	*smaragdinicollis*	Dpto. Pasco; Millpo, E Tambo de Vacas on Pozuzo-Chaglla trail	S
	128362	LSUMNS	*smaragdinicollis*	Dpto. Pasco; Millpo, E Tambo de Vacas on Pozuzo-Chaglla trail	S
21169	115538	KUMNH	*smaragdinicollis*	Dpto. Puno; Sina	T
21195		KUMNH	*smaragdinicollis*	Dpto. Puno; Sina	T
	98177	LSUMNS	*smaragdinicollis*	Dpto. Puno; Valcon, 5 km NNW Quiaca	S
	98180	LSUMNS	*smaragdinicollis*	Dpto. Puno; Valcon, 5 km NNW Quiaca	S
	98181	LSUMNS	*smaragdinicollis*	Dpto. Puno; Valcon, 5 km NNW Quiaca	S
	98182	LSUMNS	*smaragdinicollis*	Dpto. Puno; Valcon, 5 km NNW Quiaca	S
	98183	LSUMNS	*smaragdinicollis*	Dpto. Puno; Valcon, 5 km NNW Quiaca	S
	98184	LSUMNS	*smaragdinicollis*	Dpto. Puno; Valcon, 5 km NNW Quiaca	S
	98185	LSUMNS	*smaragdinicollis*	Dpto. Puno; Valcon, 5 km NNW Quiaca	S
43672	173884	LSUMNS	*smaragdinicollis*	Dpto. San Martin; ca. km ENE Florida	S
43711	173885	LSUMNS	*smaragdinicollis*	Dpto. San Martin; ca. km ENE Florida	B
43683		LSUMNS	*smaragdinicollis*	Dpto. San Martin; ca. km ENE Florida	T
	104463	LSUMNS	*smaragdinicollis*	Dpto. San Martin; Puerta del Monte, ca. 30km NE Los Alisos	S
	AQ 222	CORBIDI	*tyrianthina*	Dpto. Cajamarca; prov. Chota; distr. Queracoto, La Granja, Pagaibamba	S
	AQ 227	CORBIDI	*tyrianthina*	Dpto. Cajamarca; prov. Chota; distr. Queracoto, La Granja, Pagaibamba	S
	AQ 228	CORBIDI	*tyrianthina*	Dpto. Cajamarca; prov. Chota; distr. Queracoto, La Granja, Pagaibamba	S
	AQ 231	CORBIDI	*tyrianthina*	Dpto. Cajamarca; prov. Chota; distr. Queracoto, La Granja, Pagaibamba	S
	AQ 234	CORBIDI	*tyrianthina*	Dpto. Cajamarca; prov. Chota; distr. Queracoto, La Granja, Pagaibamba	S
	AQ 245	CORBIDI	*tyrianthina*	Dpto. Cajamarca; prov. Chota; distr. Queracoto, La Granja, Pagaibamba	S
	AQ 263	CORBIDI	*tyrianthina*	Dpto. Cajamarca; prov. Chota; distr. Queracoto, La Granja, Pagaibamba	S
	AQ 265	CORBIDI	*tyrianthina*	Dpto. Cajamarca; prov. Chota; distr. Queracoto, La Granja, Pagaibamba	S
	AQ 266	CORBIDI	*tyrianthina*	Dpto. Cajamarca; prov. Chota; distr. Queracoto, La Granja, Pagaibamba	S
	AQ 276	CORBIDI	*tyrianthina*	Dpto. Cajamarca; prov. Chota; distr. Queracoto, La Granja, Pagaibamba	S
	JAN 808	CORBIDI	*tyrianthina*	Dpto. Cajamarca; prov. Chota; distr. Queracoto, La Granja, Pagaibamba	S
	JAN 809	CORBIDI	*tyrianthina*	Dpto. Cajamarca; prov. Chota; distr. Queracoto, La Granja, Pagaibamba	S
	JAN 810	CORBIDI	*tyrianthina*	Dpto. Cajamarca; prov. Chota; distr. Queracoto, La Granja, Pagaibamba	S
	JAN 811	CORBIDI	*tyrianthina*	Dpto. Cajamarca; prov. Chota; distr. Queracoto, La Granja, Pagaibamba	S
	JNZ 335	CORBIDI	*tyrianthina*	Dpto. Cajamarca; prov. Chota; distr. Queracoto, La Granja, Pagaibamba	S
	JNZ 348	CORBIDI	*tyrianthina*	Dpto. Cajamarca; prov. Chota; distr. Queracoto, La Granja, Pagaibamba	S
	JNZ 357	CORBIDI	*tyrianthina*	Dpto. Cajamarca; prov. Chota; distr. Queracoto, La Granja, Pagaibamba	S
	LA 007	CORBIDI	*tyrianthina*	Dpto. Cajamarca; prov. Chota; distr. Queracoto, La Granja, Pagaibamba	S
	LA 010	CORBIDI	*tyrianthina*	Dpto. Cajamarca; prov. Chota; distr. Queracoto, La Granja, Pagaibamba	S
	LA 008	CORBIDI	*tyrianthina*	Dpto. Cajamarca; prov. Chota; distr. Queracoto, La Granja, Pagaibamba	S
55825	178963	LSUMNS	*tyrianthina*	Dpto. Cajamarca; Hito Jesus	S
56379	178964	LSUMNS	*tyrianthina*	Dpto. Cajamarca; Hito Jesus	S
31730	169715	LSUMNS	*tyrianthina*	Dpto. Cajamarca; Quebrada Lanchal, ca. 8km ESE Sallique	S
31729	169716	LSUMNS	*tyrianthina*	Dpto. Cajamarca; Quebrada Lanchal, ca. 8km ESE Sallique	S

31736	169717	LSUMNS	*tyrianthina*	Dpto. Cajamarca; Quebrada Lanchal, ca. 8km ESE Sallique	S
31741	169718	LSUMNS	*tyrianthina*	Dpto. Cajamarca; Quebrada Lanchal, ca. 8km ESE Sallique	S
31787	169719	LSUMNS	*tyrianthina*	Dpto. Cajamarca; Quebrada Lanchal, ca. 8km ESE Sallique	S
31774	169720	LSUMNS	*tyrianthina*	Dpto. Cajamarca; Quebrada Lanchal, ca. 8km ESE Sallique	S
32000	169721	LSUMNS	*tyrianthina*	Dpto. Cajamarca; Quebrada Lanchal, ca. 8km ESE Sallique	B
32098	169722	LSUMNS	*tyrianthina*	Dpto. Cajamarca; Quebrada Lanchal, ca. 8km ESE Sallique	B
32521	169723	LSUMNS	*tyrianthina*	Dpto. Cajamarca; Quebrada Lanchal, ca. 8km ESE Sallique	S
32582	169724	LSUMNS	*tyrianthina*	Dpto. Cajamarca; Quebrada Lanchal, ca. 8km ESE Sallique	B
32073	CCW 140	LSUMNS	*tyrianthina*	Dpto. Cajamarca; Quebrada Lanchal, ca. 8km ESE Sallique	B
32431	CCW 216	LSUMNS	*tyrianthina*	Dpto. Cajamarca; Quebrada Lanchal, ca. 8km ESE Sallique	B
31842	JPO 7871	LSUMNS	*tyrianthina*	Dpto. Cajamarca; Quebrada Lanchal, ca. 8km ESE Sallique	S
31788	RCF 646	LSUMNS	*tyrianthina*	Dpto. Cajamarca; Quebrada Lanchal, ca. 8km ESE Sallique	S
32100	RCF 702	LSUMNS	*tyrianthina*	Dpto. Cajamarca; Quebrada Lanchal, ca. 8km ESE Sallique	S
31974		LSUMNS	*tyrianthina*	Dpto. Cajamarca; Quebrada Lanchal, ca. 8km ESE Sallique	T
32101		LSUMNS	*tyrianthina*	Dpto. Cajamarca; Quebrada Lanchal, ca. 8km ESE Sallique	T
32520		LSUMNS	*tyrianthina*	Dpto. Cajamarca; Quebrada Lanchal, ca. 8km ESE Sallique	T
162602	28081	MSB	*tyrianthina*	Dpto. Lambayeque;	B
162605	28083	MSB	*tyrianthina*	Dpto. Lambayeque;	B
162606	28084	MSB	*tyrianthina*	Dpto. Lambayeque;	B
162653	28124	MSB	*tyrianthina*	Dpto. Lambayeque;	B
162653	28124	MSB	*tyrianthina*	Dpto. Lambayeque;	T
162670	31339	MSB	*tyrianthina*	Dpto. Lambayeque;	T
162768		MSB	*tyrianthina*	Dpto. Lambayeque;	S
162773		MSB	*tyrianthina*	Dpto. Lambayeque;	S
162775		MSB	*tyrianthina*	Dpto. Lambayeque;	S
162781		MSB	*tyrianthina*	Dpto. Lambayeque;	S
162782		MSB	*tyrianthina*	Dpto. Lambayeque;	S
162785		MSB	*tyrianthina*	Dpto. Lambayeque;	S
162788		MSB	*tyrianthina*	Dpto. Lambayeque;	S
162803		MSB	*tyrianthina*	Dpto. Lambayeque;	S
162815		MSB	*tyrianthina*	Dpto. Lambayeque;	S
162816		MSB	*tyrianthina*	Dpto. Lambayeque;	B
162820		MSB	*tyrianthina*	Dpto. Lambayeque;	S
162534		MSB	*tyrianthina*	Dpto. Lambayeque; Dos Lagunas	S
162572	28061	MSB	*tyrianthina*	Dpto. Lambayeque; Tres Lagunas	T
162559	31314	MSB	*tyrianthina*	Dpto. Lambayeque; Tres Lagunas	B
162566	31315	MSB	*tyrianthina*	Dpto. Lambayeque; Tres Lagunas	B
162566	31315	MSB	*tyrianthina*	Dpto. Lambayeque; Tres Lagunas	T
162584	31321	MSB	*tyrianthina*	Dpto. Lambayeque; Tres Lagunas	T
162591	31323	MSB	*tyrianthina*	Dpto. Lambayeque; Tres Lagunas	B
162600	31326	MSB	*tyrianthina*	Dpto. Lambayeque; Tres Lagunas	B
162611	31328	MSB	*tyrianthina*	Dpto. Lambayeque; Tres Lagunas	B
162689	31344	MSB	*tyrianthina*	Dpto. Lambayeque; Tres Lagunas	B
162696	31348	MSB	*tyrianthina*	Dpto. Lambayeque; Tres Lagunas	B
162699	31350	MSB	*tyrianthina*	Dpto. Lambayeque; Tres Lagunas	B
162700	31351	MSB	*tyrianthina*	Dpto. Lambayeque; Tres Lagunas	B
162704	31353	MSB	*tyrianthina*	Dpto. Lambayeque; Tres Lagunas	B
162712	31357	MSB	*tyrianthina*	Dpto. Lambayeque; Tres Lagunas	T
162719	31359	MSB	*tyrianthina*	Dpto. Lambayeque; Tres Lagunas	T

162592		MSB	*tyrianthina*	Dpto. Lambayeque; Tres Lagunas	B
162711		MSB	*tyrianthina*	Dpto. Lambayeque; Tres Lagunas	S
162740		MSB	*tyrianthina*	Dpto. Lambayeque; Tres Lagunas	S
162750		MSB	*tyrianthina*	Dpto. Lambayeque; Tres Lagunas	S
162759		MSB	*tyrianthina*	Dpto. Lambayeque; Tres Lagunas	S
162765		MSB	*tyrianthina*	Dpto. Lambayeque; Tres Lagunas	S
162771		MSB	*tyrianthina*	Dpto. Lambayeque; Tres Lagunas	S
162776		MSB	*tyrianthina*	Dpto. Lambayeque; Tres Lagunas	S
162783		MSB	*tyrianthina*	Dpto. Lambayeque; Tres Lagunas	S
162789		MSB	*tyrianthina*	Dpto. Lambayeque; Tres Lagunas	S
162801		MSB	*tyrianthina*	Dpto. Lambayeque; Tres Lagunas	S
162802		MSB	*tyrianthina*	Dpto. Lambayeque; Tres Lagunas	S
162806		MSB	*tyrianthina*	Dpto. Lambayeque; Tres Lagunas	S
162821		MSB	*tyrianthina*	Dpto. Lambayeque; Tres Lagunas	S
	78123	LSUMNS	*tyrianthina*	Dpto. Piura; 33km (by road) SW Huancabamba	S
	78122	LSUMNS	*tyrianthina*	Dpto. Piura; 35km (by road) SW Huancabamba	S

LITERATURE CITED

Akaike, H. (1974) A new look at the statistical model identification. *IEEE Transactions on Automatic Control,* **19**:716-723.

Altshuler, D.L. (2006) Flight performance and competitive displacement of hummingbirds across elevational gradients. *American Naturalist*, **167**: 216-229.

Arbogast, B.S., Edwards, S.V., Wakeley, J., Beerli, P. & Slowinski, J.B. (2002) Estimating Divergence times from molecular data on phylogenetic and population genetic timescales. *Annual Review of Ecology and Systematics,* **33**: 707-740.

Arbogast, B.S., Drovetski, S.V., Curry, R.L., Boag, P.T., Seutin, G., Grant, P.R., Grant, B.R., Anderson, D.J. (2006) The origin and diversification of Galapagos mockingbirds. *Evolution,* **60**: 370–382.

Bates, J.M. & Zink, R.M. (1994) Evolution into the Andes: molecular evidence for species relationships in the genus *Leptopogon*. *The Auk,* **111**: 507-515.

Bandelt, H.J., Forster, P. & Rohl, A. (1999) Median-joining networks for inferring intraspecific phylogenies. *Molecular Biology and Evolution,* **16**: 37-48.

Bleiweiss, R., Kirsch, J.A.W. & Matheus, J.C. (1997) DNA-hybridization evidence for the major lineages of hummingbirds (Aves: Trochilidae). *Molecular Biology and Evolution,* **14**: 325-343.

Bleiweiss, R. (1999) Joint effects of feeding and breeding behavior on trophic dimorphism in hummingbirds. *Proceedings of the Royal Society B.,* **266**: 2491-2497.

Burns, K.J. & Naoki, K. (2004) Molecular phylogenetics and biogeography of Neotropical tanagers in the genus *Tangara*. *Molecular Phylogenetics and Evolution,* **32**: 838-854.

Cadena, C.D., Klicka, J. & Ricklefs, R.E. (2007) Evolutionary differentiation in the Neotropical montane region: molecular phylogenetics and phylogeography of *Buarremon* brush-finches (Aves, Emberizidae). *Molecular Phylogenetics and Evolution,* **44**: 993-1016.

Cadena, C.D. (2007) Testing the role of interspecific competition in the evolutionary origin of elevational zonation: an example with *Buarremon* brush-finches (Aves, Emberizidae) in the Neotropical mountains. *Evolution,* 1120-1136.

Cadena, C.D. & Cuervo, A.M. (2010) Molecules, ecology, morphology, and song in concert: How many species is *Arremon torquatus* (Aves: Emberizidae)? *Biological Journal of The Linnean Society,* **199**: 152-176.

Cadena, C.D., Cheviron, Z.A. & Funk, W.C. (2011) Testing the molecular and evolutionary causes of a 'leapfrog' pattern of geographical variation in coloration. *Journal of Evolutionary Biology*, **24:** 402-414.

Chapman, F.M. (1917) The Distribution of Bird-life in Colombia. *Bulletin of the American Museum of Natural History,* **36:** 1-729.

Chapman, F.M. (1926) The Distribution of Bird-life in Ecuador: A contribution to a study Of the Origin of Andean Bird-life. *Bulletin of the American Museum of Natural History,* **55**: 1-784.

Chaves, J.A., Pollinger, J.P., Smith, T.B. & LeBuhn, G. (2007) The role of geography and ecology in shaping the phylogeography of the Speckled Hummingbird (*Adelomyia melanogenys*) in Ecuador. *Molecular Phylogenetics and Evolution,* **43**: 795-807.

Chaves, J.A. & Smith, T.B. (2011) Evolutionary patterns of diversification in the Andean hummingbird genus *Adelomyia*. *Molecular phylogenetics and Evolution,* **60**: 207-218.

Chaves, J.A., Weir, J.T. & Smith, T.B. (2011) Diversification in *Adelomyia* hummingbirds follows Andean uplift. *Molecular Ecology,* **20**: 4564-4576.

Chesser, R.T. (2000) Evolution in the high Andes: the phylogenetics of *Muscisaxicola* Ground-Tyrants. *Molecular Phylogenetics and Evolution,* **15**: 369-380.

Cory, C.B. (1918) *Catalogue of Birds of the Americas*. Field Mus. Nat. Hist. Publ., Zool. Ser., Vol. 13, Pt. 2, No. 1.

Coyne, J.A. & Price, T.D. (2000) Little evidence for sympatric speciation in island birds. *Evolution,* **54**: 2166-2171.

Coyne, J.A. & Orr, H.A. (2004) *Speciation*. Sinauer Associates, Inc., Sunderland, Massachussetts, USA.

Cracraft, J. (1985) Historical biogeography and patterns of differentiation within the South American avifauna: areas of endemism. *Ornithological Monographs,* **36**: 49-84.

Dalgaard, P. (2008) Introductory statistics with R, 2nd ed. Springer Science + Business Media, LLC, New York, New York, USA.

Diamond, J.M. (1973) Distributional ecology of New Guinea birds. *Science,* **179**: 759-

769.

Doan, T.M. (2003) A south-to-north biogeographic hypothesis for Andean speciation: evidence from lizard genus Proctoporus (Reptilia, Gymnophthalmidae). *Journal of Biogeography,* **30:** 361–374.

Doebeli, M. & Dieckmann, U. (2003) Speciation along environmental gradients. *Nature*, **421**: 259-264.

Drummond, A.J., Suchard, M.A., Xie, D. & Rambaut, A. A Bayesian phylogenetics with BEAUti and BEAST 1.7. *Molecular Biology and Evolution*, In press

Drummond, A.J., Ho, S.Y.W, Phillips, M.J. & Rambaut, A. (2006) Relaxed phylogenetics and dating with confidence. *PLoS Biology,* **4**: e88.

Drummond, A.J. & Rambaut, A (2007a) Tracer v.1.4 available from: http://beast.bio.ed.ac.uk/Tracer.

Drummond, A.J. & Rambaut, A (2007b) LogCombiner v.1.7.1 available from: http://beast.bio.ed.ac.uk/LogCombiner.

Drummond, A.J. & Rambaut, A (2007c) TreeAnnotator v.1.7.1 available from: http://beast.bio.ed.ac.uk/TreeAnnotator.

Dunning, Jr., J.B. (1993) *CRC Handbook of Avian Body Masses*. CRC Press, Boca Raton, USA.

Edgar, R.C. (2004) MUSCLE: multiple sequence alignment with high accuracy and high throughput. *Nucleic Acids Research,* **32**: 1792-1797.

Edwards, S.V. & Beerli, P. (2000) Perspective: Gene divergence, population divergence, and the variance in coalescence time in phylogeographic studies. *Evolution*, **54**: 1839-1854.

Edwards, S.V. (2009) Is a new and general theory of molecular systematics emerging? *Evolution*, **63**: 1-19.

Excoffier, L., Laval, G. & Schneider, S. (2005) Arlequin ver. 3.0: An integrated software package for population genetics data analysis. *Evolutionary Bioinformatics Online*, **1**: 47-50.

Fjeldsa, J. (1994) Geographical patterns for relict and young species of birds in Africa and South America and implications for conservation priorities. *Biodiversity and Conservation*, **3**: 207-226.

Fjeldsa, J. and Krabbe, K. (1990) *Birds of the High Andes.* Apollo Books, Copenhagen, Denmark.

Floréz-Rodríquez, A., Carling, M.D. & Cadena, C.D. (2011) Reconstructing the phylogeny of *"Buarremon"* brush-finches and near-relatives (Aves: Emberizidae) from individual gene trees. *Molecular Phylogenetics and Evolution*, **58**: 297-303.

Fuchs, J, Chen, S., Johnson, J.A. & Mindell, D.P. (2011) Pliocene diversification within the South American forest falcons (Falconidae: *Micrastur*). *Molecular Phylogenetics and Evolution,* **60:** 398-407.

Garcia-Moreno, J., Arctander, P. & Fjeldsa, J. (1999a) Strong diversification at the treeline among *Metallura* hummingbirds. *The Auk,* **116**: 702-711.

Garcia-Moreno, J., Arctander, P. & Fjeldsa, J. (1999b) A case of rapid diversification in the neotropics: phylogenetic relationships among *Cranioleuca* spinetails (Aves: Furnaraiidae). *Molecular Phylogenetics and Evolution,* **12**: 273-281.

Garzione, C.N., Hoke, G.D., Libarkin, J.C., Withers, S., MacFadden, B., Eiler, J., Gosh, P. & Mulch, A. (2008) Rise of the Andes. *Science,* **320**: 1304-1307.

Gavrilets, S. (2000) Waiting time to parapatric speciation. *Proceedings of the Royal Society B,* **267**: 2483-2492.

Gavrilets, S., Li, H. & Vose, M.D. (2000) Patterns of parapatric speciation. *Evolution*, **54**: 1126-1134.

Grant, P.R. & Grant, B.R. (2008) *How and why species multiply: the radiation of Darwin's finches.* Princeton University Press, Princeton, New Jersey, USA.

Graves, G.R. (1988) Linearity of geographic range and its possible effect on the population structure of Andean birds. *The Auk,* **105**: 47-52.

Graves, G.R. (1985) Elevational correlates of speciation and intraspecific geographic variation in Andean forest birds. *The Auk,* **103**: 556-579.

Graves, G.R. (1980) A new species of metaltail hummingbird from northern Peru. *The Wilson Bulletin,* **92:** 1-7.

Gregory-Wodzicki, K.M. (2000) Uplift history of the central and northern Andes: A review. *Geological Society of America Bulletin,* **112**: 1091-1105.

Greenberg, R., Cordero, P.J., Droege, S. & Fleischer, R.C. (1998) Morphological adaptation with no mitochondrial DNA differentiation in the coastal plain swamp sparrow. *The Auk,* **118**: 706-712.

Greenberg, R., Danner, R., Olsen, B. & Luther, D. (2011) High summer temperature explains bill size variation in salt marsh sparrows. *Ecography*, **34**: 001-007.

Guindon, S. & Gascuel, O. (2003) A simple, fast, and accurate method to estimate large phylogenies by Maximum Likelihood. *Systematic Biology,* **52**: 696-704.

Hackett, S.J., Kimball, R.T., Reddy, S., Bowie, R.C.K., Braun, E.L., Braun, M.J., Chojnowski, J.L., Cox, W.A., Han, K.-L., Harshman, J., Huddleston, C.J., Marks, B.D., Miglia, K., Moore, W.S., Sheldon, F.H., Steadman, D.W., Witt, C.C., & Yuri, T. (2008) A phylogenetic study of birds reveals their evolutionary history. *Science,* **320**: 1763-1768.

Hagan, A.A. & Heath, J.E. (1980) Regulation of heat loss in the duck by vasomotion in the bill. *Journal of Thermal Biology,* **5**: 95-101.

Harrison, C.J.O. (1984) A revision of the fossil swifts (Vertebrata, Aves, suborder: Apodi), with descriptions of three new genera and two new species. *Mededelingen van de Irkgroep voor Tertiawere en Kwartawere geologie*, **21**: 157-177.

Hawkins, B.A., Diniz-Filho, J.A.F., Jaramillo, J.A., & Soeller, S.A. (2007) Climate, niche conervatism, and the global bird diversity gradient. *The American Naturalist,* **170**: s16-s27.

Heindl, M. & Schuchmann, K.L. (1998) Biogeography, geographical variation and taxonomy of the Andean hummingbird genus *Metallura* GOULD, 1847. *J. Ornithol*., **139:** 425-473.

Heled, J. & Drummond, A.J. (2010) Bayesian inference of species trees from multilocus data. *Molecular Biology and Evolution,* **27:** 570-580.

Hewitt, G. (2000) The genetic legacy of the Quaternary ice ages. *Nature,* **405**: 907-913.

Hey, J. (2006) Recent advances in assessing gene flow betIen diverging populations and Species. *Current Opinion in Genetics and Development*, **16**: 592-596.

Hey, J. (2010) Isolation with migration models for more than two populations. *Molecular Biology and Evolution*, **27**: 905-920.

Hey, J. & Nielsen, R. (2007) Integration within the Felsenstein equation for improved Markov chain Monte Carlo methods in population genetics. *PNAS*, **104**: 2785-2790.

Hijmans, R.J., Cameron, S.E., Parra, J.L., Jones, P.G. & Jarvis, A. (2005) Very high resolution interpolated climate surfaces for global land areas. *International Journal of Climatology,* **25**: 1965-1978.

Holsinger, K.E. & Weir, B.S. (2009) Genetics in geographically structured populations: defining, estimating and interpreting Fst. *Nature Reviews Genetics,* **10**: 639-650.

Hooghiemstra, H. & Van der Hammen, T. (2004) Quaternary Ice-Age dynamics in the Colombian Andes: developing an understanding of my legacy. *Phil. Trans. R. Soc. Lond* B, **359**: 173-181.

Hooghiemstra, H., Wijninga, V.M. & Cleef, A.M. (2006) The paleobotanical record of Colombia: implications for biogeography and biodiversity. *Ann. Missouri Bot. Gard.*, **93**: 297-324.

Hoorn, C., Guerrero, J., Sarmiento, G.A. & Lorente, M.A. (1995) Andean tectonics as a cause for Changing drainage patterns in Miocene northern South America. *Geology,* **23**: 237-240.

Hoorn, C., Isselingh, F.P, ter Steege, H., Bermudez, M.A., Mora, A., Sevink, J., Sanmartín, I., Sanchez-Mesguer, A., Anderson, C.L., Figueweredo, J.P., Jaramillo, C., Riff, D., Negri, F.R., Hooghiemstra, H., Lundberg, J., Stadler, J., Sarkinen, T., & Antonelli, A. (2010) Amazonia through time: Andean uplift, climate change, landscape evolution, and biodiversity. *Science,* **330**: 927-931.

Humphries, E.M. & Winker, K. (2010) Discord reigns among nuclear, mitochondrial and Phenotypic estimates of divergence in nine lineages of trans-beringian birds. *Molecular Ecology,* **20**: 573-583.

Johnson, J.B. & Omland, K.S. (2004) Model selection in ecology and evolution. *Trends in ecology and evolution*,**19**: 101-108.

Johnson, K.P. & Weckstein, J.D. (2011) The Central American landbridge as an engine of diversification in new world doves. *Journal of Biogeography,* **38**: 1069-1076.

Kirchman, J.J., Witt, C.C., McGuire, J.A. & Graves, G.R. (2010) DNA from a 100-year-old holotype confirms the validity of a potentially extinct hummingbird species. *Biology Letters,* **6**: 112-115.

Kuhner, M.K. (2009) Coalescent genealogy samplers: windows into population history. *Trends in Ecology and Evolution,* **24**: 86-93.

Lerner, H.R.L., Meyer, M., James, H.F., Hofreiter, M., & Fleischer, R.C. (2011) Multilocus resolution of phylogeny and timescale in the extant adaptive radiation of Hawaiian Honeycreepers. *Current Biology,* **21**: 1838-1844.

Librado, P. & Rozas, J. (2009) DnaSP v5: A software for comprehensive analysis of DNA polymorphism data. *Bioinformatics,* **25**: 1451-1452.

Lovette, I.J. (2004) Mitochondrial dating and mixed-support for the ‘‘2% rule” in birds. *The Auk,* **121**: 1-6.

Mayr, E. (1942) *Systematics and the origin of species*. Columbia University Press, New York.

Mayr, G. (2003) Phylogeny of early Tertiary swifts and hummingbirds (Aves: Apodiformes). *The Auk,* **120**: 145-151.

Mayr, G. (2002) Osteological evidence for paraphyly of the avian order Caprimulgiformes (nightjars and allies). *J. Ornithol.,* **143**: 82-97.

McCormack, J.E., Heled, J. Delaney, K.S., Peterson, A.T., & Knowles, L.L. (2010) Calibrating Divergence times on species trees versus gene trees: implications for speciation history of *Aphelocoma* Jays. *Evolution,* **65**: 184-202.

McGuire, J.A., Witt, C.C., Altshuler, D.L. & Remsen, Jr., J.V. (2007) Phylogenetic systematics and biogeography of hummingbirds: Bayesian and Maximum likelihood analyses of Partitioned data and selection of an appropriate partitioning strategy. *Systematic Biology,* **56**: 837-856.

McGuire, J.A., Witt, C.C., Remsen, Jr., J.V., Dudley, R. & Altshuler, D.L. (2009) A higher-level taxonomy for hummingbirds. *J Ornithol,* **150**: 155-165.

Milá, B., Wayne, R.K., Fitze, P., & Smith, T.B. (2009) Divergence with gene flow and fine-scale phylogeographical structure in the Idge-billed woodcreeper, *Glyphorynchus spirurus,* a Neotropical rainforest bird. *Molecular Ecology,* **18**: 2979-2995.

Miller, M.J., Bermingham, E. & Ricklefs, R.E. (2007) Historical biogeography of the new world solitaires (*Myadestes spp.*). *The Auk,* **124**: 868-885.

Miller, M.A., Pfeiffer, W. & Schwartz, T (2010) “Creating the CIPRES science gateway for inference of large phylogenetic trees” in Proceedings of the Gateway Computing Environments Workshop (GCE), 14 Nov. 2010, New Orleans, LA pp. 1-8.

Moya, A., Galiana, A. & Ayala, F.J. (1995) Founder-effect speciation theory: failure of Experimental corroboration. *PNAS*, **92**: 3983-3986.

Nattero, J., Sérsic, A.N. & Cocucci, A.A. (2010) Geographic variation of floral traits in *Nicotiana glauca*: relationships with biotic and abiotic factors. *Acta Oecologica*, **37**: 503-511.

Nei, M. 1987. *Molecular Evolutionary Genetics.* Columbia University Press, New York.

Nylander, J.A.A., Olsson, U. Alstrom, P. & Sanmartín, I. (2008) Accounting for phylogenetic uncertainty in biogeography: a Bayesian approach to dispersal-vicariance analysis of the Thrushes (Aves: *Turdus*). *Systematic Biology*, **57**: 257-268.

Patel, S., Weckstein, J.D, Patané, J.S.L, Bates, J.M. & Aleixo, A. (2011) Temporal and spatial diversificaiton of *Pteroglossus* Aracaris (Aves: Ramphastidae) in the neotropics: constant rate of diversification does not support an increase in radiation during the Pleistocene. *Molecular Phylogenetics and Evolution*, **58**: 105-115.

Patton, J.L. & Smith, M.F. (1992) mtDNA phylogeny of Andean mice: a test of diversification of across ecological gradients. *Evolution,* **46:** 174-183.

Parker III, T.A., Schulenberg, T.S., Graves, G.R. & Braun, M.J. (1985) The avifauna of the Huancabamba region, Northern Peru. *Ornithological Monographs*, **36**: 169-197.

Parra, J.L., Remsen, Jr., J.V., Alvarez-Reballedo, M. & McGuwere, J.A. (2009) Molecular phylogenetics of the hummingbird genus *Coeligena*. *Molecular Phylogenetics and Evolution,* **53**: 425-434.

Pérez-Emán, J.L. (2005) Molecular phylogenetics and biogeography of the Neotropical redstarts (*Myioborus*; Aves, Parulinae). *Moleuclar Phylogenetics and Evolution,* **37**: 511-528.

Peters, J.L. (1945) *Check-list of Birds of the World, Vol. 5.* Harvard University Press, Cambridge, MA.

Peters, D.S. (1985) Ein neuer segler aus der grube Messel und seine Bedeutung fur den status der Aegialornithidae (Aves: Apodiformes). *Senckenbergiana lethaea,* **66:** 143-164.

Pigot, A.L., Phillemore, A.B., Owens, I.P.F. & Orme, C.D.L. (2010) The shape and temporal dynamics of phylogenetic trees arising from geographic speciation. *Systematic Biology*, **59:** 660-673.

Pinho, C. & Hey, J. (2010) Divergence with gene flow: Models and Data. *Annual Review of Ecology, Evolution, and Systematics*, **41**: 215-230.

Posada, D. (2008) jModelTest: Phylogenetic model averaging. *Molecular Biology and Evolution,* **25:** 1253-1256.

Price, T. (2008) *Speciation in Birds.* Roberts & Company, Greenwood Village, Colorado, USA.

Remsen, Jr., J.V. (1984) High incidence of "Leapfrog" pattern of geographic variation in Andean birds: implications for the speciation process. *Science*, **224**: 171-173.

Ribas, C.C., Moyle, R.G., Miyaki, C.Y. & Cracraft, J. (2007) The assembly of montane biotas: Linking Andean tectonics and climatic oscillations to independent regimes of diversification in *Pionus* parrots. *Proceedings of the Royal Society B,* **274**: 2399-2408.

Ribas, C.C., Aleixo, A., Nogueira, A.C.R., Miyaki, C.Y. & Cracraft, J. (2012) A paleobiogeographic model for biotic diversification within Amazonia over the past three million years. *Proceedings of the Royal Society B,* **279**: 681-689.

Ridgely, R.S. & Greenfield, P.J. (2001) *The Birds of Ecuador*. Cornell University Press, Ithaca, New York, USA.

Rheindt, F.E., Christidis, L., Cabanne, G.S., Miyaki, C. & Norman, J.A. (2009) The timing of Neotropical speciation dynamics: A reconstruction of *Myiopagis* flycatcher diversification using phylogenetic and paleogeographic data. *Molecular Phylogenetics and Evolution,* **53**: 961-971.

Ronquist, F. (1997) Dispersal-Vicariance Analysis: a new approach to the quantification of historical biogeography. *Systematic Biology,* **46**: 195-203.

Ronquist, F. & Huelsenbeck, J.P. (2003) MRBAYES 3: Bayesian phylogenetic inference under mixed models. *Bioinformatics,* **19**: 1572-1574.

Rozen, S. & Skaletsky, H.J. (2000) Primer3 on the WWW for general users and for biologist programmers. In: KraItz S, Misener S (eds) *Bioinformatics Methods and Protocols: Methods in Molecular Biology.* Humana Press, Totowa, NJ, pp 365- 386.

Rull, V. (2011) Neotropical biodiversity: timing and potential drivers. *Trends in Ecology and Evolution,* **26**: 508-513.

Rundle, H.D., Mooers, A.O. & Whitlock, M.C. (1998) Single founder-flush events and the evolution of reproductive isolation. *Evolution,* **52**: 1850-1855.

Sarkinen, T., Pennington, R.T., Lavin, M., Simon, M.F. & Hughes, C.E. (2011) Evolutionary islands in the Andes: persistence and extinction explain high endemism in Andean dry tropical forests. *Journal of Biogeography.*

Schuchmann, K.L. (1999) *Family Trochilidae (Hummingbirds)*. Lynx Edicons, Barcelona, Spain.

Schulenberg, T.S., Stotz, D.S., Lane, D.F., O'Neill, J.P. & Parker III, T.A. (2007) *Birds of Peru.* Princeton University Press, Princeton.

Sedano, R.E. & Burns, K.J. (2010) Are the northern Andes a species pump for Neotropical birds? Phylogenetics and biogeography of a clade of Neotropical tanagers (Aves: Thraupini). *Journal of Biogeography* **37**: 325-343.

Smith, T.B., Wayne, R.K., Girman, D.J. & Bruford, M.J. (1997) A role for ecotones in generating rainforest Biodiversity. *Science*, **276**: 1855-1857.

Smith, T.B., Calsbeek, R., Wayne, R.K., Holder, K.H., Pweres, D. & Bardeleben, C. (2004) Testing alternative mechanisms of evolutionary divergence in an African rain forest passerine bird. *Journal of Evolutionary Biology,* **18**: 257-268.

Smith, T.B., Thomassen, H.A., Freedman, A.H., Sehgal, R.N.M., Buermann, W., Saatchi, S., Pollinger, J., Milá, B., Pweres, D., Valkiunas, G. & Wayne, R.K. (2011) Patterns of divergence in the olive sunbird *Cyanomitra olivacea* (Aves: Nectariniidae) across the African rainforest-savanna ecotone. *Biological Journal of the Linnaean Society*, **103**: 821-835.

Stamatakis, A. (2006) RAxML-VI-HPC: Maximum Likelihood-based phylogenetic analysis with thousands of taxa and mixed models. *Bioinformatics,* **22**: 2688-2690.

Stattersfield, A. J., Crosby, M.J., Long, A.J. & Wege, D.C. (1998) *Endemic Bird Areas of the World*. Birdlife International, Cambridge, United Kingdom.

Stephens, M., Smith, N.J., & Donnely, P. (2001) A new statistical method for haplotype reconstruction from population data. *American Journal of Human Genetics,* **68**: 978-989.

Stephens, M. & Donnely, P. (2003) A comparison of Bayesian methods for haplotype reconstruction. *American Journal of Human Genetics,* **73**: 1162-1169.

Stotz, D.F., Fitzpatrick, J.W., Parker III, T.A. & Moskovits, D.K. (1996) *Neotropical Birds: Ecology and Conservation*. The University of Chicago Press, Chicago.

Stuessy, T.F., Foland, K.A., Sutter, J.F., Sanders, R.W. & Silva O., M. (1984) Botanical and Geological significance of potassium-argon dates from the Juan Fernandez Islands. *Science,* **225**: 49-51.

Symonds, M.R.E & Tattersall, G.J. (2010) Geographical variation in bill size across bird species provides evidence for Allen's rule. *American Naturalist,* **176**: 188-197.

Tattersall, G.J. Andrade, D.V. & Abe, A.S. (2009) Heat exchange from the toucan bill reveals a controllable vascular thermal radiator. *Science*, **325**: 468-470.

Temeles, E.J., Kress, W.J. (2003) Adaptation in a plant-hummingbird association. *Science*, **300**: 630-633.

Temeles, E.J., Miller, J.S., Rifkin, J.L. (2010) Evolution of sexual dimorphism in bill size and shape of Hermit hummingbirds (Phaethornithinae): a role for ecological causation. *Philosophical Transactions of the Royal Society*, **365**: 1053-1063.

Terborgh, J. (1971) Distribution on environmental gradients: theory and a preliminary interpretation of distributional patterns in the avifauna of the Cordillera Vilcabamba, Peru. *Ecology*, **52**: 23-40.

Terborgh, J. & Weske, J.S. (1975) The role of competition in the distribution of Andean birds. *Ecology*, **56**: 562-576.

Tinoco, B.A., Astudillo, P.X., Latta, S.C. & Graham, C.H. (2009) Distribution, ecology and conservation of an endangered Andean hummingbird: the Violet-throated Metaltail (*Metallura baroni*). *Bird Conservation International*, **19**: 63-76.

Tobias, J.A., Seddon, N., Spottiswoode, C.N., Pilgrim, J.D., Fishpool, L.D.C. & Collar, N.J. (2010) Quantitative criteria for species delimitation. *Ibis*, **152**: 724-746.

Vuilleumier, F. (1969) Pleistocene speciation in birds living in the high Andes. *Nature,* 1179-1180.

Walstrom, V.W., Klicka, J. & Spellman, G.M. (2011) Speciation in the White-breasted Nuthatch (*Sitta carolinensis*): a multi-locus perspective. doi: 10.1111/j.1365-294X.2011.05384.x.

Weir, J.T. (2006) Divergent timing and patterns of species accumulation in lowland and highland Neotropical birds. *Evolution*, **60**: 842-855.

Weir, J.T. (2009) Implications of genetic differentiation in neotropical montane forest birds. *Annals of the Missouri Botanical Garden*, **96**: 410-433.

Weir, J.T., Bermingham, E., Miller, M.J., Klicka, J., & González, M.A. (2008) Phylogeography of a morphologically diverse Neotropical montane species, the Common Bush-Tanager (*Chlorospingus opthalmicus*). *Molecular Phylogenetics and Evolution*, **47**: 650-664.

Weir, J.T. & Schluter, D. (2008) Calibrating the Avian molecular clock. *Molecular Ecology*, **17**: 2321-2328.

Weir, J.T. & Price, T.D. (2011) Limits to speciation inferred from times to secondary sympatry and ages of hybridizing species along a latitudinal gradient. *The American Naturalist*, **177**: 462-469.

Weir, J.T. & Price, M. (2011) Andean uplift promotes lowland speciation through vicariance and dispersal in *Dendrocincla* woodcreepers. *Molecular Ecology*, **20**: 4550-4563.

Wilgenbusch, J.C., Warren, D.L. & Swofford, D.L. (2004) AWTY: A system for graphical exploration of MCMC convergence in Bayesian phylogenetic inference. http://ceb.csit.fsu.edu/AWTY.

Yu, Y., Harris, A.J. & He, X.J. (2011) A Novel Bayesian Method for Reconstructing Geographic Ranges and Ancestral States on Phylogenies. *Systematic Biology*, in Review.

Zar, J.H. (2010) *Biostatistical Analysis,5th ed.* Pearson Prentice Hall, Upple Saddle River, New Jersey, USA.

Zimmer, J.T. (1952) Studies of Peruvian birds. No. 62 the hummingbird genera: *Patagona, Sappho, Polyonymus, Ramphomicron, Metallura, Chalcostigma, Taphrolesbia,* and *Aglaiocercus*. *American Museum Novitates***, 1595:** 1-29.

Zink RM, Remsen, Jr., JV (1986) Evolutionary processes and patterns of geographic variation in Birds. In: *Current Ornithology* (ed. Johnston RF), pp 1-69. Plenum Press, New York.